



Measurement of the CKM angle γ from a combination of LHCb results

The LHCb collaboration[†]

Abstract

A combination of measurements sensitive to the CKM angle γ from LHCb is performed. The inputs are from analyses of time-integrated $B^+ \rightarrow DK^+$, $B^0 \rightarrow DK^{*0}$, $B^0 \rightarrow DK^+\pi^-$ and $B^+ \rightarrow DK^+\pi^+\pi^-$ tree-level decays. In addition, results from a time-dependent analysis of $B_s^0 \rightarrow D_s^\mp K^\pm$ decays are included. The combination yields $\gamma = (72.2_{-7.3}^{+6.8})^\circ$, where the uncertainty includes systematic effects. The 95.5% confidence level interval is determined to be $\gamma \in [55.9, 85.2]^\circ$. A second combination is investigated, also including measurements from $B^+ \rightarrow D\pi^+$ and $B^+ \rightarrow D\pi^+\pi^-\pi^+$ decays, which yields compatible results.

Published in JHEP 12 (2016) 087

© CERN on behalf of the LHCb collaboration, licence CC-BY-4.0.

[†]Authors are listed at the end of this paper.

Contents

1	Introduction	1
2	Inputs from LHCb analyses sensitive to γ	5
3	Auxiliary inputs	7
4	Statistical treatment	9
5	Results	9
5.1	<i>DK</i> combination	10
5.2	<i>Dh</i> combination	10
5.3	Coverage of the frequentist method	12
5.4	Interpretation	16
6	Bayesian analysis	16
6.1	<i>DK</i> combination	16
6.2	<i>Dh</i> combination	19
7	Conclusion	24
	Appendices	26
A	Relationships between parameters and observables	26
B	Input observable values and uncertainties	31
C	Uncertainty correlations for the input observables	36
D	External constraint values and uncertainties	45
E	Uncertainty correlations for the external constraints	47
F	Fit parameter correlations	48
	References	49

1 Introduction

Understanding the origin of the baryon asymmetry of the Universe is one of the key issues of modern physics. Sakharov showed that such an asymmetry can arise if three conditions are fulfilled [1], one of which is the requirement that both charge (C) and charge-parity (CP) symmetries are broken. The latter phenomenon arises in the Standard Model (SM) of particle physics through the complex phase of the Cabibbo-Kobayashi-Maskawa (CKM) quark mixing matrix [2, 3], although the effect in the SM is not large enough to account for the observed baryon asymmetry in the Universe [4]. Violation of CP symmetry can be studied by measuring the angles of the CKM unitarity triangle [5–7]. The least precisely known of these angles, $\gamma \equiv \arg[-V_{ud}V_{ub}^*/V_{cd}V_{cb}^*]$, can be measured using only tree-level processes [8–11]; a method that, assuming new physics is not present in tree-level decays [12], has negligible theoretical uncertainty [13]. Disagreement between such direct measurements of γ and the value inferred from global CKM fits, assuming the validity of the SM, would indicate new physics beyond the SM.

The value of γ can be determined by exploiting the interference between favoured $b \rightarrow cW$ (V_{cb}) and suppressed $b \rightarrow uW$ (V_{ub}) transition amplitudes using decay channels such as $B^+ \rightarrow Dh^+$, $B^0 \rightarrow DK^{*0}$, $B^0 \rightarrow DK^+\pi^-$, $B^+ \rightarrow Dh^+\pi^-\pi^+$ and $B_s^0 \rightarrow D_s^\mp K^\pm$ [8–11, 14–21], where h is a kaon or pion and D refers to a neutral charm meson that is a mixture of the D^0 and \bar{D}^0 flavour eigenstates. The inclusion of charge conjugate processes is implied throughout, unless otherwise stated. The most precise way to determine γ is through a combination of measurements from analyses of many decay modes. Hadronic parameters such as those that describe the ratio (r_B^X) or strong phase difference (δ_B^X) between the V_{cb} and V_{ub} transition amplitudes and where X is a specific final state of a B meson decay, are also simultaneously determined. The ratio of the suppressed to favoured B decay amplitudes is related to γ and the hadronic parameters by $\mathcal{A}_{\text{sup}}/\mathcal{A}_{\text{fav}} = r_B^X e^{i(\delta_B^X \pm \gamma)}$, where the $+$ ($-$) sign refers to the decay of a meson containing a \bar{b} (b). The statistical uncertainty with which γ can be measured is approximately inversely proportional to the value of r_B^X , which is around 0.1 for $B^+ \rightarrow DK^+$ decays [22]. In the $B^+ \rightarrow D\pi^+$ channel, $r_B^{D\pi}$ is expected to be of order 0.005 [23] because the favoured amplitude is enhanced by $|V_{ud}|/|V_{us}|$ while the suppressed amplitude is further reduced by $|V_{cd}|/|V_{cs}|$ with respect to $B^+ \rightarrow DK^+$ decays. Consequently, the expected sensitivity to γ in $B^+ \rightarrow D\pi^+$ decays is considerably lower than for $B^+ \rightarrow DK^+$ decays, although the signal yields are higher. For $B^0 \rightarrow DK^{*0}$ (and also $B_s^0 \rightarrow D_s^\mp K^\pm$) decays a higher value is expected [24], $r_B^{DK^{*0}} \sim r_B^{D_s K} \sim 0.3$, which compensates for the lower branching fraction [25], whilst the expected value for $r_B^{DK\pi\pi}$ is similar to r_B^{DK} . The current world average, using only direct measurements of $B \rightarrow DK$ -like decays, is $\gamma = (73.2_{-7.0}^{+6.3})^\circ$ [26] (or, using different inputs with an alternative statistical approach, $\gamma = (68.3 \pm 7.5)^\circ$ [27]). The previous LHCb combination found $\gamma = (73_{-10}^{+9})^\circ$ [28].

This paper presents the latest combination of LHCb measurements of tree-level decays that are sensitive to γ . The results supersede those previously reported in Refs. [28–31], including more decay channels and updating selected channels to the full Run 1 dataset of pp collisions at $\sqrt{s} = 7$ and 8 TeV, corresponding to an integrated luminosity of 3 fb^{-1} . Two combinations are performed, one including all inputs from $B \rightarrow DK$ -like modes (referred to as DK) and one additionally including inputs from $B^+ \rightarrow D\pi^+$ and $B^+ \rightarrow D\pi^+\pi^-\pi^+$ decays (referred to as Dh). The DK combination includes 71 observables depending on 32 parameters, whilst the Dh combination has 89 observables

and 38 parameters.

The analyses included in the combinations use a variety of methods to measure γ , which are reviewed in Ref. [32]. The observables are briefly summarised below; their dependence on γ and various hadronic parameters is given in Appendix A. The Gronau-London-Wyler (GLW) method [8,9] considers the decays of D mesons to CP eigenstates, for example the CP -even decays $D \rightarrow K^+K^-$ and $D \rightarrow \pi^+\pi^-$. The Atwood-Dunietz-Soni (ADS) approach [10,11] extends this to include final states that are not CP eigenstates, for example $D^0 \rightarrow \pi^-K^+$, where the interference between the Cabibbo-allowed and doubly Cabibbo-suppressed decay modes in both the B and D decays gives rise to large charge asymmetries. This introduces an additional dependence on the D decay dynamics through the ratio of suppressed and favoured D decay amplitudes, r_D , and their phase difference, δ_D . The GLW/ADS formalism is easily extended to multibody D decays [10,11,33] although the multiple interfering amplitudes dilute the sensitivity to γ . For multibody ADS modes this dilution is parameterised in terms of a coherence factor, κ_D , and for the GLW modes it is parametrised by F_+ , which describes the fraction of CP -even content in a multibody decay. For multibody D decays these parameters are measured independently and used as external constraints in the combination as discussed in Sec. 3. The GLW/ADS observables are constructed from decay-rate ratios, double ratios and charge asymmetries as outlined in the following.

For GLW analyses the observables are the charge-averaged rate and the partial-rate asymmetry. The former is defined as

$$R_{CP} = 2 \frac{\Gamma(B^- \rightarrow D_{CP}K^-) + \Gamma(B^+ \rightarrow D_{CP}K^+)}{\Gamma(B^- \rightarrow D^0K^-) + \Gamma(B^+ \rightarrow \bar{D}^0K^+)}, \quad (1)$$

where D_{CP} refers to the final state of a D meson decay into a CP eigenstate. Experimentally it is convenient to measure R_{CP} , for a given final state f , by forming a double ratio that is normalised using the rate for a Cabibbo-favoured decay (*e.g.* $D^0 \rightarrow K^-\pi^+$), and the equivalent quantities from the relevant $B^+ \rightarrow D\pi^-$ decay mode. Defining the ratio of the favoured $B^+ \rightarrow \bar{D}^0K^+$ and $B^+ \rightarrow \bar{D}^0\pi^+$ partial widths, for a given final state f , as

$$R_{K/\pi}^f = \frac{\Gamma(B^- \rightarrow D[\rightarrow f]K^-) + \Gamma(B^+ \rightarrow D[\rightarrow \bar{f}]K^+)}{\Gamma(B^- \rightarrow D[\rightarrow f]\pi^-) + \Gamma(B^+ \rightarrow D[\rightarrow \bar{f}]\pi^+)}, \quad (2)$$

the double ratios are constructed as

$$R_{CP}^{KK} \approx \frac{R_{K/\pi}^{KK}}{R_{K/\pi}^{K\pi}}, \quad R_{CP}^{\pi\pi} \approx \frac{R_{K/\pi}^{\pi\pi}}{R_{K/\pi}^{K\pi}}, \quad R_{CP}^{KK\pi^0} \approx \frac{R_{K/\pi}^{KK\pi^0}}{R_{K/\pi}^{K\pi\pi^0}}, \quad R_{CP}^{\pi\pi\pi^0} \approx \frac{R_{K/\pi}^{\pi\pi\pi^0}}{R_{K/\pi}^{K\pi\pi^0}}, \quad \textit{etc.} \quad (3)$$

These relations are exact when the suppressed $B^+ \rightarrow D\pi^+$ decay amplitude ($b \rightarrow u$) vanishes and the flavour specific rates, given in the denominator of Eq. (1), are measured using the appropriate flavour-specific D decay channel. The GLW partial-rate asymmetry, for a given D meson decay into a CP eigenstate f , is defined as

$$A_{CP}^{Dh,f} = \frac{\Gamma(B^- \rightarrow D_{CP}h^-) - \Gamma(B^+ \rightarrow D_{CP}h^+)}{\Gamma(B^- \rightarrow D_{CP}h^-) + \Gamma(B^+ \rightarrow D_{CP}h^+)}. \quad (4)$$

Similarly, observables associated to the ADS modes, for a suppressed $D \rightarrow f$ decay, are the charge-averaged rate and the partial-rate asymmetry. For the charge-averaged rate, it

is adequate to use a single ratio (normalised to the favoured $D \rightarrow \bar{f}$ decay) because the detection asymmetries cancel out. The charge-averaged rate is defined as

$$R_{\text{ADS}}^{Dh,\bar{f}} = \frac{\Gamma(B^- \rightarrow D[\rightarrow \bar{f}]h^-) + \Gamma(B^+ \rightarrow D[\rightarrow f]h^+)}{\Gamma(B^- \rightarrow D[\rightarrow f]h^-) + \Gamma(B^+ \rightarrow D[\rightarrow \bar{f}]h^+)}, \quad (5)$$

whilst the partial-rate asymmetry is defined as

$$A_{\text{ADS}}^{Dh,\bar{f}} = \frac{\Gamma(B^- \rightarrow D[\rightarrow \bar{f}]h^-) - \Gamma(B^+ \rightarrow D[\rightarrow f]h^+)}{\Gamma(B^- \rightarrow D[\rightarrow \bar{f}]h^-) + \Gamma(B^+ \rightarrow D[\rightarrow f]h^+)}. \quad (6)$$

The equivalent charge asymmetry for favoured ADS modes is defined as

$$A_{\text{fav}}^{Dh,f} = \frac{\Gamma(B^- \rightarrow D[\rightarrow f]h^-) - \Gamma(B^+ \rightarrow D[\rightarrow \bar{f}]h^+)}{\Gamma(B^- \rightarrow D[\rightarrow f]h^-) + \Gamma(B^+ \rightarrow D[\rightarrow \bar{f}]h^+)}. \quad (7)$$

Some of the input analyses determined two statistically independent observables instead of those in Eqs. (5) and (6), namely the ratio of partial widths for the suppressed and favoured decays of each initial B flavour,

$$R_+^{Dh,\bar{f}} = \frac{\Gamma(B^+ \rightarrow D[\rightarrow f]h^+)}{\Gamma(B^+ \rightarrow D[\rightarrow \bar{f}]h^+)}, \quad (8)$$

$$R_-^{Dh,\bar{f}} = \frac{\Gamma(B^- \rightarrow D[\rightarrow \bar{f}]h^-)}{\Gamma(B^- \rightarrow D[\rightarrow f]h^-)}. \quad (9)$$

It should be noted that Eqs. (5) and (6) are related to Eqs. (8) and (9) by

$$R_{\text{ADS}} = \frac{R_+ + R_-}{2}, \quad A_{\text{ADS}} = \frac{R_- - R_+}{R_- + R_+}, \quad (10)$$

if the rates of the Cabibbo-favoured decays for B^- and B^+ are identical.

Similar to the ADS approach is the Grossman-Ligeti-Soffer (GLS) method [16] that exploits singly Cabibbo-suppressed decays such as $D \rightarrow K_s^0 K^- \pi^+$. The GLS observables are defined in analogy to Eqs. (5–7). Note that in the GLS method the favoured decay has sensitivity to γ because the ratio between the suppressed and favoured amplitudes is much larger than in the ADS approach. It is therefore worthwhile to include the favoured GLS decays in the combinations, which is not the case for the favoured ADS channels alone.

The Giri-Grossman-Soffer-Zupan (GGSZ) method [14,15] uses self-conjugate multibody D meson decay modes like $K_s^0 \pi^+ \pi^-$. Sensitivity to γ is obtained by comparing the distributions of decays in the $D \rightarrow f$ Dalitz plot for opposite-flavour initial-state B and \bar{B} mesons. The population of candidates in the Dalitz plot depends on four variables, referred to as Cartesian variables which, for a given B decay final state X , are defined as

$$x_{\pm}^X = r_B^X \cos(\delta_B^X \pm \gamma), \quad (11)$$

$$y_{\pm}^X = r_B^X \sin(\delta_B^X \pm \gamma). \quad (12)$$

These are the preferred observables for GGSZ analyses. The GLW/ADS and GGSZ formalisms can also be extended to multibody B decays by including a coherence factor, κ_B , that accounts for dilution from interference between competing amplitudes. This

inclusive approach is used for all multibody and quasi-two-body B decays, with the exception of the GLW-Dalitz analysis of $B^0 \rightarrow DK^+\pi^-$ decays where an amplitude analysis is performed to determine x_{\pm}^X and y_{\pm}^X . Here the term quasi-two-body decays refer to a two body resonant decay that contributes to a three body final state (*e.g.* $B^0 \rightarrow DK^*(892)^0$ decays in the $B^0 \rightarrow DK^+\pi^-$ final state).

Time-dependent (TD) analyses of $B_s^0 \rightarrow D_s^\mp K^\pm$ are also sensitive to γ [17–19]. Due to the interference between the mixing and decay amplitudes, the CP -sensitive observables, which are the coefficients of the time evolution of $B_s^0 \rightarrow D_s^\mp K^\pm$ decays, have a dependence on $(\gamma - 2\beta_s)$, where $\beta_s \equiv \arg(-V_{ts}V_{tb}^*/V_{cs}V_{cb}^*)$. In the SM, to a good approximation, $-2\beta_s$ is equal to the phase ϕ_s determined from $B_s^0 \rightarrow J/\psi\phi$ and similar decays, and therefore an external constraint on the value of ϕ_s provides sensitivity to γ . The time-dependent decay rates for the initially pure B_s^0 and \bar{B}_s^0 flavour eigenstates are given by

$$\frac{d\Gamma_{B_s^0 \rightarrow f}(t)}{dt} = \frac{1}{2}|A_f|^2(1 + |\lambda_f|^2)e^{-\Gamma_s t} \left[\cosh\left(\frac{\Delta\Gamma_s t}{2}\right) + A_f^{\Delta\Gamma} \sinh\left(\frac{\Delta\Gamma_s t}{2}\right) + C_f \cos(\Delta m_s t) - S_f \sin(\Delta m_s t) \right], \quad (13)$$

$$\frac{d\Gamma_{\bar{B}_s^0 \rightarrow f}(t)}{dt} = \frac{1}{2}|A_f|^2 \left| \frac{p}{q} \right|^2 (1 + |\lambda_f|^2)e^{-\Gamma_s t} \left[\cosh\left(\frac{\Delta\Gamma_s t}{2}\right) + A_f^{\Delta\Gamma} \sinh\left(\frac{\Delta\Gamma_s t}{2}\right) - C_f \cos(\Delta m_s t) + S_f \sin(\Delta m_s t) \right], \quad (14)$$

where $\lambda_f \equiv (q/p) \cdot (\bar{A}_f/A_f)$ and A_f (\bar{A}_f) is the decay amplitude of a B_s^0 (\bar{B}_s^0) to a final state f . In the convention used, f (\bar{f}) is the $D_s^- K^+$ ($D_s^+ K^-$) final state. The parameter Δm_s is the oscillation frequency for B_s^0 mesons, Γ_s is the average B_s^0 decay width, and $\Delta\Gamma_s$ is the decay-width difference between the heavy and light mass eigenstates in the B_s^0 system, which is known to be positive [34] as expected in the SM. The observables sensitive to γ are $A_f^{\Delta\Gamma}$, C_f and S_f . The complex coefficients p and q relate the B_s^0 meson mass eigenstates, $|B_{L,H}\rangle$, to the flavour eigenstates, $|B_s^0\rangle$ and $|\bar{B}_s^0\rangle$, as $|B_L\rangle = p|B_s^0\rangle + q|\bar{B}_s^0\rangle$ and $|B_H\rangle = p|B_s^0\rangle - q|\bar{B}_s^0\rangle$ with $|p|^2 + |q|^2 = 1$. Similar equations can be written for the CP -conjugate decays replacing S_f by $S_{\bar{f}}$, and $A_f^{\Delta\Gamma}$ by $A_{\bar{f}}^{\Delta\Gamma}$, and, assuming no CP violation in either the decay or mixing amplitudes, $C_{\bar{f}} = -C_f$. The relationships between the observables, γ and the hadronic parameters are given in Appendix A.10.

The combinations are potentially sensitive to subleading effects from D^0 – \bar{D}^0 mixing [35–37]. These are corrected for where necessary, by taking into account the D^0 decay-time acceptances of the individual measurements. The size of the correction is inversely proportional to r_B^X and so is particularly important for the $B^+ \rightarrow D\pi^+(\pi^+\pi^-)$ modes. For consistency, the correction is also applied in the corresponding $B^+ \rightarrow DK^+(\pi^+\pi^-)$ modes. The correction for other decay modes would be small and is not applied. There can also be an effect from CP violation in $D \rightarrow h^+h^-$ decays [38–41], which is included in the relevant $B^+ \rightarrow \bar{D}^0 h^+(\pi^+\pi^-)$ analyses using the world average values [22], although the latest measurements indicate that the effect is negligible [42]. Final states that include a K_s^0 meson are potentially affected by corrections due to CP violation and mixing in the neutral kaon system, parametrised by the non-zero parameter ϵ_K [43]. The effect is expected to be $\mathcal{O}(\epsilon_K/r_B^h)$, which is negligible for $B^+ \rightarrow DK^+$ decays since $|\epsilon_K| \approx 0.002$ and $r_B^{DK} \approx 0.1$ [22]. For $B^+ \rightarrow D\pi^+$ decays this ratio is expected to be $\mathcal{O}(1)$ since $r_B^{D\pi}$ is

expected to be around 0.5% [23]. Consequently, the $B^+ \rightarrow D\pi^+$ decay modes affected, such as those with $D \rightarrow K_s^0 K^\mp \pi^\pm$, are not included in the Dh combination.

To determine γ with the best possible precision, auxiliary information on some of the hadronic parameters is used in conjunction with observables measured in other LHCb analyses. More information on these quantities can be found in Secs. 2 and 3, with a summary provided in Tables 1 and 2. Frequentist and Bayesian treatments are both studied. Section 4 describes the frequentist treatment with results and coverage studies reported in Sec. 5. Section 6 describes the results of a Bayesian analysis.

2 Inputs from LHCb analyses sensitive to γ

The LHCb measurements used as inputs in the combinations are summarised in Table 1 and described briefly below. The values and uncertainties of the observables are provided in Appendix B and the correlations are given in Appendix C. The relationships between the observables and the physics parameters are listed in Appendix A. All analyses use a data sample corresponding to an integrated luminosity of 3 fb^{-1} , unless otherwise stated.

Table 1: List of the LHCb measurements used in the combinations.

B decay	D decay	Method	Ref.	Status since last combination [28]
$B^+ \rightarrow Dh^+$	$D \rightarrow h^+h^-$	GLW/ADS	[44]	Updated to 3 fb^{-1}
$B^+ \rightarrow Dh^+$	$D \rightarrow h^+\pi^-\pi^+\pi^-$	GLW/ADS	[44]	Updated to 3 fb^{-1}
$B^+ \rightarrow Dh^+$	$D \rightarrow h^+h^-\pi^0$	GLW/ADS	[45]	New
$B^+ \rightarrow DK^+$	$D \rightarrow K_s^0 h^+h^-$	GGSZ	[46]	As before
$B^+ \rightarrow DK^+$	$D \rightarrow K_s^0 K^-\pi^+$	GLS	[47]	As before
$B^+ \rightarrow Dh^+\pi^-\pi^+$	$D \rightarrow h^+h^-$	GLW/ADS	[48]	New
$B^0 \rightarrow DK^{*0}$	$D \rightarrow K^+\pi^-$	ADS	[49]	As before
$B^0 \rightarrow DK^+\pi^-$	$D \rightarrow h^+h^-$	GLW-Dalitz	[50]	New
$B^0 \rightarrow DK^{*0}$	$D \rightarrow K_s^0 \pi^+\pi^-$	GGSZ	[51]	New
$B_s^0 \rightarrow D_s^\mp K^\pm$	$D_s^+ \rightarrow h^+h^-\pi^+$	TD	[52]	As before

- $B^+ \rightarrow Dh^+$, $D \rightarrow h^+h^-$. The GLW/ADS measurement using $B^+ \rightarrow Dh^+$, $D^0 \rightarrow h^+h^-$ decays [44] is an update of a previous analysis [53]. The observables are defined in analogy to Eqs. (3–7).
- $B^+ \rightarrow Dh^+$, $D \rightarrow h^+\pi^-\pi^+\pi^-$. The ADS measurement using the $B^+ \rightarrow Dh^+$, $D \rightarrow K^\pm \pi^\mp \pi^+\pi^-$ decay mode [44] is an update of a previous measurement [54]. The quasi-GLW measurement with $B^+ \rightarrow Dh^+$, $D \rightarrow \pi^+\pi^-\pi^+\pi^-$ decays is included in the combination for the first time. The label “quasi” is used because the $D \rightarrow \pi^+\pi^-\pi^+\pi^-$ decay is not completely CP -even; the fraction of CP -even content

is given by $F_{\pi\pi\pi\pi}$ as described in Sec. 3. The method for constraining γ using these decays is described in Ref. [33], with observables defined in analogy to Eqs. (3–7).

- $B^+ \rightarrow Dh^+$, $D \rightarrow h^+h^-\pi^0$. Inputs from the quasi-GLW/ADS analysis of $B^+ \rightarrow Dh^+$, $D \rightarrow h^+h^-\pi^0$ decays [45] are new to this combination. The CP -even content of the $D \rightarrow K^+K^-\pi^0$ ($D \rightarrow \pi^+\pi^-\pi^0$) decay mode is given by the parameter $F_{KK\pi^0}$ ($F_{\pi\pi\pi^0}$), as described in Sec. 3. The observables are defined in analogy to Eqs. (3–7).
- $B^+ \rightarrow DK^+$, $D \rightarrow K_s^0h^+h^-$. The inputs from the model-independent GGSZ analysis of $B^+ \rightarrow DK^+$, $D \rightarrow K_s^0h^+h^-$ decays [46] are the same as those used in the previous combination [28]. The variables, defined in analogy to Eqs. (11–12), are obtained from a simultaneous fit to the Dalitz plots of $D \rightarrow K_s^0\pi^+\pi^-$ and $D \rightarrow K_s^0K^+K^-$ decays. Inputs from a model-dependent GGSZ analysis of the same decay [55] using data corresponding to 1 fb^{-1} are not included due to the overlap of the datasets.
- $B^+ \rightarrow DK^+$, $D \rightarrow K_s^0K^-\pi^+$. The inputs from the GLS analysis of $B^+ \rightarrow DK^+$, $D \rightarrow K_s^0K^-\pi^+$ decays [47] are the same as those included in the last combination [28]. The observables are defined in analogy to Eqs. (5–7). The negligible statistical and systematic correlations are not taken into account.
- $B^+ \rightarrow Dh^+\pi^-\pi^+$, $D \rightarrow h^+h^-$. The inputs from the LHCb GLW/ADS analysis of $B^+ \rightarrow Dh^+\pi^-\pi^+$, $D^0 \rightarrow h^+h^-$ decays [48] are included in the combination for the first time. The observables are defined in analogy to Eqs. (3–4,7–9). The only non-negligible correlations are statistical, $\rho(A_{CP}^{DK\pi\pi, KK}, A_{CP}^{DK\pi\pi, \pi\pi}) = 0.20$ and $\rho(A_{CP}^{D\pi\pi\pi, KK}, A_{CP}^{D\pi\pi\pi, \pi\pi}) = 0.08$.
- $B^0 \rightarrow DK^{*0}$, $D \rightarrow K^+\pi^-$. The inputs from the ADS analysis of $B^0 \rightarrow D^0K^*(892)^0$, $D^0 \rightarrow K^\pm\pi^\mp$ decays [49] are included as they were in the previous combination [28]. However, the GLW part of this analysis (with $D^0 \rightarrow K^+K^-$ and $D^0 \rightarrow \pi^+\pi^-$) has been superseded by the Dalitz plot analysis. The ADS observables are defined in analogy to Eqs. (7–9).
- $B^0 \rightarrow DK^+\pi^-$, $D \rightarrow h^+h^-$. Information from the GLW-Dalitz analysis of $B^0 \rightarrow DK^+\pi^-$, $D^0 \rightarrow h^+h^-$ decays [50] is added to the combination for the first time. The “Dalitz” label indicates the method used to determine information about CP violation in this mode. The variables, defined in analogy to Eqs. (11–12), are determined from a simultaneous Dalitz plot fit to $B^0 \rightarrow DK^+\pi^-$ with $D^0 \rightarrow K^-\pi^+$, $D \rightarrow K^+K^-$ and $D \rightarrow \pi^+\pi^-$ samples, as described in Refs. [20,21]. Note that the observables are those associated with the $DK^*(892)^0$ amplitudes. Constraints on hadronic parameters are also obtained in this analysis, as described in Sec. 3.
- $B^0 \rightarrow DK^{*0}$, $D \rightarrow K_s^0\pi^+\pi^-$. Inputs from the model-dependent GGSZ analysis of $B^0 \rightarrow DK^{*0}(892)$, $D \rightarrow K_s^0\pi^+\pi^-$ decays [51] are included in the combination for the first time. The observables, defined in analogy to Eqs. (11–12), are measured by fitting the $D \rightarrow K_s^0\pi^+\pi^-$ Dalitz plot using a model developed by the BaBar collaboration [56].

A model-independent GGSZ analysis [57] is also performed by LHCb on the same data sample. Currently, the model-dependent analysis has the best sensitivity to the parameters x_{\pm} and y_{\pm} . Therefore the model-dependent results are used in the combination. The numerical results of the combination change insignificantly if the model-independent results are used instead.

- $B_s^0 \rightarrow D_s^{\mp} K^{\pm}$. The inputs used from the time-dependent analysis of $B_s^0 \rightarrow D_s^{\mp} K^{\pm}$ decays using data corresponding to 1 fb^{-1} [52] are identical to those used in Ref. [28]. Note however that a different sign convention is used here, as defined in Eqs.(13–14) and Appendix A.10.

3 Auxiliary inputs

The external inputs are briefly described below and summarised in Table 2. These measurements provide constraints on unknown parameters and result in better precision on γ . The values and uncertainties of the observables are provided in Appendix D and the correlations are given in Appendix E.

- **Input from global fit to charm data.** The GLW/ADS measurements need input to constrain the charm system in three areas: the ratio and strong phase difference for $D^0 \rightarrow K^-\pi^+$ and $D^0 \rightarrow \pi^-K^+$ decays ($r_D^{K\pi}$, $\delta_D^{K\pi}$), charm mixing (x_D , y_D) and direct CP violation in $D^0 \rightarrow h^+h^-$ decays (A_{KK}^{dir} , $A_{\pi\pi}^{\text{dir}}$), taken from a recent HFAG charm fit [22]. These do not include the latest results on ΔA_{CP} from LHCb [42] but their impact has been checked and found to be negligible. The value of $\delta_D^{K\pi}$ is shifted by 180° compared to the HFAG result in order to match the phase convention adopted in this paper. The parameter $R_D^{K\pi}$ is related to the amplitude ratio $r_D^{K\pi}$ through $R_D^{K\pi} \equiv (r_D^{K\pi})^2$.

Table 2: List of the auxiliary inputs used in the combinations.

Decay	Parameters	Source	Ref.
$D^0-\bar{D}^0$ -mixing	x_D, y_D	HFAG	[22]
$D \rightarrow K^+\pi^-$	$r_D^{K\pi}, \delta_D^{K\pi}$	HFAG	[22]
$D \rightarrow h^+h^-$	$A_{KK}^{\text{dir}}, A_{\pi\pi}^{\text{dir}}$	HFAG	[22]
$D \rightarrow K^{\pm}\pi^{\mp}\pi^+\pi^-$	$\delta_D^{K3\pi}, \kappa_D^{K3\pi}, r_D^{K3\pi}$	CLEO+LHCb	[58]
$D \rightarrow \pi^+\pi^-\pi^+\pi^-$	$F_{\pi\pi\pi\pi}$	CLEO	[59]
$D \rightarrow K^{\pm}\pi^{\mp}\pi^0$	$\delta_D^{K2\pi}, \kappa_D^{K2\pi}, r_D^{K2\pi}$	CLEO+LHCb	[58]
$D \rightarrow h^+h^-\pi^0$	$F_{\pi\pi\pi^0}, F_{KK\pi^0}$	CLEO	[59]
$D \rightarrow K_S^0K^-\pi^+$	$\delta_D^{K_S K\pi}, \kappa_D^{K_S K\pi}, r_D^{K_S K\pi}$	CLEO	[60]
$D \rightarrow K_S^0K^-\pi^+$	$r_D^{K_S K\pi}$	LHCb	[61]
$B^0 \rightarrow DK^{*0}$	$\kappa_B^{DK^{*0}}, \bar{R}_B^{DK^{*0}}, \Delta\bar{\delta}_B^{DK^{*0}}$	LHCb	[50]
$B_s^0 \rightarrow D_s^{\mp}K^{\pm}$	ϕ_s	LHCb	[62]

- **Input for $D^0 \rightarrow K^\pm \pi^\mp \pi^0$ and $D^0 \rightarrow K^\pm \pi^\mp \pi^+ \pi^-$ decays.** The ADS measurements with $D^0 \rightarrow K^\pm \pi^\mp \pi^0$ and $D^0 \rightarrow K^\pm \pi^\mp \pi^+ \pi^-$ decays require knowledge of the hadronic parameters describing the D decays. These are the ratio, strong phase difference and coherence factors of the two decays: $r_D^{K2\pi}$, $\delta_D^{K2\pi}$, $\kappa_D^{K2\pi}$, $r_D^{K3\pi}$, $\delta_D^{K3\pi}$ and $\kappa_D^{K3\pi}$. Recently an analysis of $D^0 \rightarrow K^\pm \pi^\mp \pi^+ \pi^-$ decays has been performed by LHCb [63] that is sensitive to $r_D^{K3\pi}$, $\delta_D^{K3\pi}$ and $\kappa_D^{K3\pi}$. Furthermore, an updated measurement has been performed using CLEO-c data, and the results have been combined with those from LHCb [58] to yield constraints and correlations of the six parameters. These are included as Gaussian constraints in this combination, in line with the treatment of the other auxiliary inputs.
- **CP content of $D \rightarrow h^+ h^- \pi^0$ and $D \rightarrow \pi^+ \pi^- \pi^+ \pi^-$ decays.** For both the three-body $D \rightarrow h^+ h^- \pi^0$ and four-body $D \rightarrow \pi^+ \pi^- \pi^+ \pi^-$ quasi-GLW measurements the fractional CP -even content of the decays, $F_{KK\pi^0}$, $F_{\pi\pi\pi^0}$ and $F_{\pi\pi\pi\pi}$, are used as inputs. These parameters were measured by the CLEO collaboration [59]. The uncertainty for the CP -even content of $D \rightarrow \pi^+ \pi^- \pi^+ \pi^-$ decays is increased from ± 0.028 to ± 0.032 to account for the non-uniform acceptance of the LHCb detector following the recommendation in Ref. [44]. For the $D \rightarrow h^+ h^- \pi^0$ decay the LHCb efficiency is sufficiently uniform to avoid the need to increase the F_+ uncertainty for these modes.
- **Input for $D \rightarrow K_s^0 K^- \pi^+$ parameters.** The $B^+ \rightarrow DK^+$, $D \rightarrow K_s^0 K^- \pi^+$ GLS measurement needs inputs for the charm system parameters $r_D^{K_S K\pi}$, $\delta_D^{K_S K\pi}$, and $\kappa_D^{K_S K\pi}$. Constraints from Ref. [60] on all three are included, along with an additional constraint on the branching fraction ratio $R_D^{K_S K\pi}$ from Ref. [61]. The results corresponding to a limited region of the Dalitz plot, dominated by the $K^*(892)^+$ resonance, are used here. The quantity $R_D^{K_S K\pi}$ is related to $r_D^{K_S K\pi}$ through

$$R_D^{K_S K\pi} = \frac{(r_D^{K_S K\pi})^2 - \kappa_D^{K_S K\pi} r_D^{K_S K\pi} (y_D \cos \delta_D^{K_S K\pi} - x_D \sin \delta_D^{K_S K\pi})}{1 - r_D^{K_S K\pi} \kappa_D^{K_S K\pi} (y_D \cos \delta_D^{K_S K\pi} + x_D \sin \delta_D^{K_S K\pi})}. \quad (15)$$

The linear correlation coefficient between $\delta_D^{K_S K\pi}$ and $\kappa_D^{K_S K\pi}$ is extracted from the experimental likelihood as $\rho(\delta_D^{K_S K\pi}, \kappa_D^{K_S K\pi}) = -0.60$.

- **Constraints on the $B^0 \rightarrow DK^{*0}$ hadronic parameters.** The quasi-two-body $B^0 \rightarrow DK^{*0}$ ADS and model-dependent GGSZ measurements need input on the coherence factor $\kappa_B^{DK^{*0}}$ and the parameters $\bar{R}_B^{DK^{*0}} = \bar{r}_B^{DK^{*0}} / r_B^{DK^{*0}}$ and $\Delta \bar{\delta}_B^{DK^{*0}} = \bar{\delta}_B^{DK^{*0}} - \delta_B^{DK^{*0}}$, which relate the hadronic parameters of the quasi-two-body $B^0 \rightarrow DK^{*0}$ ADS and GGSZ measurements (barred symbols) to those of the $B^0 \rightarrow DK^+ \pi^-$ amplitude analysis (unbarred symbols). The resulting values are taken from the LHCb GLW-Dalitz analysis described in Ref. [50]. These are taken to be uncorrelated with each other and with the $x_\pm^{DK^{*0}}$, $y_\pm^{DK^{*0}}$ parameters that are determined from the same analysis.
- **Constraint on ϕ_s .** The time-dependent measurement of $B_s^0 \rightarrow D_s^\mp K^\pm$ determines the quantity $\gamma - 2\beta_s$. In order to interpret this as a measurement of γ , the weak phase $-2\beta_s \equiv \phi_s$ is constrained to the value measured by LHCb in $B_s^0 \rightarrow J/\psi hh$ decays [62]. It has been checked that using the world average instead has a negligible impact on the results.

4 Statistical treatment

The baseline results of the combinations are presented using a frequentist treatment, starting from a likelihood function built from the product of the probability density functions (PDFs), f_i , of experimental observables \vec{A}_i ,

$$\mathcal{L}(\vec{\alpha}) = \prod_i f_i(\vec{A}_i^{\text{obs}}|\vec{\alpha}), \quad (16)$$

where \vec{A}_i^{obs} are the measured values of the observables from an input analysis i , and $\vec{\alpha}$ is the set of parameters. For each of the inputs it is assumed that the observables follow a Gaussian distribution

$$f_i(\vec{A}_i^{\text{obs}}|\vec{\alpha}) \propto \exp\left(-\frac{1}{2}(\vec{A}_i(\vec{\alpha}) - \vec{A}_i^{\text{obs}})^T V_i^{-1} (\vec{A}_i(\vec{\alpha}) - \vec{A}_i^{\text{obs}})\right), \quad (17)$$

where V_i is the experimental covariance matrix, which includes statistical and systematic uncertainties and their correlations. Correlations in the systematic uncertainties between the statistically independent input measurements are assumed to be zero.

A χ^2 -function is defined as $\chi^2(\vec{\alpha}) = -2 \ln \mathcal{L}(\vec{\alpha})$. The best-fit point is given by the global minimum of the χ^2 -function, $\chi^2(\vec{\alpha}_{\text{min}})$. To evaluate the confidence level (CL) for a given value of a parameter, *e.g.* $\gamma = \gamma_0$ in the following, the value of the χ^2 -function at the new minimum is considered, $\chi^2(\vec{\alpha}'_{\text{min}}(\gamma_0))$. The associated profile likelihood function for the parameters is $\mathcal{L}(\vec{\alpha}'_{\text{min}}(\gamma_0))$. Then a test statistic is defined as $\Delta\chi^2 = \chi^2(\vec{\alpha}'_{\text{min}}) - \chi^2(\vec{\alpha}_{\text{min}})$. The p -value, or $1 - \text{CL}$, is calculated by means of a Monte Carlo procedure, described in Ref. [64] and briefly recapitulated here. For each value of γ_0 the test statistic $\Delta\chi^2$ is calculated, and a set of pseudoexperiments, \vec{A}_j , is generated according to Eq. (17) with parameters $\vec{\alpha}$ set to the values at $\vec{\alpha}'_{\text{min}}$. A new value of the test statistic, $\Delta\chi^{2'}$, is calculated for each pseudoexperiment by replacing $\vec{A}_{\text{obs}} \rightarrow \vec{A}_j$ and minimising with respect to $\vec{\alpha}$, once with γ as a free parameter, and once with γ fixed to γ_0 . The value of $1 - \text{CL}$ is then defined as the fraction of pseudoexperiments for which $\Delta\chi^2 < \Delta\chi^{2'}$. This method is sometimes referred to as the “ $\hat{\mu}$ ”, or the PLUGIN method. Its coverage cannot be guaranteed [64] for the full parameter space, but can be verified for the best-fit point. The reason is that for each value of γ_0 , the nuisance parameters, *i.e.* the components of $\vec{\alpha}$ other than the parameter of interest, are set to their best-fit values for this point, as opposed to computing an n -dimensional confidence region, which is computationally impractical. The coverage of the frequentist combinations is discussed in Sec. 5.3.

5 Results

Results for the DK combination are presented in Sec. 5.1 and for the Dh combination in Sec. 5.2. The coverage of the frequentist method is discussed in Sec. 5.3 whilst an interpretation of the results is provided in Sec. 5.4. The rate equations from which the observables are determined are invariant under the simultaneous transformation $\gamma \rightarrow \gamma + 180^\circ$, $\delta_B^X \rightarrow \delta_B^X + 180^\circ$, where δ_B^X is the strong phase for each $B \rightarrow DX$ decay considered. Only the solution most consistent with the determination of γ from the global CKM fit [26, 27] is shown.

5.1 DK combination

The DK combination consists of 71 observables and 32 parameters. The goodness of fit computed from the χ^2 value at the best fit point given the number of degrees of freedom is $p = 91.5\%$. The equivalent value calculated from the fraction of pseudoexperiments, generated from the best fit point, which have a χ^2 larger than that found in the data is $p = (90.5 \pm 0.2)\%$.

Table 3 summarises the resulting central values and confidence intervals that are obtained from five separate one-dimensional PLUGIN scans for the parameters: γ , r_B^{DK} , δ_B^{DK} , $r_B^{DK^{*0}}$ and $\delta_B^{DK^{*0}}$. These are shown in Fig. 1. Due to computational constraints the two-dimensional contours, shown in Fig. 2, are obtained via the profile likelihood method in which the value of the test statistic itself ($\Delta\chi^2$) is used. Except for the coverage, as described in Sec. 5.3, this is verified to be a good approximation of the PLUGIN method. The parameter correlations obtained from the profile likelihood method are given in Appendix F.1.

Table 3: Confidence intervals and central values for the parameters of interest in the frequentist DK combination.

Observable	Central value	68.3% Interval	95.5% Interval	99.7% Interval
γ ($^\circ$)	72.2	[64.9, 79.0]	[55.9, 85.2]	[43.7, 90.9]
r_B^{DK}	0.1019	[0.0963, 0.1075]	[0.0907, 0.1128]	[0.0849, 0.1182]
δ_B^{DK} ($^\circ$)	142.6	[136.0, 148.3]	[127.8, 153.6]	[116.2, 158.7]
$r_B^{DK^{*0}}$	0.218	[0.171, 0.263]	[0.118, 0.305]	[0.000, 0.348]
$\delta_B^{DK^{*0}}$ ($^\circ$)	189	[169, 212]	[148, 241]	[123, 283]

5.2 Dh combination

The Dh combination includes observables measured from $B^+ \rightarrow D\pi^+$ and $B^+ \rightarrow D\pi^+\pi^-\pi^+$ decays, in addition to those measured in the DK combination, for a total of 89 observables and 38 parameters. The goodness of fit calculated from the χ^2 is $p = 72.9\%$ and calculated from the pseudoexperiments is $p = (71.4 \pm 0.3)\%$.

Table 4 gives the results of the one-dimensional PLUGIN scans for γ , $r_B^{D\pi}$, $\delta_B^{D\pi}$, r_B^{DK} , δ_B^{DK} , $r_B^{DK^{*0}}$ and $\delta_B^{DK^{*0}}$. The scans are shown in Fig. 3. Two solutions are found, corresponding to $r_B^{D\pi}$ values of 0.027 and 0.0045 for the favoured and secondary solutions, respectively. Figure 3 shows that the secondary solution is suppressed by slightly more than 1σ . Consequently, the 1σ interval for γ is very narrow because the uncertainty scales inversely with the central value of $r_B^{D\pi}$. As with the DK combination, the two-dimensional scans are performed using the profile likelihood method and are shown in Fig. 4. The two solutions and the non-Gaussian contours are clearly visible. The parameter correlations obtained from the profile likelihood method for both solutions are given in Appendix F.2. The coverage for the Dh analysis is examined in Sec. 5.3, where it is found that the coverage is slightly low and then starts to degrade when the true value of $r_B^{D\pi}$ is less than 0.01, reaching a minimum around 0.006, before the behaviour of the DK combination is recovered at very low values.

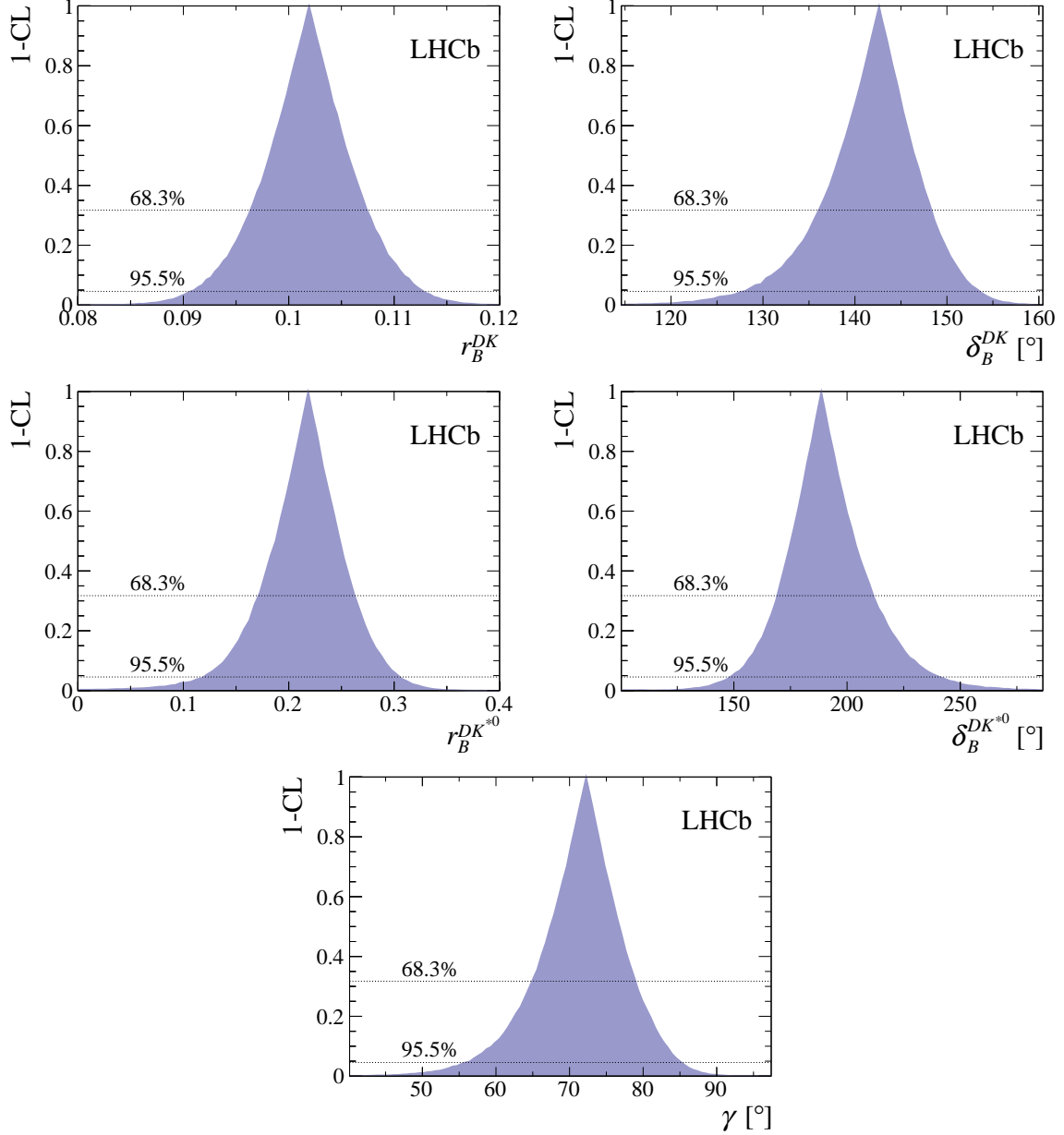


Figure 1: $1 - \text{CL}$ curves for the DK combination obtained with the `PLUGIN` method. The 1σ and 2σ levels are indicated by the horizontal dotted lines.

Recently, attempts have been made to estimate the value of $r_B^{D\pi}$ using the known branching fractions of $B^0 \rightarrow \bar{D}^0 K^0$ and $B^0 \rightarrow \bar{D}^0 \pi^0$ decays and $\text{SU}(3)$ symmetry [23], predicting a value of $r_B^{D\pi} = 0.0053 \pm 0.0007$, consistent with the secondary solution observed in the data. Using this as an additional external input in the Dh combination gives $\gamma = (71.8_{-8.6}^{+7.2})^\circ$, which shows that when $r_B^{D\pi}$ is small the uncertainties on γ are dominated by the $B \rightarrow DK$ inputs. This behaviour is similarly reflected by the 95.5% and 99.7% confidence intervals for the Dh combination when no external constraint on $r_B^{D\pi}$ is used. The goodness of fit calculated from the χ^2 is $p = 70.5\%$ and calculated from pseudoexperiments is $p = (69.7 \pm 0.6)\%$.

Given the poor expected additional sensitivity from the $B \rightarrow D\pi$ -like modes, coupled

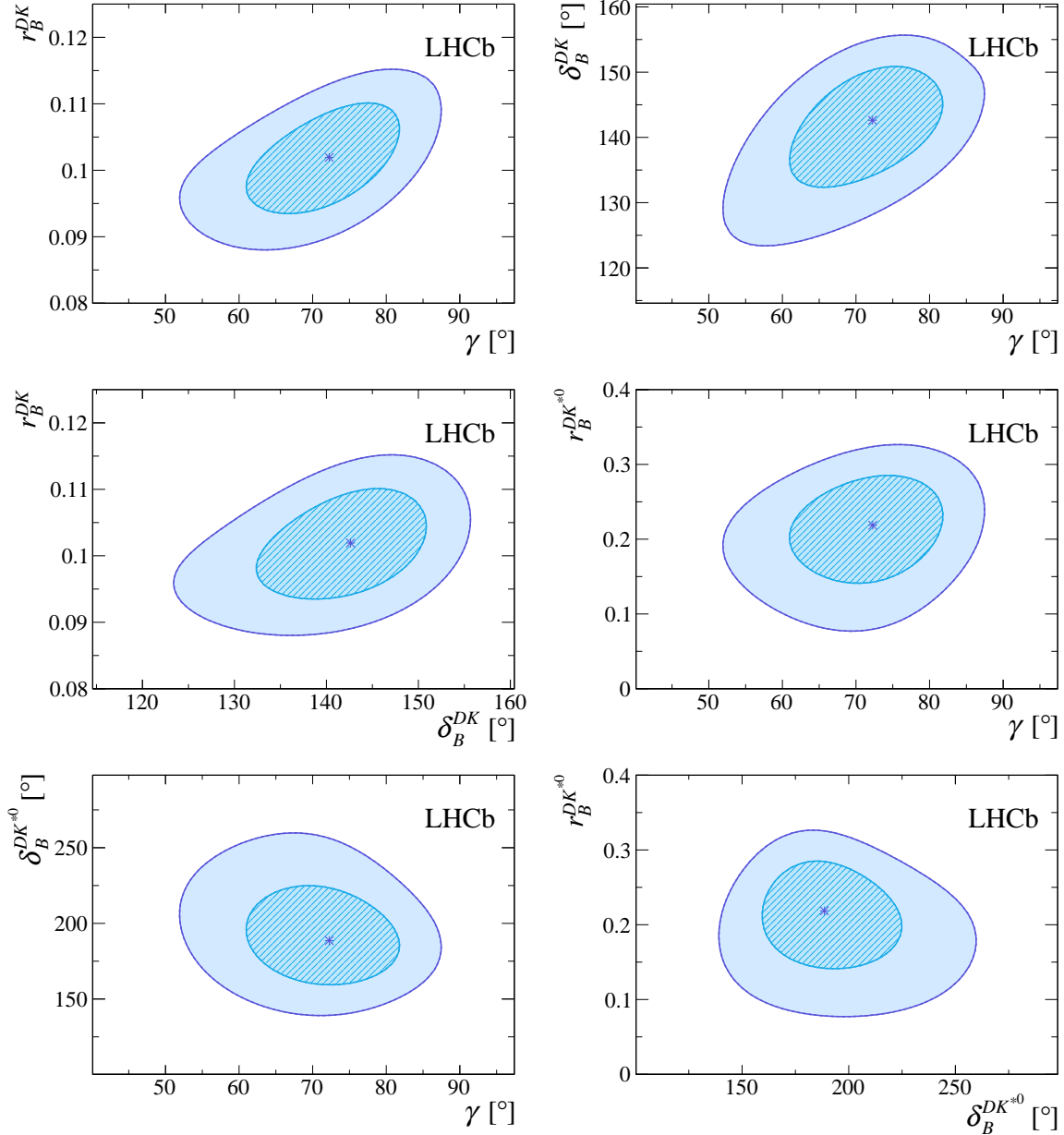


Figure 2: Profile likelihood contours from the DK combination. The contours show the two-dimensional 1σ and 2σ boundaries, corresponding to 68.3% and 95.5% CL, respectively.

with the highly non-Gaussian p -value distribution of the Dh combination, and the fact that the coverage of the Dh combination is low near the expected value of $r_B^{D\pi}$ (see Sec. 5.3), we choose to quote as the nominal result that of the DK combination, namely $\gamma = (72.2^{+6.8}_{-7.3})^\circ$.

5.3 Coverage of the frequentist method

The coverage of the PLUGIN (and the profile likelihood) method is tested by generating pseudoexperiments and evaluating the fraction for which the p -value is less than that obtained for the data. In general, the coverage depends on the point in parameter space.

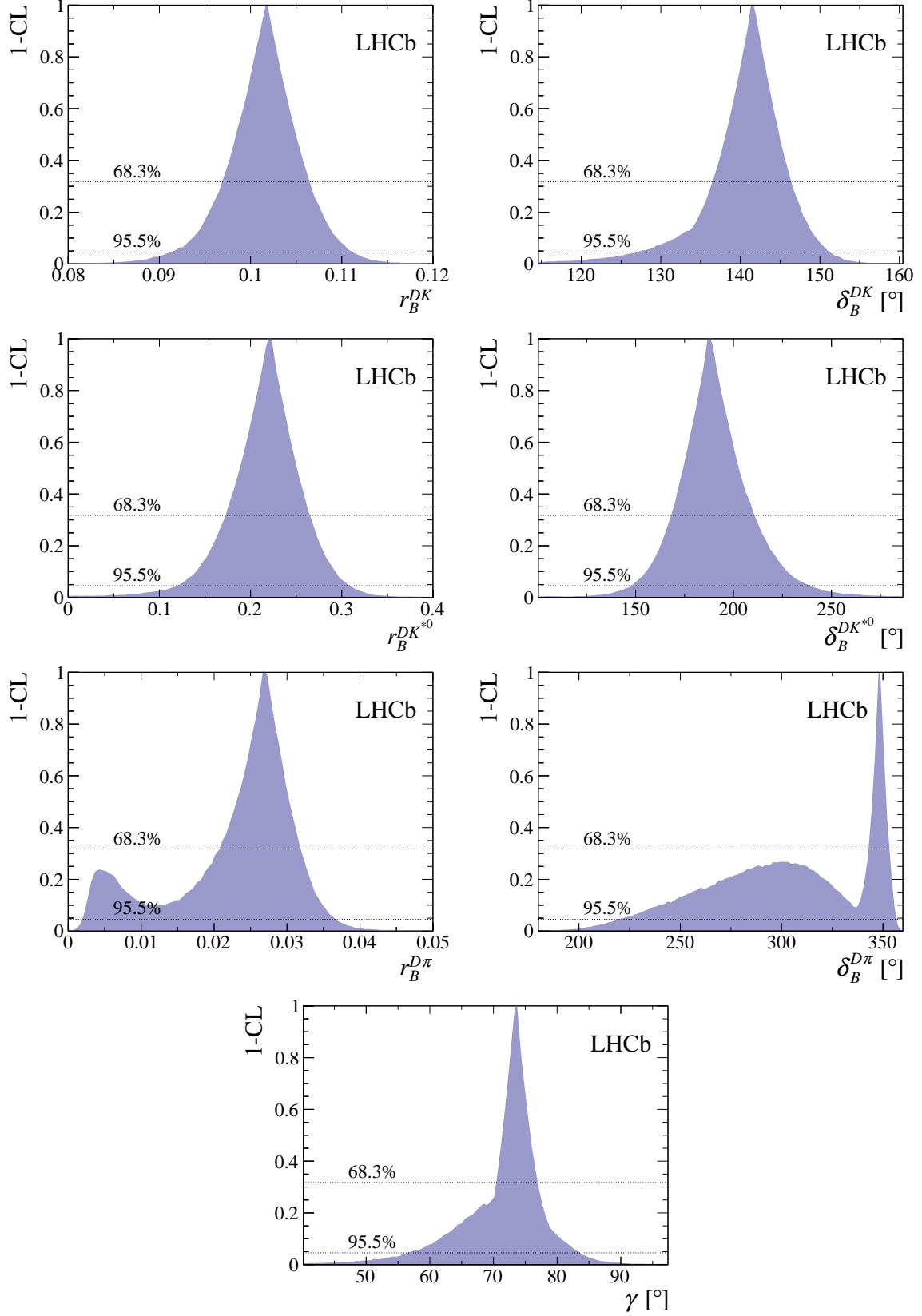


Figure 3: $1 - \text{CL}$ curves for the Dh combination obtained with the PLUGIN method. The 1σ and 2σ levels are indicated by the horizontal dotted lines.

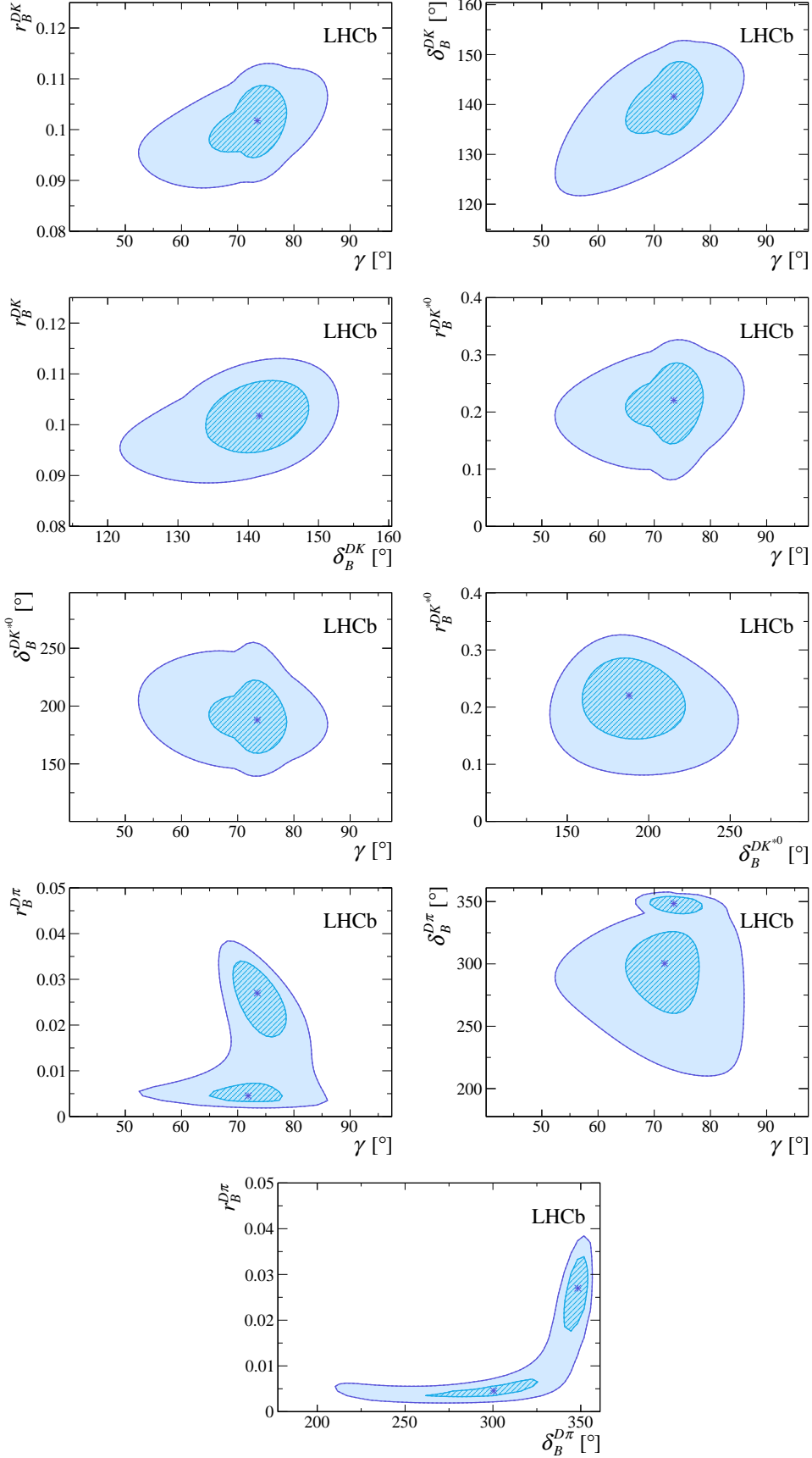


Figure 4: Profile likelihood contours from the Dh combination. The contours show the two-dimensional 1σ and 2σ boundaries, corresponding to 68.3% and 95.5% CL, respectively.

Table 4: Confidence intervals and central values for the parameters of interest in the frequentist Dh combination.

Observable	Central value	68.3% Interval	95.5% Interval	99.7% Interval
γ ($^\circ$)	73.5	[70.5, 76.8]	[56.7, 83.4]	[40.1, 90.8]
r_B^{DK}	0.1017	[0.0970, 0.1064]	[0.0914, 0.1110]	[0.0844, 0.1163]
δ_B^{DK} ($^\circ$)	141.6	[136.6, 146.3]	[127.2, 151.1]	[114.6, 155.7]
$r_B^{DK^{*0}}$	0.220	[0.173, 0.264]	[0.121, 0.307]	[0.000, 0.355]
$\delta_B^{DK^{*0}}$ ($^\circ$)	188	[168, 211]	[148, 239]	[120, 280]
$r_B^{D\pi}$	0.027	[0.0207, 0.0318]	[0.0020, 0.0365]	[0.0008, 0.0425]
$\delta_B^{D\pi}$ ($^\circ$)	348.3	[343.2, 352.9]	[220.5, 356.4]	[192.9, 359.8]

Table 5: Measured coverage α of the confidence intervals for γ , determined at the best fit points, for both the one-dimensional PLUGIN and profile likelihood methods. The nominal coverage is denoted as η .

	η [%]	α (profile likelihood) [%]	α (PLUGIN) [%]
DK	68.3	65.1 ± 0.7	67.1 ± 0.7
	95.5	93.5 ± 0.4	94.3 ± 0.3
	99.7	98.7 ± 0.2	98.8 ± 0.2
Dh	68.3	63.0 ± 0.7	64.3 ± 0.7
	95.5	90.9 ± 0.4	91.7 ± 0.4
	99.7	95.3 ± 0.3	95.6 ± 0.3

Following the procedure described in Ref. [30], the coverage of the profile likelihood and one-dimensional PLUGIN method intervals are tested. The coverage is determined for each method using the same pseudoexperiments; consequently their uncertainties are correlated. The results for the best fit points are shown in Table 5. Figure 5 shows the coverage of the 1σ intervals as determined from pseudoexperiments for the DK (Dh) combination as a function of the value of r_B^{DK} ($r_B^{D\pi}$) used to generate the pseudoexperiments. It can be seen that the coverage for the DK combination degrades as the true value of r_B^{DK} gets smaller. This behaviour has previously been observed by the CKMfitter group [26]. The fitted value found in this combination, $r_B^{DK} \approx 0.1$, is well within the regime of accurate coverage. The dependence of the coverage for the Dh combination on $r_B^{D\pi}$ shows similar behaviour, where the coverage begins to degrade when the true value reaches $r_B^{D\pi} < 0.01$, worsening until the true value of $r_B^{D\pi}$ becomes so small that the $D\pi$ modes offer no sensitivity and the behaviour seen in the DK combination is recovered. The fitted value of $r_B^{D\pi}$ in the Dh combination (~ 0.03) falls in the regime with good coverage, whilst the expected value, and indeed the value of the second minimum (~ 0.005), is in the regime in which the coverage starts to deteriorate. No correction for under-coverage is applied to the confidence intervals quoted in Tables 3 and 4.

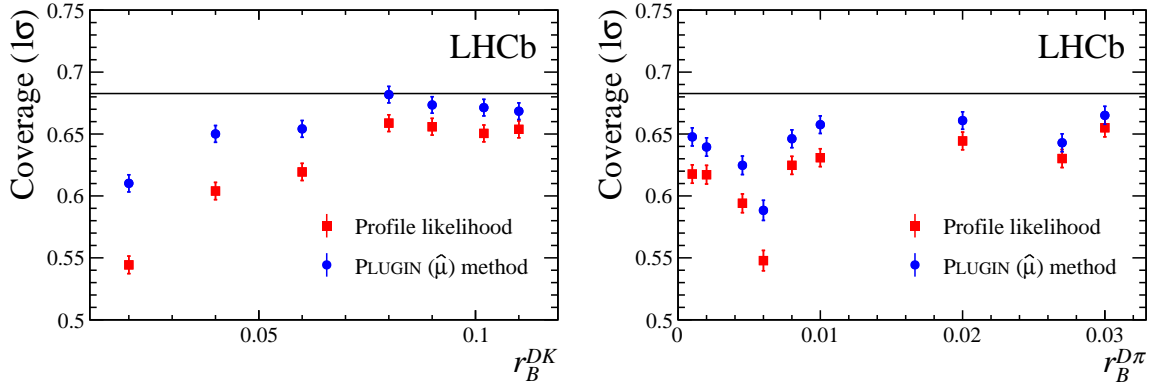


Figure 5: Dependence of the coverage for the one-dimensional PLUGIN method (blue circles) and the profile likelihood method (red squares) on r_B^{DK} for the DK combination (left) and on $r_B^{D\pi}$ for the Dh combination (right). The solid horizontal line shows the nominal coverage at 1σ of 68.3%.

5.4 Interpretation

Using the nominal DK combination and the simple profile likelihood method some further interpretation of the results is presented in this section. Performing the DK combination with statistical uncertainties only suggests that the systematic contribution to the uncertainty on γ is approximately 3° . Performing the combination without use of the external constraints (described in Sec. 3) roughly doubles the uncertainty on γ , demonstrating the value of including this information.

The origin of the sensitivity to γ of the various decay modes and analysis methods in the DK combination is demonstrated in Fig. 6. It can be seen that $B^+ \rightarrow DK^+$ decays offer the best sensitivity (see Fig. 6 left) and that the GLW/ADS methods offer multiple narrow solutions compared to the single broader solution of the GGSZ method (see Fig. 6 right). Figures 7 and 8 further demonstrate the complementarity of the input methods in the (γ vs. δ_B^X) and (γ vs. r_B^X) planes, for the B^+ and B^0 systems respectively.

6 Bayesian analysis

The combinations are also performed using a Bayesian procedure. Probability (or credible) intervals (or regions) are obtained according to a highest posterior density approach. A highest posterior density interval (region) is defined by the property that the minimum density of any point within the interval (region) is equal to, or larger than, the density of any point outside that interval (region).

6.1 DK combination

Uniform prior probability distributions (hereafter referred to as priors) are used for γ and the B -meson hadronic parameters in the DK combination, allowing them to vary inside the following ranges: $\gamma \in [0^\circ, 180^\circ]$, $\delta_B^{DK} \in [-180^\circ, 180^\circ]$, $r_B^{DK} \in [0.06, 0.14]$. The priors for $\delta_B^{DK\pi\pi}$ and $\delta_B^{D_s K}$ are identical to that for δ_B^{DK} ; the range for $\delta_B^{DK^*0}$ is $[0^\circ, 360^\circ]$. The allowed ranges for $r_B^{DK^*0}$, $r_B^{DK\pi\pi}$ and $r_B^{D_s K}$ are $[0, 0.45]$, $[0, 0.16]$ and $[0, 0.2]$. The remaining

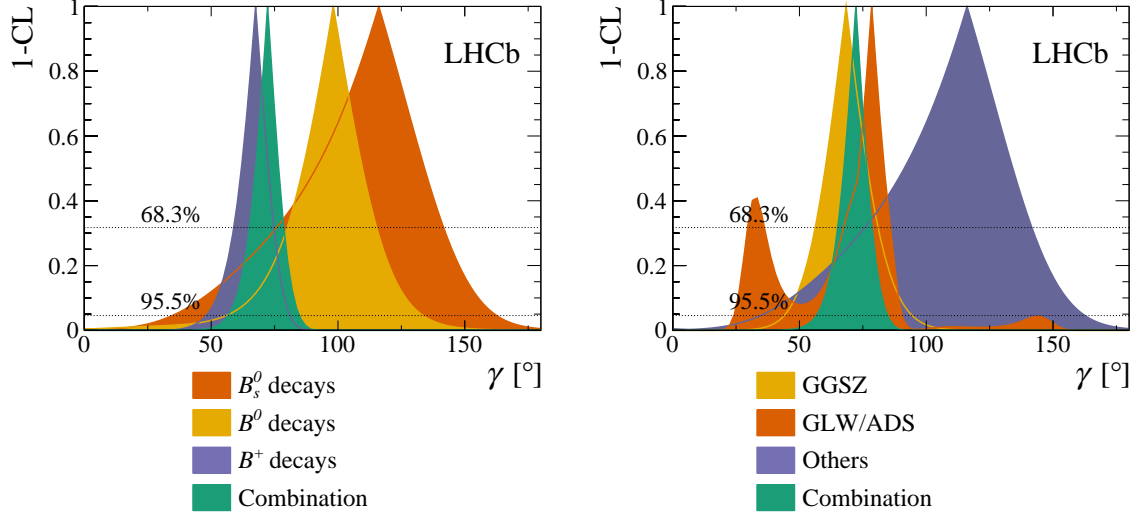


Figure 6: $1 - \text{CL}$ plots, using the profile likelihood method, for DK combinations split by the initial B meson flavour (left) and split by analysis method (right). Left: (orange) B_s^0 initial state, (yellow) B^0 initial states, (blue) B^+ initial states and (green) the full combination. Right: (yellow) GGSZ methods, (orange) GLW/ADS methods, (blue) other methods and (green) the full combination.

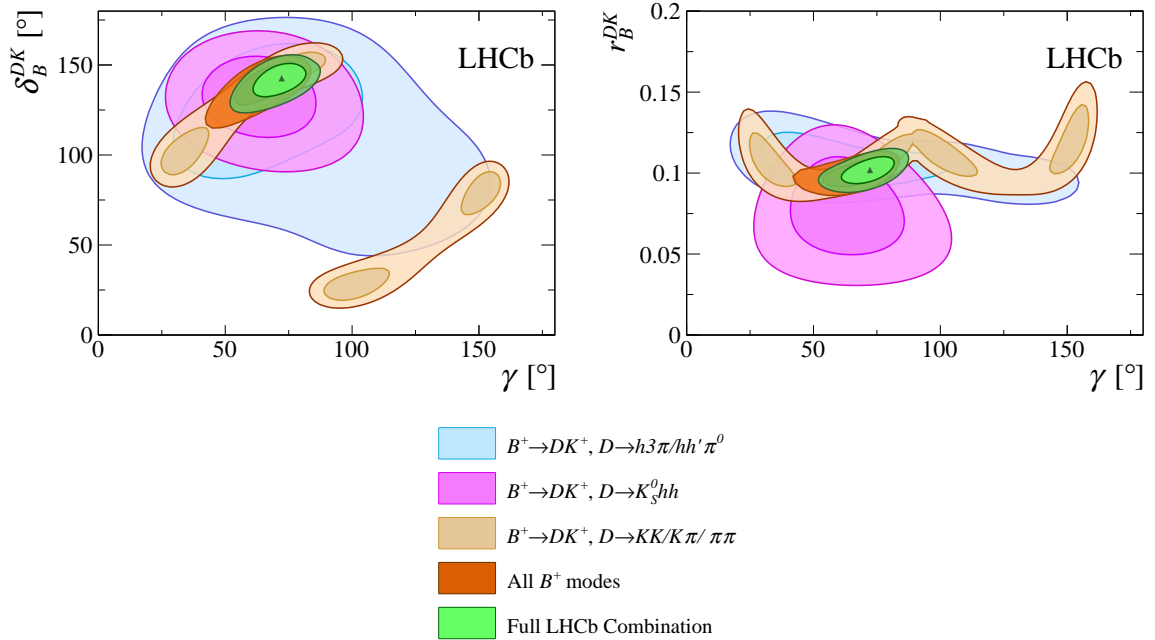


Figure 7: Profile likelihood contours of γ vs. δ_B^{DK} (left) and γ vs. r_B^{DK} (right) for various DK sub-combinations: (blue) $B^+ \rightarrow DK^+, D^0 \rightarrow h\pi\pi\pi/hh'\pi^0$, (pink) $B^+ \rightarrow DK^+, D^0 \rightarrow K_s^0 hh$, (light brown) $B^+ \rightarrow DK^+, D^0 \rightarrow KK/K\pi/\pi\pi$, (orange) all B^+ modes and (green) the full combination. Dark and light regions show the intervals containing 68.3% and 95.5% respectively.

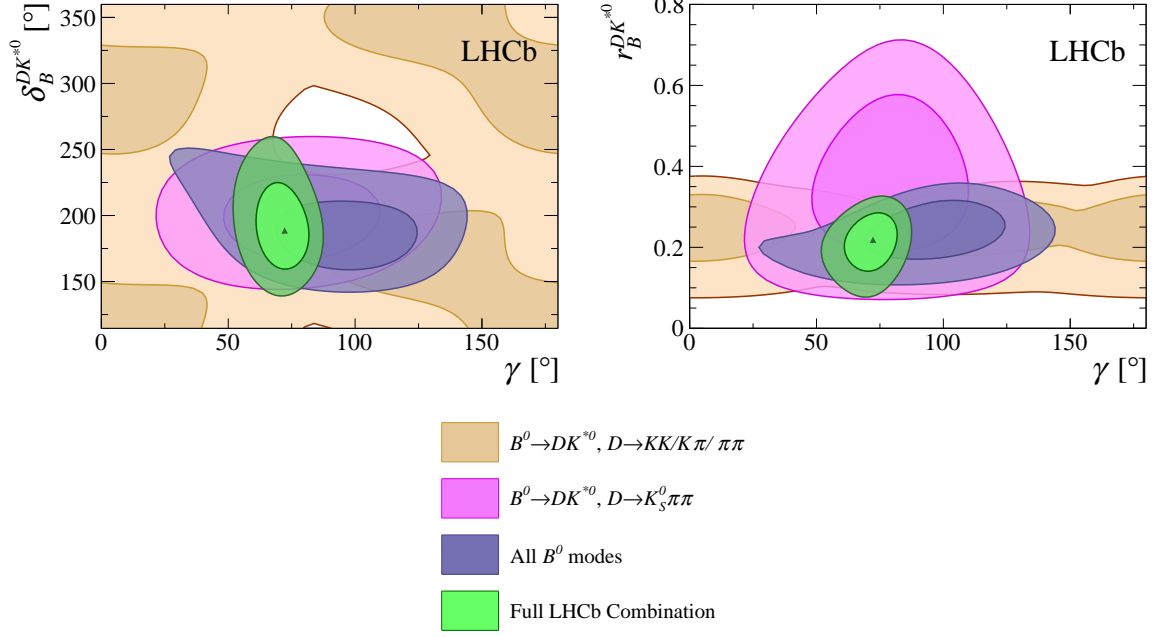


Figure 8: Profile likelihood contours of γ vs. $\delta_B^{DK^*0}$ (left) and γ vs. $r_B^{DK^*0}$ (right) for various DK sub-combinations: (brown) $B^0 \rightarrow DK^*0$, $D^0 \rightarrow KK/K\pi/\pi\pi$, (pink) $B^0 \rightarrow DK^*0$, $D^0 \rightarrow K_s^0\pi\pi$, (purple) all B^0 modes and (green) the full combination. Dark and light regions show the intervals containing 68.3% and 95.5% respectively.

auxiliary parameters are constrained with Gaussian priors according to the externally measured values and their uncertainties. A range of alternative prior distributions have been found to have negligible impact on the results for γ . The results are shown in Table 6 and in Figs. 9 and 10. The Bayesian credible intervals are found to be in good agreement with the frequentist confidence intervals.

Table 6: Credible intervals and most probable values for the hadronic parameters determined from the DK Bayesian combination.

Observable	Central value	68.3% Interval	95.5% Interval	99.7% Interval
γ ($^\circ$)	70.3	[62.4, 77.4]	[52.6, 83.5]	[42.1, 88.4]
r_B^{DK}	0.1012	[0.0954, 0.1064]	[0.0900, 0.1120]	[0.0846, 0.1171]
δ_B^{DK} ($^\circ$)	142.2	[134.7, 148.1]	[125.3, 153.7]	[113.2, 157.9]
$r_B^{DK^*0}$	0.204	[0.149, 0.253]	[0.073, 0.299]	[0.000, 0.322]
$\delta_B^{DK^*0}$ ($^\circ$)	190.3	[165.8, 218.4]	[139.5, 263.4]	[117.8, 292.4]

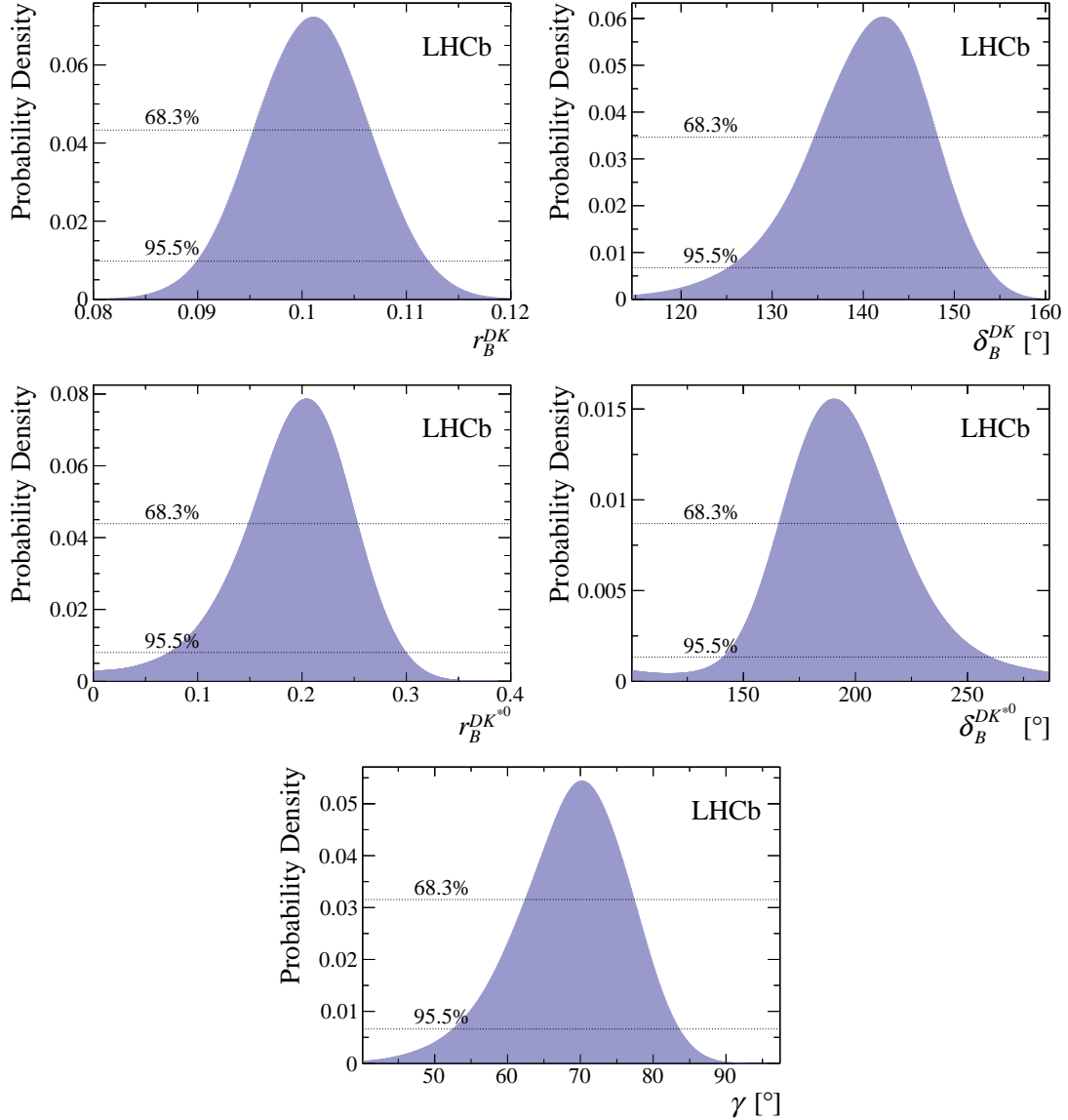


Figure 9: Posterior probability density from the Bayesian interpretation for the DK combination.

6.2 Dh combination

For the Dh combination additional uniform priors are introduced: $r_B^{D\pi} \in [0, 0.06]$, $\delta_B^{D\pi} \in [180^\circ, 360^\circ]$, $r_B^{D\pi\pi\pi} \in [0, 0.13]$ and $\delta_B^{D\pi\pi\pi} \in [0^\circ, 360^\circ]$. All other priors are as described above for the DK combination.

The results are given in Table 7 and shown in Figs. 11 and 12. Comparison with the frequentist treatment (Sec. 5.2) shows that the 1σ intervals and regions differ between the two treatments, but satisfactory agreement is recovered at 2σ . Such differences are not uncommon when comparing confidence and credible intervals or regions with low enough confidence level and probability, in the presence of a highly non-Gaussian likelihood function.

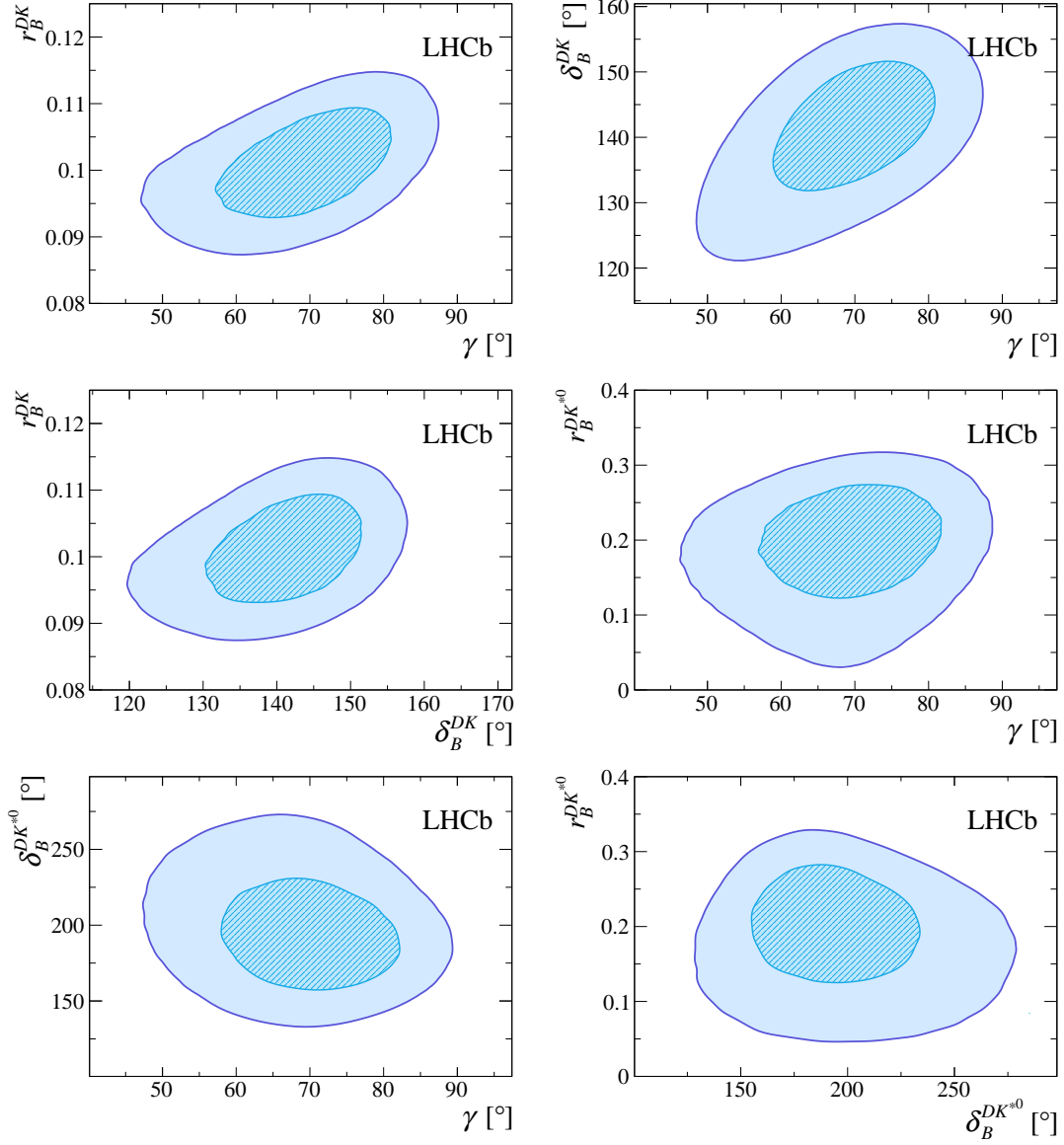


Figure 10: Two-dimensional posterior probability regions from the Bayesian interpretation for the DK combination. Light and dark regions show the 68.3% and 95.5% credible intervals respectively.

Table 7: Credible intervals and most probable values for the hadronic parameters determined from the Dh Bayesian combination.

Observable	Central value	68.3% Interval	95.5% Interval	99.7% Interval
γ ($^\circ$)	72.4	[63.9, 79.0]	[52.1, 84.6]	[40.1, 89.5]
r_B^{DK}	0.1003	[0.0948, 0.1057]	[0.0893, 0.1109]	[0.0838, 0.1159]
δ_B^{DK} ($^\circ$)	141.0	[133.3, 147.5]	[122.1, 153.1]	[108.6, 157.5]
$r_B^{DK^*0}$	0.2072	[0.1514, 0.2555]	[0.0788, 0.3007]	[0.0031, 0.3291]
$\delta_B^{DK^*0}$ ($^\circ$)	189.8	[166.3, 216.5]	[143.9, 255.2]	[120.2, 286.0]
$r_B^{D\pi}$	0.0043	[0.0027, 0.0063]	[0.0011, 0.0281]	[0.0008, 0.0329]
$\delta_B^{D\pi}$ ($^\circ$)	303.7	[264.7, 332.7]	[231.5, 355.2]	[202.7, 359.0]

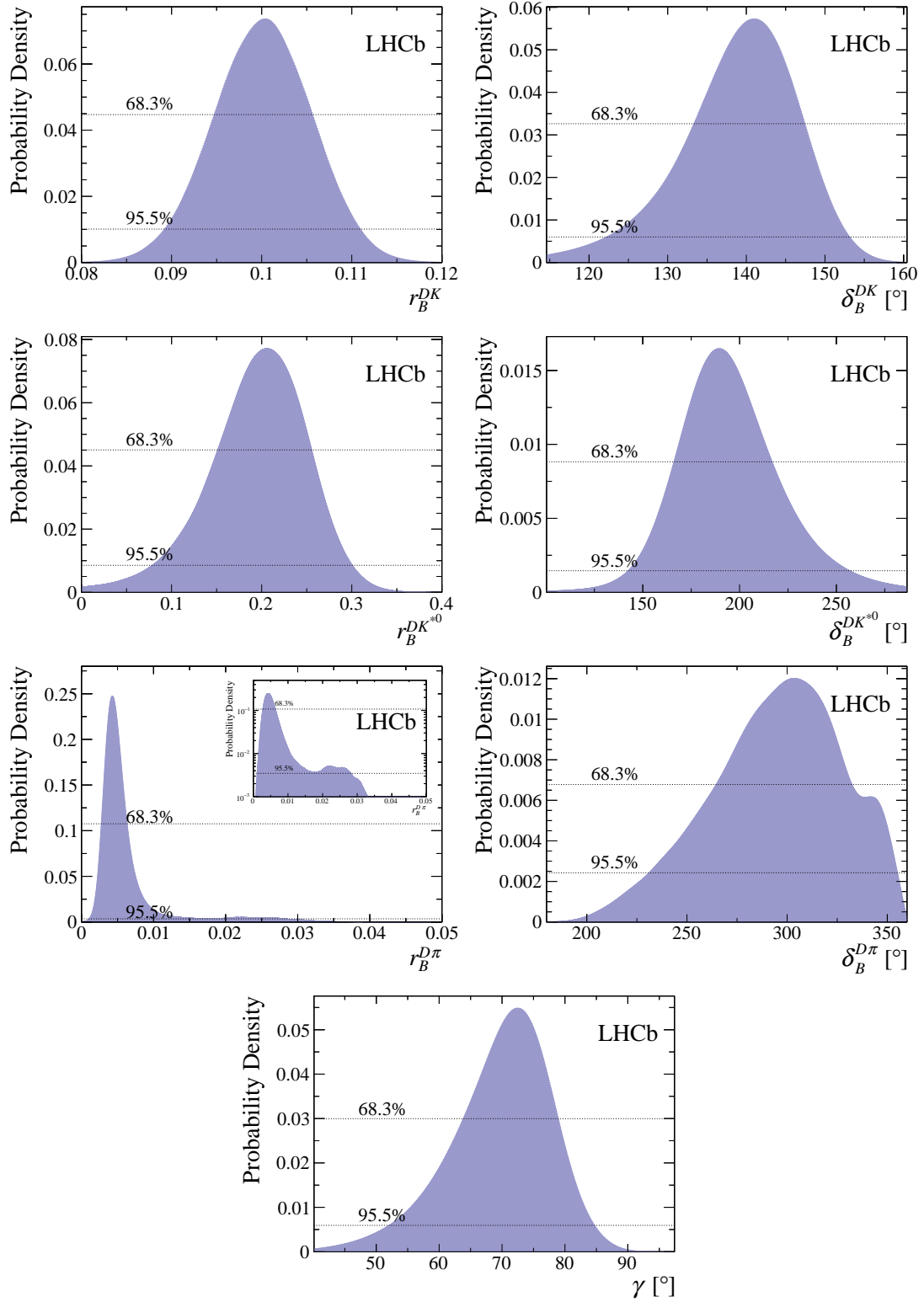


Figure 11: Posterior probability density from the Bayesian interpretation for the Dh combination. The inset for $r_B^{D\pi}$ shows the same distribution on a logarithmic scale.

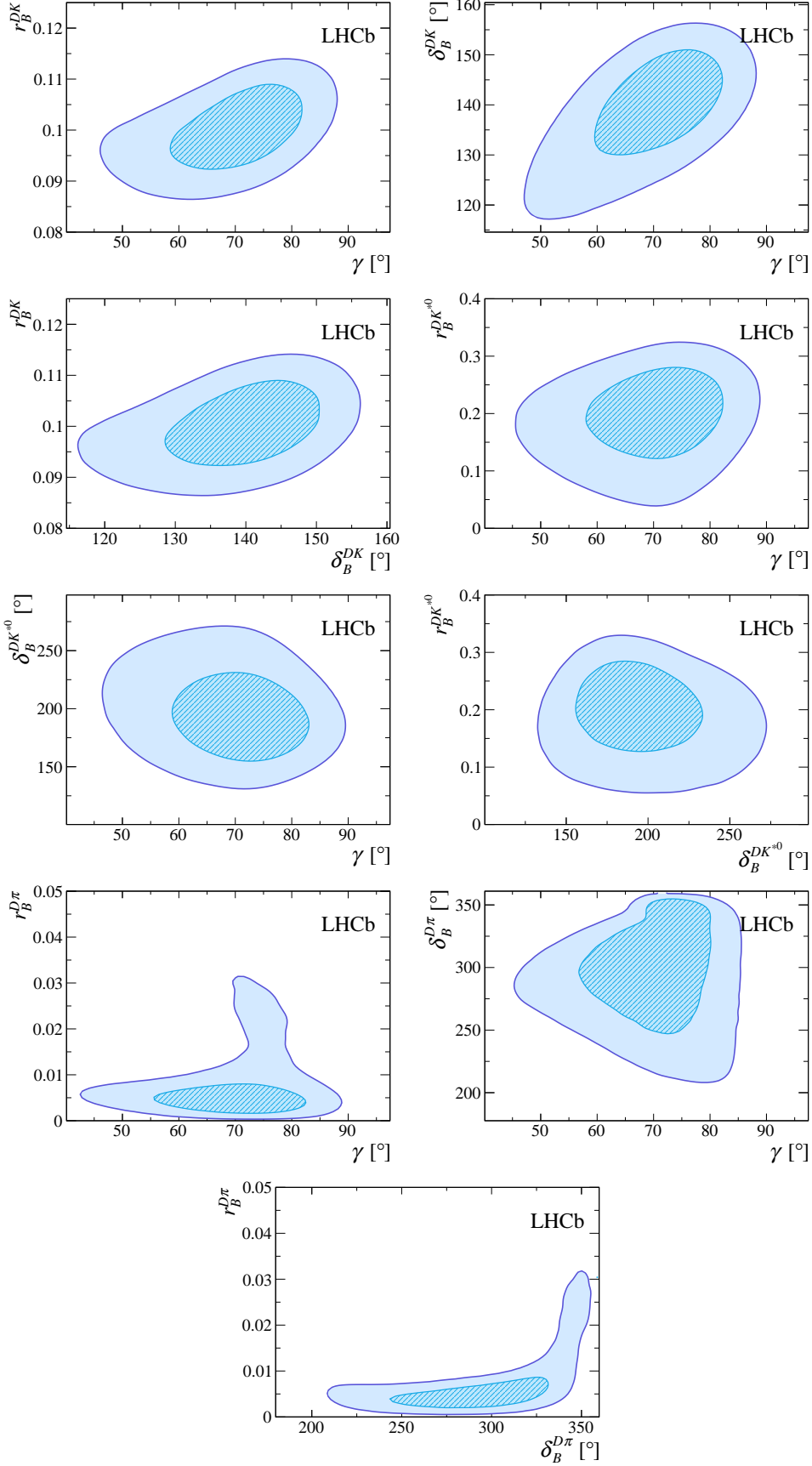


Figure 12: Two-dimensional posterior probability regions from the Bayesian interpretation for the Dh combination. Light and dark regions show the 68.3% and 95.5% credible intervals respectively.

7 Conclusion

Observables measured by LHCb that have sensitivity to the CKM angle γ , along with auxiliary information from other experiments, are combined to determine an improved constraint on γ . Combination of all $B \rightarrow DK$ -like modes results in a best fit value of $\gamma = 72.2^\circ$ and the confidence intervals

$$\begin{aligned}\gamma &\in [64.9, 79.0]^\circ \text{ at } 68.3\% \text{ CL}, \\ \gamma &\in [55.9, 85.2]^\circ \text{ at } 95.5\% \text{ CL}.\end{aligned}$$

A second combination is investigated with additional inputs from $B \rightarrow D\pi$ -like modes. The frequentist and Bayesian approaches are in agreement at the 2σ level, giving intervals of $\gamma \in [56.7, 83.4]^\circ$ and $\gamma \in [52.1, 84.6]^\circ$ at 95.5% CL, respectively.

Taking the best fit value and the 68.3% CL interval of the DK combination γ is found to be

$$\gamma = (72.2_{-7.3}^{+6.8})^\circ,$$

where the uncertainty includes both statistical and systematic effects. A Bayesian interpretation yields similar results, with credible intervals found to be consistent with the corresponding confidence intervals of the frequentist treatment. The result for γ is compatible with the world averages [26, 27] and the previous LHCb average, $\gamma = (73_{-10}^{+9})^\circ$ [28]. This combination has a significantly smaller uncertainty than the previous one and replaces it as the most precise determination of γ from a single experiment to date.

Additional inputs to the combinations in the future will add extra sensitivity, this includes use of new decay modes (such as $B^+ \rightarrow DK^{*+}$), updates of current measurements to the full Run I data sample (such as $B_s^0 \rightarrow D_s^\mp K^\pm$) and inclusion of the Run II data sample. Exploiting the full LHCb Run II data sample over the coming years is expected to reduce the uncertainty on γ to approximately 4° .

Acknowledgements

We would like to acknowledge the significant efforts of our late friend and colleague Moritz Karbach who invested considerable time and hard work into the studies presented in this paper. We express our gratitude to our colleagues in the CERN accelerator departments for the excellent performance of the LHC. We thank the technical and administrative staff at the LHCb institutes. We acknowledge support from CERN and from the national agencies: CAPES, CNPq, FAPERJ and FINEP (Brazil); NSFC (China); CNRS/IN2P3 (France); BMBF, DFG and MPG (Germany); INFN (Italy); FOM and NWO (The Netherlands); MNiSW and NCN (Poland); MEN/IFA (Romania); MinES and FASO (Russia); MinECo (Spain); SNSF and SER (Switzerland); NASU (Ukraine); STFC (United Kingdom); NSF (USA). We acknowledge the computing resources that are provided by CERN, IN2P3 (France), KIT and DESY (Germany), INFN (Italy), SURF (The Netherlands), PIC (Spain), GridPP (United Kingdom), RRCKI and Yandex LLC (Russia), CSCS (Switzerland), IFIN-HH (Romania), CBPF (Brazil), PL-GRID (Poland) and OSC (USA). We are indebted to the communities behind the multiple open source software packages on which we depend. Individual groups or members have received

support from AvH Foundation (Germany), EPLANET, Marie Skłodowska-Curie Actions and ERC (European Union), Conseil Général de Haute-Savoie, Labex ENIGMASS and OCEVU, Région Auvergne (France), RFBR and Yandex LLC (Russia), GVA, XuntaGal and GENCAT (Spain), Herchel Smith Fund, The Royal Society, Royal Commission for the Exhibition of 1851 and the Leverhulme Trust (United Kingdom).

Appendices

A Relationships between parameters and observables

The equations given in this section reflect the relationship between the experimental observables and the parameters of interest. For simplicity, the equations are given in the absence of $D^0-\bar{D}^0$ mixing. In order to include the small ($< 0.5^\circ$) effects from $D^0-\bar{D}^0$ mixing, the equations should be modified following the recommendation in Ref. [37], making use of the D^0 decay time acceptance coefficients, M_{xy} , given in Table 8.

Table 8: D^0 decay time acceptance coefficients (see Ref. [37]) for each analysis.

Analysis	M_{xy}
$D \rightarrow h^+h^-$ GLW/ADS	0.594
$D \rightarrow h^+h^-\pi^0$ GLW/ADS	0.592
$D \rightarrow h^+\pi^-\pi^+\pi^-$ GLW/ADS	0.570
$B^+ \rightarrow Dh^+\pi^-\pi^+$ GLW/ADS	0.6
$D \rightarrow K_s^0K^-\pi^+$ GLS	0.6
$B^0 \rightarrow DK^{*0}$ ADS	0.6

A.1 $B^+ \rightarrow Dh^+$, $D \rightarrow h^+h^-$ observables

$$A_{\text{ADS}}^{DK,\pi K} = \frac{2r_B^{DK}r_D^{K\pi} \sin(\delta_B^{DK} + \delta_D^{K\pi}) \sin \gamma}{(r_B^{DK})^2 + (r_D^{K\pi})^2 + 2r_B^{DK}r_D^{K\pi} \cos(\delta_B^{DK} + \delta_D^{K\pi}) \cos \gamma}$$

$$A_{\text{ADS}}^{D\pi,\pi K} = \frac{2r_B^{D\pi}r_D^{K\pi} \sin(\delta_B^{D\pi} + \delta_D^{K\pi}) \sin \gamma}{(r_B^{D\pi})^2 + (r_D^{K\pi})^2 + 2r_B^{D\pi}r_D^{K\pi} \cos(\delta_B^{D\pi} + \delta_D^{K\pi}) \cos \gamma}$$

$$A_{\text{CP}}^{DK, KK} = \frac{2r_B^{DK} \sin \delta_B^{DK} \sin \gamma}{1 + (r_B^{DK})^2 + 2r_B^{DK} \cos \delta_B^{DK} \cos \gamma} + A_{KK}^{\text{dir}}$$

$$A_{\text{CP}}^{DK,\pi\pi} = \frac{2r_B^{DK} \sin \delta_B^{DK} \sin \gamma}{1 + (r_B^{DK})^2 + 2r_B^{DK} \cos \delta_B^{DK} \cos \gamma} + A_{\pi\pi}^{\text{dir}}$$

$$A_{\text{CP}}^{D\pi, KK} = \frac{2r_B^{D\pi} \sin \delta_B^{D\pi} \sin \gamma}{1 + (r_B^{D\pi})^2 + 2r_B^{D\pi} \cos \delta_B^{D\pi} \cos \gamma} + A_{KK}^{\text{dir}}$$

$$\begin{aligned}
A_{CP}^{D\pi,\pi\pi} &= \frac{2r_B^{D\pi} \sin \delta_B^{D\pi} \sin \gamma}{1 + (r_B^{D\pi})^2 + 2r_B^{D\pi} \cos \delta_B^{D\pi} \cos \gamma} + A_{\pi\pi}^{\text{dir}} \\
A_{\text{fav}}^{DK,K\pi} &= \frac{2r_B^{DK} r_D^{K\pi} \sin (\delta_B^{DK} - \delta_D^{K\pi}) \sin \gamma}{1 + (r_B^{DK} r_D^{K\pi})^2 + 2r_B^{DK} r_D^{K\pi} \cos (\delta_B^{DK} - \delta_D^{K\pi}) \cos \gamma} \\
R_{\text{ADS}}^{DK,\pi K} &= \frac{(r_B^{DK})^2 + (r_D^{K\pi})^2 + 2r_B^{DK} r_D^{K\pi} \cos (\delta_B^{DK} + \delta_D^{K\pi}) \cos \gamma}{1 + (r_B^{DK} r_D^{K\pi})^2 + 2r_B^{DK} r_D^{K\pi} \cos (\delta_B^{DK} - \delta_D^{K\pi}) \cos \gamma} \\
R_{\text{ADS}}^{D\pi,\pi K} &= \frac{(r_B^{D\pi})^2 + (r_D^{K\pi})^2 + 2r_B^{D\pi} r_D^{K\pi} \cos (\delta_B^{D\pi} + \delta_D^{K\pi}) \cos \gamma}{1 + (r_B^{D\pi} r_D^{K\pi})^2 + 2r_B^{D\pi} r_D^{K\pi} \cos (\delta_B^{D\pi} - \delta_D^{K\pi}) \cos \gamma} \\
R_{K/\pi}^{K\pi} &= R \frac{1 + (r_B^{DK} r_D^{K\pi})^2 + 2r_B^{DK} r_D^{K\pi} \cos (\delta_B^{DK} - \delta_D^{K\pi}) \cos \gamma}{1 + (r_B^{D\pi} r_D^{K\pi})^2 + 2r_B^{D\pi} r_D^{K\pi} \cos (\delta_B^{D\pi} - \delta_D^{K\pi}) \cos \gamma} \\
R_{CP}^{KK} &= \frac{R_{K/\pi}^{KK}}{R_{K/\pi}^{K\pi}} = R \frac{1 + (r_B^{DK})^2 + 2r_B^{DK} \cos(\delta_B^{DK}) \cos(\gamma)}{1 + (r_B^{D\pi})^2 + 2r_B^{D\pi} \cos(\delta_B^{D\pi}) \cos(\gamma)} \\
R_{CP}^{\pi\pi} &= \frac{R_{K/\pi}^{\pi\pi}}{R_{K/\pi}^{K\pi}} = R \frac{1 + (r_B^{DK})^2 + 2r_B^{DK} \cos(\delta_B^{DK}) \cos(\gamma)}{1 + (r_B^{D\pi})^2 + 2r_B^{D\pi} \cos(\delta_B^{D\pi}) \cos(\gamma)}
\end{aligned}$$

A.2 $B^+ \rightarrow Dh^+, D \rightarrow h^+ \pi^- \pi^+ \pi^-$ observables

$$\begin{aligned}
A_{\text{ADS}}^{DK,\pi K\pi\pi} &= \frac{2\kappa_D^{K3\pi} r_B^{DK} r_D^{K3\pi} \sin (\delta_B^{DK} + \delta_D^{K3\pi}) \sin \gamma}{(r_B^{DK})^2 + (r_D^{K3\pi})^2 + 2\kappa_D^{K3\pi} r_B^{DK} r_D^{K3\pi} \cos (\delta_B^{DK} + \delta_D^{K3\pi}) \cos \gamma} \\
A_{\text{ADS}}^{D\pi,\pi K\pi\pi} &= \frac{2\kappa_D^{K3\pi} r_B^{D\pi} r_D^{K3\pi} \sin (\delta_B^{D\pi} + \delta_D^{K3\pi}) \sin \gamma}{(r_B^{D\pi})^2 + (r_D^{K3\pi})^2 + 2\kappa_D^{K3\pi} r_B^{D\pi} r_D^{K3\pi} \cos (\delta_B^{D\pi} + \delta_D^{K3\pi}) \cos \gamma} \\
A_{CP}^{DK,\pi\pi\pi\pi} &= \frac{2(2F_{\pi\pi\pi\pi} - 1)r_B^{DK} \sin \delta_B^{DK} \sin \gamma}{1 + (r_B^{DK})^2 + 2(2F_{\pi\pi\pi\pi} - 1)r_B^{DK} \cos \delta_B^{DK} \cos \gamma} \\
A_{CP}^{D\pi,\pi\pi\pi\pi} &= \frac{2(2F_{\pi\pi\pi\pi} - 1)r_B^{D\pi} \sin \delta_B^{D\pi} \sin \gamma}{1 + (r_B^{D\pi})^2 + 2(2F_{\pi\pi\pi\pi} - 1)r_B^{D\pi} \cos \delta_B^{D\pi} \cos \gamma} \\
A_{\text{fav}}^{DK,\pi K\pi\pi} &= \frac{2\kappa_D^{K3\pi} r_B^{DK} r_D^{K3\pi} \sin (\delta_B^{DK} - \delta_D^{K3\pi}) \sin \gamma}{1 + (r_B^{DK} r_D^{K3\pi})^2 + 2\kappa_D^{K3\pi} r_B^{DK} r_D^{K3\pi} \cos (\delta_B^{DK} - \delta_D^{K3\pi}) \cos \gamma}
\end{aligned}$$

$$R_{\text{ADS}}^{DK,\pi K\pi\pi} = \frac{(r_B^{DK})^2 + (r_D^{K3\pi})^2 + 2\kappa_D^{K3\pi} r_B^{DK} r_D^{K3\pi} \cos(\delta_B^{DK} + \delta_D^{K3\pi}) \cos \gamma}{1 + (r_B^{DK} r_D^{K3\pi})^2 + 2\kappa_D^{K3\pi} r_B^{DK} r_D^{K3\pi} \cos(\delta_B^{DK} - \delta_D^{K3\pi}) \cos \gamma}$$

$$R_{\text{ADS}}^{D\pi,\pi K\pi\pi} = \frac{(r_B^{D\pi})^2 + (r_D^{K3\pi})^2 + 2\kappa_D^{K3\pi} r_B^{D\pi} r_D^{K3\pi} \cos(\delta_B^{D\pi} + \delta_D^{K3\pi}) \cos \gamma}{1 + (r_B^{D\pi} r_D^{K3\pi})^2 + 2\kappa_D^{K3\pi} r_B^{D\pi} r_D^{K3\pi} \cos(\delta_B^{D\pi} - \delta_D^{K3\pi}) \cos \gamma}$$

$$R_{K/\pi}^{K\pi\pi\pi} = R \frac{1 + (r_B^{DK} r_D^{K3\pi})^2 + 2\kappa_D^{K3\pi} r_B^{DK} r_D^{K3\pi} \cos(\delta_B^{DK} - \delta_D^{K3\pi}) \cos \gamma}{1 + (r_B^{D\pi} r_D^{K3\pi})^2 + 2\kappa_D^{K3\pi} r_B^{D\pi} r_D^{K3\pi} \cos(\delta_B^{D\pi} - \delta_D^{K3\pi}) \cos \gamma}$$

$$R_{CP}^{\pi\pi\pi\pi} = \frac{R_{K/\pi}^{4\pi}}{R_{K/\pi}^{K\pi\pi\pi}} = R \frac{1 + (r_B^{DK})^2 + 2r_B^{DK} (2F_{\pi\pi\pi\pi} - 1) \cos(\delta_B^{DK}) \cos(\gamma)}{1 + (r_B^{D\pi})^2 + 2r_B^{D\pi} (2F_{\pi\pi\pi\pi} - 1) \cos(\delta_B^{D\pi}) \cos(\gamma)}$$

A.3 $B^+ \rightarrow Dh^+, D \rightarrow h^+h^-\pi^0$ observables

$$A_{\text{ADS}}^{DK,\pi K\pi^0} = \frac{2\kappa_D^{K2\pi} r_B^{DK} r_D^{K2\pi} \sin(\delta_B^{DK} + \delta_D^{K2\pi}) \sin \gamma}{(r_B^{DK})^2 + (r_D^{K2\pi})^2 + 2\kappa_D^{K2\pi} r_B^{DK} r_D^{K2\pi} \cos(\delta_B^{DK} + \delta_D^{K2\pi}) \cos \gamma}$$

$$A_{\text{ADS}}^{D\pi,\pi K\pi^0} = \frac{2\kappa_D^{K2\pi} r_B^{D\pi} r_D^{K2\pi} \sin(\delta_B^{D\pi} + \delta_D^{K2\pi}) \sin \gamma}{(r_B^{D\pi})^2 + (r_D^{K2\pi})^2 + 2\kappa_D^{K2\pi} r_B^{D\pi} r_D^{K2\pi} \cos(\delta_B^{D\pi} + \delta_D^{K2\pi}) \cos \gamma}$$

$$A_{CP}^{DK,KK\pi^0} = \frac{2(2F_{KK\pi^0} - 1)r_B^{DK} \sin \delta_B^{DK} \sin \gamma}{1 + (r_B^{DK})^2 + 2(2F_{KK\pi^0} - 1)r_B^{DK} \cos \delta_B^{DK} \cos \gamma}$$

$$A_{CP}^{DK,\pi\pi\pi^0} = \frac{2(2F_{\pi\pi\pi^0} - 1)r_B^{DK} \sin \delta_B^{DK} \sin \gamma}{1 + (r_B^{DK})^2 + 2(2F_{\pi\pi\pi^0} - 1)r_B^{DK} \cos \delta_B^{DK} \cos \gamma}$$

$$A_{CP}^{D\pi,KK\pi^0} = \frac{2(2F_{KK\pi^0} - 1)r_B^{D\pi} \sin \delta_B^{D\pi} \sin \gamma}{1 + (r_B^{D\pi})^2 + 2(2F_{KK\pi^0} - 1)r_B^{D\pi} \cos \delta_B^{D\pi} \cos \gamma}$$

$$A_{CP}^{D\pi,\pi\pi\pi^0} = \frac{2(2F_{\pi\pi\pi^0} - 1)r_B^{D\pi} \sin \delta_B^{D\pi} \sin \gamma}{1 + (r_B^{D\pi})^2 + 2(2F_{\pi\pi\pi^0} - 1)r_B^{D\pi} \cos \delta_B^{D\pi} \cos \gamma}$$

$$A_{\text{fav}}^{DK,K\pi\pi^0} = \frac{2\kappa_D^{K2\pi} r_B^{DK} r_D^{K2\pi} \sin(\delta_B^{DK} - \delta_D^{K2\pi}) \sin \gamma}{1 + (r_B^{DK} r_D^{K2\pi})^2 + 2\kappa_D^{K2\pi} r_B^{DK} r_D^{K2\pi} \cos(\delta_B^{DK} - \delta_D^{K2\pi}) \cos \gamma}$$

$$R_{\text{ADS}}^{DK,\pi K\pi^0} = \frac{(r_B^{DK})^2 + (r_D^{K2\pi})^2 + 2\kappa_D^{K2\pi} r_B^{DK} r_D^{K2\pi} \cos(\delta_B^{DK} + \delta_D^{K2\pi}) \cos \gamma}{1 + (r_B^{DK} r_D^{K2\pi})^2 + 2\kappa_D^{K2\pi} r_B^{DK} r_D^{K2\pi} \cos(\delta_B^{DK} - \delta_D^{K2\pi}) \cos \gamma}$$

$$\begin{aligned}
R_{\text{ADS}}^{D\pi, \pi K \pi^0} &= \frac{(r_B^{D\pi})^2 + (r_D^{K2\pi})^2 + 2\kappa_D^{K2\pi} r_B^{D\pi} r_D^{K2\pi} \cos(\delta_B^{D\pi} + \delta_D^{K2\pi}) \cos \gamma}{1 + (r_B^{D\pi} r_D^{K2\pi})^2 + 2\kappa_D^{K2\pi} r_B^{D\pi} r_D^{K2\pi} \cos(\delta_B^{D\pi} - \delta_D^{K2\pi}) \cos \gamma} \\
R_{\text{CP}}^{KK\pi^0} &= \frac{R_{K/\pi}^{KK\pi^0}}{R_{K/\pi}^{K\pi\pi^0}} = R \frac{1 + (r_B^{DK})^2 + 2r_B^{DK} (2F_{KK\pi^0} - 1) \cos(\delta_B^{DK}) \cos(\gamma)}{1 + (r_B^{D\pi})^2 + 2r_B^{D\pi} (2F_{KK\pi^0} - 1) \cos(\delta_B^{D\pi}) \cos(\gamma)} \\
R_{\text{CP}}^{\pi\pi\pi^0} &= \frac{R_{K/\pi}^{\pi\pi\pi^0}}{R_{K/\pi}^{K\pi\pi^0}} = R \frac{1 + (r_B^{DK})^2 + 2r_B^{DK} (2F_{\pi\pi\pi^0} - 1) \cos(\delta_B^{DK}) \cos(\gamma)}{1 + (r_B^{D\pi})^2 + 2r_B^{D\pi} (2F_{\pi\pi\pi^0} - 1) \cos(\delta_B^{D\pi}) \cos(\gamma)}
\end{aligned}$$

A.4 $B^+ \rightarrow DK^+, D \rightarrow K_s^0 h^+ h^-$ observables

$$\begin{aligned}
x_- &= r_B^{DK} \cos(\delta_B^{DK} - \gamma) \\
y_- &= r_B^{DK} \sin(\delta_B^{DK} - \gamma) \\
x_+ &= r_B^{DK} \cos(\delta_B^{DK} + \gamma) \\
y_+ &= r_B^{DK} \sin(\delta_B^{DK} + \gamma)
\end{aligned}$$

A.5 $B^+ \rightarrow Dh^+, D \rightarrow K_s^0 K^- \pi^+$ observables

$$\begin{aligned}
R_{\text{ADS}}^{DK, K_s K \pi} &= \frac{1 + (r_B^{DK})^2 (r_D^{K_s K \pi})^2 + 2\kappa_D^{K_s K \pi} r_B^{DK} r_D^{K_s K \pi} \cos(\delta_B^{DK} - \delta_D^{K_s K \pi}) \cos \gamma}{(r_B^{DK})^2 + (r_D^{K_s K \pi})^2 + 2\kappa_D^{K_s K \pi} r_B^{DK} r_D^{K_s K \pi} \cos(\delta_B^{DK} + \delta_D^{K_s K \pi}) \cos \gamma} \\
A_{\text{fav}}^{DK, K_s K \pi} &= \frac{2\kappa_D^{K3\pi} r_B^{DK} r_D^{K3\pi} \sin(\delta_B^{DK} - \delta_D^{K3\pi}) \sin \gamma}{1 + (r_B^{DK})^2 (r_D^{K3\pi})^2 + 2\kappa_D^{K3\pi} r_B^{DK} r_D^{K3\pi} \cos(\delta_B^{DK} - \delta_D^{K3\pi}) \cos \gamma} \\
A_{\text{ADS}}^{DK, K_s K \pi} &= \frac{2\kappa_D^{K3\pi} r_B^{DK} r_D^{K3\pi} \sin(\delta_B^{DK} + \delta_D^{K3\pi}) \sin \gamma}{(r_B^{DK})^2 + (r_D^{K_s K \pi})^2 + 2\kappa_D^{K_s K \pi} r_B^{DK} r_D^{K_s K \pi} \cos(\delta_B^{DK} + \delta_D^{K_s K \pi}) \cos \gamma}
\end{aligned}$$

A.6 $B^+ \rightarrow Dh^+ \pi^- \pi^+, D \rightarrow h^+ h^-$ observables

$$\begin{aligned}
R_{\text{CP}}^{DK\pi\pi} &= 1 + (r_B^{DK\pi\pi})^2 + 2\kappa_B^{DK\pi\pi} r_B^{DK\pi\pi} \cos \delta_B^{DK\pi\pi} \cos \gamma, \\
A_{\text{fav}}^{DK\pi\pi, K\pi} &= \frac{2\kappa_B^{DK\pi\pi} r_B^{DK\pi\pi} r_D^{K\pi} \sin(\delta_B^{DK\pi\pi} - \delta_D^{K\pi}) \sin \gamma}{1 + (r_B^{DK\pi\pi})^2 (r_D^{K\pi})^2 + 2\kappa_B^{DK\pi\pi} r_B^{DK\pi\pi} r_D^{K\pi} \cos(\delta_B^{DK\pi\pi} - \delta_D^{K\pi}) \cos \gamma} \\
A_{\text{fav}}^{D\pi\pi\pi, K\pi} &= \frac{2\kappa_B^{D\pi\pi\pi} r_B^{D\pi\pi\pi} r_D^{K\pi} \sin(\delta_B^{D\pi\pi\pi} - \delta_D^{K\pi}) \sin \gamma}{1 + (r_B^{D\pi\pi\pi})^2 (r_D^{K\pi})^2 + 2\kappa_B^{D\pi\pi\pi} r_B^{D\pi\pi\pi} r_D^{K\pi} \cos(\delta_B^{D\pi\pi\pi} - \delta_D^{K\pi}) \cos \gamma}
\end{aligned}$$

$$A_{CP}^{DK\pi\pi, KK} = \frac{2\kappa_B^{DK\pi\pi} r_B^{DK\pi\pi} \sin \delta_B^{DK\pi\pi} \sin \gamma}{1 + (r_B^{DK\pi\pi})^2 + 2\kappa_B^{DK\pi\pi} r_B^{DK\pi\pi} \cos \delta_B^{DK\pi\pi} \cos \gamma} + A_{KK}^{\text{dir}}$$

$$A_{CP}^{DK\pi\pi, \pi\pi} = \frac{2\kappa_B^{DK\pi\pi} r_B^{DK\pi\pi} \sin \delta_B^{DK\pi\pi} \sin \gamma}{1 + (r_B^{DK\pi\pi})^2 + 2\kappa_B^{DK\pi\pi} r_B^{DK\pi\pi} \cos \delta_B^{DK\pi\pi} \cos \gamma} + A_{\pi\pi}^{\text{dir}}$$

$$A_{CP}^{D\pi\pi\pi, KK} = \frac{2\kappa_B^{D\pi\pi\pi} r_B^{D\pi\pi\pi} \sin \delta_B^{D\pi\pi\pi} \sin \gamma}{1 + (r_B^{D\pi\pi\pi})^2 + 2\kappa_B^{D\pi\pi\pi} r_B^{D\pi\pi\pi} \cos \delta_B^{D\pi\pi\pi} \cos \gamma} + A_{KK}^{\text{dir}}$$

$$A_{CP}^{D\pi\pi\pi, \pi\pi} = \frac{2\kappa_B^{DK\pi\pi} r_B^{DK\pi\pi} \sin \delta_B^{DK\pi\pi} \sin \gamma}{1 + (r_B^{DK\pi\pi})^2 + 2\kappa_B^{DK\pi\pi} r_B^{DK\pi\pi} \cos \delta_B^{DK\pi\pi} \cos \gamma} + A_{\pi\pi}^{\text{dir}}$$

$$R_+^{DK\pi\pi, K\pi} = \frac{(r_B^{DK\pi\pi})^2 + (r_D^{K\pi})^2 + 2\kappa_B^{DK\pi\pi} r_B^{DK\pi\pi} r_D^{K\pi} \cos(\delta_B^{DK\pi\pi} + \delta_D^{K\pi} + \gamma)}{1 + (r_B^{DK\pi\pi})^2 (r_D^{K\pi})^2 + 2\kappa_B^{DK\pi\pi} r_B^{DK\pi\pi} r_D^{K\pi} \cos(\delta_B^{DK\pi\pi} - \delta_D^{K\pi} + \gamma)}$$

$$R_-^{DK\pi\pi, K\pi} = \frac{(r_B^{DK\pi\pi})^2 + (r_D^{K\pi})^2 + 2\kappa_B^{DK\pi\pi} r_B^{DK\pi\pi} r_D^{K\pi} \cos(\delta_B^{DK\pi\pi} + \delta_D^{K\pi} - \gamma)}{1 + (r_B^{DK\pi\pi})^2 (r_D^{K\pi})^2 + 2\kappa_B^{DK\pi\pi} r_B^{DK\pi\pi} r_D^{K\pi} \cos(\delta_B^{DK\pi\pi} - \delta_D^{K\pi} - \gamma)}$$

$$R_+^{D\pi\pi\pi, K\pi} = \frac{(r_B^{D\pi\pi\pi})^2 + (r_D^{K\pi})^2 + 2\kappa_B^{D\pi\pi\pi} r_B^{D\pi\pi\pi} r_D^{K\pi} \cos(\delta_B^{D\pi\pi\pi} + \delta_D^{K\pi} + \gamma)}{1 + (r_B^{D\pi\pi\pi})^2 (r_D^{K\pi})^2 + 2\kappa_B^{D\pi\pi\pi} r_B^{D\pi\pi\pi} r_D^{K\pi} \cos(\delta_B^{D\pi\pi\pi} - \delta_D^{K\pi} + \gamma)}$$

$$R_-^{D\pi\pi\pi, K\pi} = \frac{(r_B^{DK\pi\pi})^2 + (r_D^{K\pi})^2 + 2\kappa_B^{DK\pi\pi} r_B^{DK\pi\pi} r_D^{K\pi} \cos(\delta_B^{DK\pi\pi} + \delta_D^{K\pi} - \gamma)}{1 + (r_B^{DK\pi\pi})^2 (r_D^{K\pi})^2 + 2\kappa_B^{DK\pi\pi} r_B^{DK\pi\pi} r_D^{K\pi} \cos(\delta_B^{DK\pi\pi} - \delta_D^{K\pi} - \gamma)}$$

A.7 $B^0 \rightarrow DK^{*0}, D \rightarrow K^+\pi^-$ observables

$$\bar{A}_{\text{fav}}^{DK^{*0}, K\pi} = \frac{2\kappa_B^{DK^{*0}} \bar{R}_B^{DK^{*0}} r_B^{DK^{*0}} r_D^{K\pi} \sin(\delta_B^{DK^{*0}} + \Delta\bar{\delta}_B^{DK^{*0}} - \delta_D^{K\pi}) \sin \gamma}{1 + (\bar{R}_B^{DK^{*0}} r_B^{DK^{*0}})^2 (r_D^{K\pi})^2 + 2\kappa_B^{DK^{*0}} \bar{R}_B^{DK^{*0}} r_B^{DK^{*0}} r_D^{K\pi} \cos(\delta_B^{DK^{*0}} + \Delta\bar{\delta}_B^{DK^{*0}} - \delta_D^{K\pi}) \cos \gamma}$$

$$\bar{R}_+^{DK^{*0}, K\pi} = \frac{(\bar{R}_B^{DK^{*0}} r_B^{DK^{*0}})^2 + (r_D^{K\pi})^2 + 2\kappa_B^{DK^{*0}} \bar{R}_B^{DK^{*0}} r_B^{DK^{*0}} r_D^{K\pi} \cos(\delta_B^{DK^{*0}} + \Delta\bar{\delta}_B^{DK^{*0}} + \delta_D^{K\pi} + \gamma)}{1 + (\bar{R}_B^{DK^{*0}} r_B^{DK^{*0}})^2 (r_D^{K\pi})^2 + 2\kappa_B^{DK^{*0}} \bar{R}_B^{DK^{*0}} r_B^{DK^{*0}} r_D^{K\pi} \cos(\delta_B^{DK^{*0}} + \Delta\bar{\delta}_B^{DK^{*0}} - \delta_D^{K\pi} + \gamma)}$$

$$\bar{R}_-^{DK^{*0}, K\pi} = \frac{(\bar{R}_B^{DK^{*0}} r_B^{DK^{*0}})^2 + (r_D^{K\pi})^2 + 2\kappa_B^{DK^{*0}} \bar{R}_B^{DK^{*0}} r_B^{DK^{*0}} r_D^{K\pi} \cos(\delta_B^{DK^{*0}} + \Delta\bar{\delta}_B^{DK^{*0}} + \delta_D^{K\pi} - \gamma)}{1 + (\bar{R}_B^{DK^{*0}} r_B^{DK^{*0}})^2 (r_D^{K\pi})^2 + 2\kappa_B^{DK^{*0}} \bar{R}_B^{DK^{*0}} r_B^{DK^{*0}} r_D^{K\pi} \cos(\delta_B^{DK^{*0}} + \Delta\bar{\delta}_B^{DK^{*0}} - \delta_D^{K\pi} - \gamma)}$$

A.8 $B^0 \rightarrow DK^+\pi^-$, $D \rightarrow h^+h^-$ observables

$$\begin{aligned}x_-^{DK^{*0}} &= r_B^{DK^{*0}} \cos(\delta_B^{DK^{*0}} - \gamma) \\y_-^{DK^{*0}} &= r_B^{DK^{*0}} \sin(\delta_B^{DK^{*0}} - \gamma) \\x_+^{DK^{*0}} &= r_B^{DK^{*0}} \cos(\delta_B^{DK^{*0}} + \gamma) \\y_+^{DK^{*0}} &= r_B^{DK^{*0}} \sin(\delta_B^{DK^{*0}} + \gamma)\end{aligned}$$

A.9 $B^0 \rightarrow DK^{*0}$, $D \rightarrow K_s^0\pi^+\pi^-$ observables

$$\begin{aligned}\bar{x}_-^{DK^{*0}} &= \bar{R}_B^{DK^{*0}} r_B^{DK^{*0}} \cos(\delta_B^{DK^{*0}} + \Delta\bar{\delta}_B^{DK^{*0}} - \gamma) \\ \bar{y}_-^{DK^{*0}} &= \bar{R}_B^{DK^{*0}} r_B^{DK^{*0}} \sin(\delta_B^{DK^{*0}} + \Delta\bar{\delta}_B^{DK^{*0}} - \gamma) \\ \bar{x}_+^{DK^{*0}} &= \bar{R}_B^{DK^{*0}} r_B^{DK^{*0}} \cos(\delta_B^{DK^{*0}} + \Delta\bar{\delta}_B^{DK^{*0}} + \gamma) \\ \bar{y}_+^{DK^{*0}} &= \bar{R}_B^{DK^{*0}} r_B^{DK^{*0}} \sin(\delta_B^{DK^{*0}} + \Delta\bar{\delta}_B^{DK^{*0}} + \gamma)\end{aligned}$$

A.10 $B_s^0 \rightarrow D_s^\mp K^\pm$ observables

$$\begin{aligned}C_f &= \frac{1 - (r_B^{D_s K})^2}{1 + (r_B^{D_s K})^2}, \\ A_f^{\Delta\Gamma} &= \frac{2r_B^{D_s K} \cos(\delta_B^{D_s K} - (\gamma + \phi_s))}{1 + (r_B^{D_s K})^2} \\ A_{\bar{f}}^{\Delta\Gamma} &= \frac{2r_B^{D_s K} \cos(\delta_B^{D_s K} + (\gamma + \phi_s))}{1 + (r_B^{D_s K})^2} \\ S_f &= \frac{2r_B^{D_s K} \sin(\delta_B^{D_s K} - (\gamma + \phi_s))}{1 + (r_B^{D_s K})^2} \\ S_{\bar{f}} &= \frac{2r_B^{D_s K} \sin(\delta_B^{D_s K} + (\gamma + \phi_s))}{1 + (r_B^{D_s K})^2}\end{aligned}$$

B Input observable values and uncertainties

The input observable values and their statistical and systematic uncertainties are listed below. The observables labelled $D\pi$ are only used in the Dh combination.

B.1 $B^+ \rightarrow Dh^+$, $D \rightarrow h^+h^-$ analysis

The values and uncertainties are taken from Ref. [44]. The observables are defined in analogy to Eqs. (3-7), and the measured values are

$$A_{\text{ADS}}^{DK,\pi K} = -0.403 \pm 0.056 \pm 0.011,$$

$$\begin{aligned}
A_{\text{ADS}}^{D\pi,\pi K} &= 0.100 \pm 0.031 \pm 0.009, \\
A_{\text{CP}}^{DK,KK} &= 0.087 \pm 0.020 \pm 0.008, \\
A_{\text{CP}}^{DK,\pi\pi} &= 0.128 \pm 0.037 \pm 0.012, \\
A_{\text{CP}}^{D\pi,KK} &= -0.0145 \pm 0.0050 \pm 0.0017, \\
A_{\text{CP}}^{D\pi,\pi\pi} &= 0.0043 \pm 0.0086 \pm 0.0031, \\
A_{\text{fav}}^{DK,K\pi} &= -0.0194 \pm 0.0072 \pm 0.0060, \\
R_{\text{ADS}}^{DK,\pi K} &= 0.0188 \pm 0.0011 \pm 0.0010, \\
R_{\text{ADS}}^{D\pi,\pi K} &= 0.0036 \pm 0.0001 \pm 0.0001, \\
R_{\text{CP}}^{KK} &= 0.968 \pm 0.022 \pm 0.021 \pm 0.010, \\
R_{\text{CP}}^{\pi\pi} &= 1.002 \pm 0.040 \pm 0.026 \pm 0.010, \\
R_{K/\pi}^{K\pi} &= 0.0779 \pm 0.0006 \pm 0.0019,
\end{aligned}$$

where the first uncertainties are statistical and the second are systematic. For R_{CP}^{KK} and $R_{\text{CP}}^{\pi\pi}$ the third uncertainties arise from the assumption that $r_B^{D\pi} = 0$ as discussed in Ref. [44] and subsequently applies only for the DK combination. Their statistical and systematic correlations are given in Tables 9 and 10. The relationships between observables and parameters are given in Appendix A.1.

B.2 $B^+ \rightarrow Dh^+$, $D \rightarrow h^+\pi^-\pi^+\pi^-$ analysis

The values and uncertainties are taken from Ref. [44]. The observables are defined in analogy to Eqs. (3–7), and the measured values are

$$\begin{aligned}
A_{\text{ADS}}^{DK,\pi K\pi\pi} &= -0.313 \pm 0.102 \pm 0.038, \\
A_{\text{ADS}}^{D\pi,\pi K\pi\pi} &= 0.023 \pm 0.048 \pm 0.005, \\
A_{\text{CP}}^{DK,\pi\pi\pi\pi} &= 0.100 \pm 0.034 \pm 0.018, \\
A_{\text{CP}}^{D\pi,\pi\pi\pi\pi} &= -0.0041 \pm 0.0079 \pm 0.0024, \\
A_{\text{fav}}^{DK,\pi K\pi\pi} &= -0.000 \pm 0.012 \pm 0.002, \\
R_{\text{ADS}}^{DK,\pi K\pi\pi} &= 0.0140 \pm 0.0015 \pm 0.0006, \\
R_{\text{ADS}}^{D\pi,\pi K\pi\pi} &= 0.0038 \pm 0.0002 \pm 0.0001, \\
R_{\text{CP}}^{\pi\pi\pi\pi} &= 0.975 \pm 0.037 \pm 0.019 \pm 0.005, \\
R_{K/\pi}^{K\pi\pi\pi} &= 0.0793 \pm 0.0010 \pm 0.0018,
\end{aligned}$$

where the first uncertainty is statistical and the second is systematic. The third uncertainty for $R_{\text{CP}}^{\pi\pi\pi\pi}$ is again from the assumption that $r_B^{D\pi} = 0$ and subsequently applies only for the DK combination. Their statistical and systematic correlations are given in Tables 11 and 12. The relationships between observables and parameters are given in Appendix A.2.

B.3 $B^+ \rightarrow Dh^+$, $D \rightarrow h^+h^-\pi^0$ analysis

The values and uncertainties are taken from Ref. [45]. The observables are defined in analogy to Eqs. (3–7), and the measured values are

$$A_{\text{ADS}}^{DK,\pi K\pi^0} = -0.20 \pm 0.27 \pm 0.04,$$

$$\begin{aligned}
A_{\text{ADS}}^{D\pi,\pi K\pi^0} &= 0.44 \pm 0.19 \pm 0.01, \\
A_{\text{CP}}^{DK,KK\pi^0} &= 0.30 \pm 0.20 \pm 0.02, \\
A_{\text{CP}}^{DK,\pi\pi\pi^0} &= 0.054 \pm 0.091 \pm 0.011, \\
A_{\text{CP}}^{D\pi,KK\pi^0} &= -0.030 \pm 0.040 \pm 0.005, \\
A_{\text{CP}}^{D\pi,\pi\pi\pi^0} &= -0.016 \pm 0.020 \pm 0.004, \\
A_{\text{fav}}^{DK,K\pi\pi^0} &= 0.010 \pm 0.026 \pm 0.005, \\
R_{\text{ADS}}^{DK,\pi K\pi^0} &= 0.014 \pm 0.005 \pm 0.002, \\
R_{\text{ADS}}^{D\pi,\pi K\pi^0} &= 0.00235 \pm 0.00049 \pm 0.00006, \\
R_{\text{CP}}^{KK\pi^0} &= 0.95 \pm 0.22 \pm 0.05, \\
R_{\text{CP}}^{\pi\pi\pi^0} &= 0.98 \pm 0.11 \pm 0.05,
\end{aligned}$$

where the first uncertainty is statistical and the second is systematic. The statistical and systematic correlations are given in Tables 13 and 14. The relationships between observables and parameters are given in Appendix A.3.

B.4 $B^+ \rightarrow DK^+$, $D \rightarrow K_s^0 h^+ h^-$ analysis

The values and uncertainties are taken from Ref. [46]. The results are

$$\begin{aligned}
x_-^{DK} &= 0.025 \pm 0.025 \pm 0.010 \pm 0.005, \\
y_-^{DK} &= 0.075 \pm 0.029 \pm 0.005 \pm 0.014, \\
x_+^{DK} &= -0.077 \pm 0.024 \pm 0.010 \pm 0.004, \\
y_+^{DK} &= -0.022 \pm 0.025 \pm 0.004 \pm 0.010,
\end{aligned}$$

where the first uncertainty is statistical, the second is systematic, and the third is an external uncertainty due to the information on the strong phase variation across the $D \rightarrow K_s^0 h^+ h^-$ phase space. Correlations between the statistical and systematic uncertainties are given in Tables 15 and 16. The relationships between observables and parameters are given in Appendix A.4.

B.5 $B^+ \rightarrow Dh^+$, $D \rightarrow K_s^0 K^- \pi^+$ analysis

The values and uncertainties are taken from Ref. [47]. The observables are defined in analogy to Eqs. (5–7) and are

$$\begin{aligned}
R_{\text{ADS}}^{DK,K_S K\pi} &= 3.855 \pm 0.961 \pm 0.060, \\
A_{\text{fav}}^{DK,K_S K\pi} &= 0.026 \pm 0.109 \pm 0.029, \\
A_{\text{ADS}}^{DK,K_S K\pi} &= 0.336 \pm 0.208 \pm 0.026,
\end{aligned}$$

where the first uncertainty is statistical and the second is systematic. The statistical and systematic correlations are found to be negligible and not included. The relationships between observables and parameters are given in Appendix A.5.

B.6 $B^+ \rightarrow Dh^+ \pi^- \pi^+$, $D \rightarrow h^+ h^-$ analysis

The values and uncertainties are taken from Ref. [48]. The observables are defined in analogy to Eqs. (3,4,7–9) and are

$$R_{\text{CP}}^{DK\pi\pi} = 1.040 \pm 0.064$$

$$\begin{aligned}
A_{\text{fav}}^{DK\pi\pi, K\pi} &= 0.013 \pm 0.019 \pm 0.013, \\
A_{\text{fav}}^{D\pi\pi\pi, K\pi} &= -0.002 \pm 0.003 \pm 0.011, \\
A_{CP}^{DK\pi\pi, KK} &= -0.045 \pm 0.064 \pm 0.011, \\
A_{CP}^{DK\pi\pi, \pi\pi} &= -0.054 \pm 0.101 \pm 0.011, \\
A_{CP}^{D\pi\pi\pi, KK} &= -0.019 \pm 0.011 \pm 0.010, \\
A_{CP}^{D\pi\pi\pi, \pi\pi} &= -0.013 \pm 0.016 \pm 0.010, \\
R_+^{DK\pi\pi, K\pi} &= 0.0107 \pm 0.0060 \pm 0.0011, \\
R_-^{DK\pi\pi, K\pi} &= 0.0053 \pm 0.0045 \pm 0.0006, \\
R_+^{D\pi\pi\pi, K\pi} &= 0.0043 \pm 0.0005 \pm 0.0002, \\
R_-^{D\pi\pi\pi, K\pi} &= 0.0042 \pm 0.0005 \pm 0.0002,
\end{aligned}$$

where the first uncertainty is statistical and the second is systematic. For $R_{CP}^{DK\pi\pi}$, the single uncertainty includes both statistical and systematic contributions. The only non-negligible correlations are the statistical correlations, $\rho(A_{CP}^{DK\pi\pi, KK}, A_{CP}^{DK\pi\pi, \pi\pi}) = 0.20$ and $\rho(A_{CP}^{D\pi\pi\pi, KK}, A_{CP}^{D\pi\pi\pi, \pi\pi}) = 0.08$. The relationships between observables and parameters are given in Appendix A.6.

B.7 $B^0 \rightarrow DK^{*0}$, $D \rightarrow K^+\pi^-$ analysis

The values and uncertainties are taken from Ref. [49]. The ADS observables are defined in analogy to Eqs. (7–9) and are

$$\begin{aligned}
\bar{A}_{\text{fav}}^{DK^{*0}, K\pi} &= -0.03 \pm 0.04 \pm 0.02, \\
\bar{R}_+^{DK^{*0}, K\pi} &= 0.06 \pm 0.03 \pm 0.01, \\
\bar{R}_-^{DK^{*0}, K\pi} &= 0.06 \pm 0.03 \pm 0.01,
\end{aligned}$$

where the first uncertainty is statistical and the second is systematic. The statistical correlations are given in Table 17, and the systematic correlations in Table 18. The relationships between observables and parameters are given in Appendix A.7.

B.8 $B^0 \rightarrow DK^+\pi^-$, $D \rightarrow h^+h^-$ analysis

The values and uncertainties are taken from Ref. [50]. The results are

$$\begin{aligned}
x_-^{DK^{*0}} &= -0.02 \pm 0.13 \pm 0.14, \\
y_-^{DK^{*0}} &= -0.35 \pm 0.26 \pm 0.41, \\
x_+^{DK^{*0}} &= 0.04 \pm 0.16 \pm 0.11, \\
y_+^{DK^{*0}} &= -0.47 \pm 0.28 \pm 0.22,
\end{aligned}$$

where the first uncertainty is statistical and the second is systematic. The correlations are given in Tables 19 and 20. The relationships between observables and parameters are given in Appendix A.8.

B.9 $B^0 \rightarrow DK^{*0}, D \rightarrow K_s^0 \pi^+ \pi^-$ analysis

The values and uncertainties are taken from Ref. [51]. The results are

$$\begin{aligned}\bar{x}_-^{DK^{*0}} &= -0.15 \pm 0.14 \pm 0.03 \pm 0.01, \\ \bar{y}_-^{DK^{*0}} &= 0.25 \pm 0.15 \pm 0.06 \pm 0.01, \\ \bar{x}_+^{DK^{*0}} &= 0.05 \pm 0.24 \pm 0.04 \pm 0.01, \\ \bar{y}_+^{DK^{*0}} &= -0.65 \pm 0.24 \pm 0.08 \pm 0.01,\end{aligned}$$

where the first uncertainty is statistical, the second is systematic and the third is from the Dalitz plot fit model. The correlations are given in Table 21. The relationships between observables and parameters are given in Appendix A.9.

B.10 $B_s^0 \rightarrow D_s^\mp K^\pm$ analysis

The values and uncertainties are taken from Ref. [52] (with a change in the sign convention, see Appendix A.10 for the explicit definition). The results are

$$\begin{aligned}C_f &= 0.53 \pm 0.25 \pm 0.04, \\ A_f^{\Delta\Gamma} &= -0.37 \pm 0.42 \pm 0.20, \\ A_{\bar{f}}^{\Delta\Gamma} &= -0.20 \pm 0.41 \pm 0.20, \\ S_f &= -1.09 \pm 0.33 \pm 0.08, \\ S_{\bar{f}} &= 0.36 \pm 0.34 \pm 0.08,\end{aligned}$$

where the first uncertainty is statistical and the second is systematic. The statistical correlations are given in Table 22, and the systematic correlations in Table 23. The relationships between observables and parameters are given in Appendix A.10.

C Uncertainty correlations for the input observables

The correlation matrices of the statistical and systematic uncertainties are given below. The observables labelled $D\pi$ are only used in the Dh combination.

Table 9: Correlation matrix of the statistical uncertainties for the $B^+ \rightarrow Dh^+$, $D^0 \rightarrow h^+h^-$ observables [44].

	$A_{\text{ADS}}^{DK,\pi K}$	$A_{\text{ADS}}^{D\pi,\pi K}$	$A_{CP}^{DK,KK}$	$A_{CP}^{DK,\pi\pi}$	$A_{CP}^{D\pi,KK}$	$A_{CP}^{D\pi,\pi\pi}$	$A_{\text{fav}}^{DK,K\pi}$	$R_{\text{ADS}}^{DK,\pi K}$	$R_{\text{ADS}}^{D\pi,\pi K}$	R_{CP}^{KK}	$R_{CP}^{\pi\pi}$	$R_{K/\pi}^{K\pi}$
$A_{\text{ADS}}^{DK,\pi K}$	1	-0.047	0.002	0.001	0.009	0.005	0.008	0.102	-0.003	0	0	0
$A_{\text{ADS}}^{D\pi,\pi K}$	-0.047	1	0.004	0.003	0.017	0.010	0.014	0.015	-0.043	0	0	0
$A_{CP}^{DK,KK}$	0.002	0.004	1	0.004	-0.007	0.016	0.024	0	0	-0.014	0	-0.001
$A_{CP}^{DK,\pi\pi}$	0.001	0.003	0.004	1	0.016	-0.036	0.014	-0.001	0	0	-0.038	-0.002
$A_{CP}^{D\pi,KK}$	0.009	0.017	-0.007	0.016	1	0.064	0.092	0	0	-0.001	0	-0.001
$A_{CP}^{D\pi,\pi\pi}$	0.005	0.010	0.016	-0.036	0.064	1	0.053	0	0	0	-0.003	0
$A_{\text{fav}}^{DK,K\pi}$	0.008	0.014	0.024	0.014	0.092	0.053	1	0	0	0	0	0
$R_{\text{ADS}}^{DK,\pi K}$	0.102	0.015	0	-0.001	0	0	0	1	-0.022	0.040	0.025	-0.114
$R_{\text{ADS}}^{D\pi,\pi K}$	-0.003	-0.043	0	0	0	0	0	-0.022	1	-0.005	-0.003	0.011
R_{CP}^{KK}	0	0	-0.014	0	-0.001	0	0	0.040	-0.005	1	0.060	-0.317
$R_{CP}^{\pi\pi}$	0	0	0	-0.038	0	-0.003	0	0.025	-0.003	0.060	1	-0.176
$R_{K/\pi}^{K\pi}$	0	0	-0.001	-0.002	-0.001	0	0	-0.114	0.011	-0.317	-0.176	1

Table 10: Correlation matrix of the systematic uncertainties for the $B^+ \rightarrow Dh^+$, $D^0 \rightarrow h^+h^-$ observables [44].

	$A_{\text{ADS}}^{DK,\pi K}$	$A_{\text{ADS}}^{D\pi,\pi K}$	$A_{CP}^{DK,KK}$	$A_{CP}^{DK,\pi\pi}$	$A_{CP}^{D\pi,KK}$	$A_{CP}^{D\pi,\pi\pi}$	$A_{\text{fav}}^{DK,K\pi}$	$R_{\text{ADS}}^{DK,\pi K}$	$R_{\text{ADS}}^{D\pi,\pi K}$	R_{CP}^{KK}	$R_{CP}^{\pi\pi}$	$R_{K/\pi}^{K\pi}$
$A_{\text{ADS}}^{DK,\pi K}$	1	0.36	-0.06	0.27	0.30	0.04	0.09	0.78	-0.43	-0.04	0.23	-0.14
$A_{\text{ADS}}^{D\pi,\pi K}$	0.36	1	-0.03	0.31	0.22	-0.06	-0.55	0.59	-0.47	-0.01	0.12	-0.04
$A_{CP}^{DK,KK}$	-0.06	-0.03	1	-0.02	-0.80	0.09	0.09	-0.10	-0.06	0.03	-0.28	0.07
$A_{CP}^{DK,\pi\pi}$	0.27	0.31	-0.02	1	0.19	-0.42	-0.01	0.35	-0.28	-0.22	0.11	-0.07
$A_{CP}^{D\pi,KK}$	0.30	0.22	-0.80	0.19	1	0.11	0.09	0.37	-0.21	-0.16	0.20	-0.13
$A_{CP}^{D\pi,\pi\pi}$	0.04	-0.06	0.09	-0.42	0.11	1	0.30	-0.03	0.06	-0.08	-0.03	-0.09
$A_{\text{fav}}^{DK,K\pi}$	0.09	-0.55	0.09	-0.01	0.09	0.30	1	-0.11	0.05	-0.01	-0.02	-0.02
$R_{\text{ADS}}^{DK,\pi K}$	0.78	0.59	-0.10	0.35	0.37	-0.03	-0.11	1	-0.57	-0.14	0.33	-0.22
$R_{\text{ADS}}^{D\pi,\pi K}$	-0.43	-0.47	-0.06	-0.28	-0.21	0.06	0.05	-0.57	1	0.19	0.10	0.02
R_{CP}^{KK}	-0.04	-0.01	0.03	-0.22	-0.16	-0.08	-0.01	-0.14	0.19	1	0.17	0.21
$R_{CP}^{\pi\pi}$	0.23	0.12	-0.28	0.11	0.20	-0.03	-0.02	0.33	0.10	0.17	1	-0.11
$R_{K/\pi}^{K\pi}$	-0.14	-0.04	0.07	-0.07	-0.13	-0.09	-0.02	-0.22	0.02	0.21	-0.11	1

Table 11: Correlation matrix of the statistical uncertainties for the $B^+ \rightarrow Dh^+$, $D^0 \rightarrow h^\pm \pi^\mp \pi^+ \pi^-$ observables [44].

	$A_{\text{ADS}}^{DK,\pi K\pi\pi}$	$A_{\text{ADS}}^{D\pi,\pi K\pi\pi}$	$A_{CP}^{DK,\pi\pi\pi\pi}$	$A_{CP}^{D\pi,\pi\pi\pi\pi}$	$A_{\text{fav}}^{DK,\pi K\pi\pi}$	$R_{\text{ADS}}^{DK,\pi K\pi\pi}$	$R_{\text{ADS}}^{D\pi,\pi K\pi\pi}$	$R_{CP}^{\pi\pi\pi\pi}$	$R_{K/\pi}^{K\pi\pi\pi}$
$A_{\text{ADS}}^{DK,\pi K\pi\pi}$	1	-0.062	0.002	0.009	0.006	0.082	-0.004	0.002	0.003
$A_{\text{ADS}}^{D\pi,\pi K\pi\pi}$	-0.062	1	0.005	0.020	0.017	0.013	-0.022	0	0
$A_{CP}^{DK,\pi\pi\pi\pi}$	0.002	0.005	1	-0.020	0.024	-0.001	0	-0.018	-0.002
$A_{CP}^{D\pi,\pi\pi\pi\pi}$	0.009	0.020	-0.020	1	0.097	0	0	-0.004	0
$A_{\text{fav}}^{DK,\pi K\pi\pi}$	0.006	0.017	0.024	0.097	1	0	0	0	0.001
$R_{\text{ADS}}^{DK,\pi K\pi\pi}$	0.082	0.013	-0.001	0	0	1	-0.046	0.041	-0.099
$R_{\text{ADS}}^{D\pi,\pi K\pi\pi}$	-0.004	-0.022	0	0	0	-0.046	1	-0.004	0.012
$R_{CP}^{\pi\pi\pi\pi}$	0.002	0	-0.018	-0.004	0	0.041	-0.004	1	-0.308
$R_{K/\pi}^{K\pi\pi\pi}$	0.003	0	-0.002	0	0.001	-0.099	0.012	-0.308	1

Table 12: Correlation matrix of the systematic uncertainties for the $B^+ \rightarrow Dh^+$, $D^0 \rightarrow h^\pm \pi^\mp \pi^+ \pi^-$ observables [44].

	$A_{\text{ADS}}^{DK,\pi K\pi\pi}$	$A_{\text{ADS}}^{D\pi,\pi K\pi\pi}$	$A_{CP}^{DK,\pi\pi\pi\pi}$	$A_{CP}^{D\pi,\pi\pi\pi\pi}$	$A_{\text{fav}}^{DK,\pi K\pi\pi}$	$R_{\text{ADS}}^{DK,\pi K\pi\pi}$	$R_{\text{ADS}}^{D\pi,\pi K\pi\pi}$	$R_{CP}^{\pi\pi\pi\pi}$	$R_{K/\pi}^{K\pi\pi\pi}$
$A_{\text{ADS}}^{DK,\pi K\pi\pi}$	1	-0.09	-0.04	0.02	0.02	0.87	0.05	-0.04	-0.13
$A_{\text{ADS}}^{D\pi,\pi K\pi\pi}$	-0.09	1	-0.34	0.43	0.05	0.10	0.46	-0.04	0.17
$A_{CP}^{DK,\pi\pi\pi\pi}$	-0.04	-0.34	1	0.31	0.09	0.03	-0.35	0.07	-0.14
$A_{CP}^{D\pi,\pi\pi\pi\pi}$	0.02	0.43	0.31	1	0.32	0.01	0.24	-0.07	0.08
$A_{\text{fav}}^{DK,\pi K\pi\pi}$	0.02	0.05	0.09	0.32	1	0.02	-0.02	0.02	0
$R_{\text{ADS}}^{DK,\pi K\pi\pi}$	0.87	0.10	0.03	0.01	0.02	1	0.14	0.04	-0.04
$R_{\text{ADS}}^{D\pi,\pi K\pi\pi}$	0.05	0.46	-0.35	0.24	-0.02	0.14	1	-0.06	0.13
$R_{CP}^{\pi\pi\pi\pi}$	-0.04	-0.04	0.07	-0.07	0.02	0.04	-0.06	1	0.11
$R_{K/\pi}^{K\pi\pi\pi}$	-0.13	0.17	-0.14	0.08	0	-0.04	0.13	0.11	1

Table 13: Correlation matrix of the statistical uncertainties for the $B^+ \rightarrow Dh^+$, $D^0 \rightarrow h^\pm h^\mp \pi^0$ observables [52].

	$A_{\text{ADS}}^{DK,\pi K\pi^0}$	$A_{\text{ADS}}^{D\pi,\pi K\pi^0}$	$A_{CP}^{DK, KK\pi^0}$	$A_{CP}^{DK,\pi\pi\pi^0}$	$A_{CP}^{D\pi, KK\pi^0}$	$A_{CP}^{D\pi,\pi\pi\pi^0}$	$A_{\text{fav}}^{DK, K\pi\pi^0}$	$R_{\text{ADS}}^{DK,\pi K\pi^0}$	$R_{\text{ADS}}^{D\pi,\pi K\pi^0}$	$R_{CP}^{KK\pi^0}$	$R_{CP}^{\pi\pi\pi^0}$
$A_{\text{ADS}}^{DK,\pi K\pi^0}$	1	-0.04	0	0	0	0.01	0.01	0.13	0	0	0
$A_{\text{ADS}}^{D\pi,\pi K\pi^0}$	-0.04	1	0	0	0	0.01	0.01	-0.01	-0.34	0	0
$A_{CP}^{DK, KK\pi^0}$	0	0	1	0	-0.04	0.01	0.01	0	0	-0.20	-0.01
$A_{CP}^{DK,\pi\pi\pi^0}$	0	0	0	1	0.01	-0.04	0.02	0	0	0	-0.04
$A_{CP}^{D\pi, KK\pi^0}$	0	0	-0.04	0.01	1	0.04	0.04	0	0	0	0
$A_{CP}^{D\pi,\pi\pi\pi^0}$	0.01	0.01	0.01	-0.04	0.04	1	0.08	0	0	0	0
$A_{\text{fav}}^{DK, K\pi\pi^0}$	0.01	0.01	0.01	0.02	0.04	0.08	1	0	0	0	0
$R_{\text{ADS}}^{DK,\pi K\pi^0}$	0.13	-0.01	0	0	0	0	0	1	0.03	0	0.01
$R_{\text{ADS}}^{D\pi,\pi K\pi^0}$	0	-0.34	0	0	0	0	0	0.03	1	0	0
$R_{CP}^{KK\pi^0}$	0	0	-0.20	0	0	0	0	0	0	1	0.02
$R_{CP}^{\pi\pi\pi^0}$	0	0	-0.01	-0.04	0	0	0	0.01	0	0.02	1

Table 14: Correlation matrix of the systematic uncertainties for the $B^+ \rightarrow Dh^+$, $D^0 \rightarrow h^\pm h^\mp \pi^0$ observables [52].

	$A_{\text{ADS}}^{DK,\pi K\pi^0}$	$A_{\text{ADS}}^{D\pi,\pi K\pi^0}$	$A_{CP}^{DK,KK\pi^0}$	$A_{CP}^{DK,\pi\pi\pi^0}$	$A_{CP}^{D\pi,KK\pi^0}$	$A_{CP}^{D\pi,\pi\pi\pi^0}$	$A_{\text{fav}}^{DK,K\pi\pi^0}$	$R_{\text{ADS}}^{DK,\pi K\pi^0}$	$R_{\text{ADS}}^{D\pi,\pi K\pi^0}$	$R_{CP}^{KK\pi^0}$	$R_{CP}^{\pi\pi\pi^0}$
$A_{\text{ADS}}^{DK,\pi K\pi^0}$	1	0.03	0.07	0.07	0.18	0.17	-0.16	0.81	0.32	0.02	0.13
$A_{\text{ADS}}^{D\pi,\pi K\pi^0}$	0.03	1	0.28	0.31	0.67	0.68	-0.63	-0.18	-0.49	0	-0.04
$A_{CP}^{DK,KK\pi^0}$	0.07	0.28	1	0.77	0.07	0.05	0.05	0.08	-0.08	-0.33	-0.18
$A_{CP}^{DK,\pi\pi\pi^0}$	0.07	0.31	0.77	1	0.05	0.02	-0.06	0.13	-0.11	-0.14	-0.25
$A_{CP}^{D\pi,KK\pi^0}$	0.18	0.67	0.07	0.05	1	0.88	-0.82	-0.04	0.02	-0.04	0.02
$A_{CP}^{D\pi,\pi\pi\pi^0}$	0.17	0.68	0.05	0.02	0.88	1	-0.87	-0.03	0	0	0.01
$A_{\text{fav}}^{DK,K\pi\pi^0}$	-0.16	-0.63	0.05	-0.06	-0.82	-0.87	1	-0.05	0.06	0.04	0
$R_{\text{ADS}}^{DK,\pi K\pi^0}$	0.81	-0.18	0.08	0.13	-0.04	-0.03	-0.05	1	0.33	-0.03	-0.02
$R_{\text{ADS}}^{D\pi,\pi K\pi^0}$	0.32	-0.49	-0.08	-0.11	0.02	0	0.06	0.33	1	0.02	-0.02
$R_{CP}^{KK\pi^0}$	0.02	0	-0.33	-0.14	-0.04	0	0.04	-0.03	0.02	1	0.38
$R_{CP}^{\pi\pi\pi^0}$	0.13	-0.04	-0.18	-0.25	0.02	0.01	0	-0.02	-0.02	0.38	1

Table 15: Correlation matrix of the statistical uncertainties for the $B^+ \rightarrow DK^+$, $D^0 \rightarrow K_s^0 h^+ h^-$ observables [46].

	x_-^{DK}	y_-^{DK}	x_+^{DK}	y_+^{DK}
x_-^{DK}	1	-0.247	0.038	-0.003
y_-^{DK}	-0.247	1	-0.011	0.012
x_+^{DK}	0.038	-0.011	1	0.002
y_+^{DK}	-0.003	0.012	0.002	1

Table 16: Correlation matrix of the systematic uncertainties for the $B^+ \rightarrow DK^+$, $D^0 \rightarrow K_s^0 h^+ h^-$ observables [46].

	x_-^{DK}	y_-^{DK}	x_+^{DK}	y_+^{DK}
x_-^{DK}	1	0.005	-0.025	0.070
y_-^{DK}	0.005	1	0.009	-0.141
x_+^{DK}	-0.025	0.009	1	0.008
y_+^{DK}	0.070	-0.141	0.008	1

Table 17: Correlation matrix of the statistical uncertainties for the $B^0 \rightarrow DK^{*0}$, $D \rightarrow K^+ \pi^-$ observables [49].

	$\bar{A}_{\text{fav}}^{DK^{*0}, K\pi}$	$\bar{R}_+^{DK^{*0}, K\pi}$	$\bar{R}_-^{DK^{*0}, K\pi}$
$\bar{A}_{\text{fav}}^{DK^{*0}, K\pi}$	1	0.091	0.083
$\bar{R}_+^{DK^{*0}, K\pi}$	0.091	1	-0.081
$\bar{R}_-^{DK^{*0}, K\pi}$	-0.083	-0.081	1

Table 18: Correlation matrix of the systematic uncertainties for the $B^0 \rightarrow DK^{*0}$, $D \rightarrow K^+ \pi^-$ observables [49].

	$\bar{A}_{\text{fav}}^{DK^{*0}, K\pi}$	$\bar{R}_+^{DK^{*0}, K\pi}$	$\bar{R}_-^{DK^{*0}, K\pi}$
$\bar{A}_{\text{fav}}^{DK^{*0}, K\pi}$	1	0.008	0.008
$\bar{R}_+^{DK^{*0}, K\pi}$	0.008	1	0.997
$\bar{R}_-^{DK^{*0}, K\pi}$	0.008	0.997	1

Table 19: Correlation matrix of the statistical uncertainties for $B^0 \rightarrow D^0 K \pi$, $D \rightarrow h^+ h^-$ observables [50].

	$x_-^{DK^{*0}}$	$y_-^{DK^{*0}}$	$x_+^{DK^{*0}}$	$y_+^{DK^{*0}}$
$x_-^{DK^{*0}}$	1	0.341	0.104	0.130
$y_-^{DK^{*0}}$	0.341	1	0.054	0.154
$x_+^{DK^{*0}}$	0.104	0.054	1	0.501
$y_+^{DK^{*0}}$	0.130	0.154	0.501	1

Table 20: Correlation matrix of the systematic uncertainties for $B^0 \rightarrow D^0 K \pi$, $D \rightarrow h^+ h^-$ observables [50].

	$x_-^{DK^{*0}}$	$y_-^{DK^{*0}}$	$x_+^{DK^{*0}}$	$y_+^{DK^{*0}}$
$x_-^{DK^{*0}}$	1	0.872	0.253	0.368
$y_-^{DK^{*0}}$	0.872	1	0.293	0.414
$x_+^{DK^{*0}}$	0.253	0.293	1	0.731
$y_+^{DK^{*0}}$	0.368	0.414	0.731	1

Table 21: Correlation matrix of the statistical uncertainties for the $B^0 \rightarrow DK^{*0}$, $D \rightarrow K_S^0 \pi^+ \pi^-$ observables [51].

	$\bar{x}_-^{DK^{*0}}$	$\bar{y}_-^{DK^{*0}}$	$\bar{x}_+^{DK^{*0}}$	$\bar{y}_+^{DK^{*0}}$
$\bar{x}_-^{DK^{*0}}$	1	0.143	0	0
$\bar{y}_-^{DK^{*0}}$	0.143	1	0	0
$\bar{x}_+^{DK^{*0}}$	0	0	1	0.143
$\bar{y}_+^{DK^{*0}}$	0	0	0.143	1

Table 22: Correlation matrix of the statistical uncertainties for the $B_s^0 \rightarrow D_s^\mp K^\pm$ observables [52].

	C_f	$A_f^{\Delta\Gamma}$	$A_{\bar{f}}^{\Delta\Gamma}$	S_f	$S_{\bar{f}}$
C_f	1	-0.084	-0.103	-0.008	0.045
$A_f^{\Delta\Gamma}$	-0.084	1	0.544	0.117	-0.022
$A_{\bar{f}}^{\Delta\Gamma}$	-0.103	0.544	1	0.067	-0.032
S_f	-0.008	0.117	0.067	1	-0.002
$S_{\bar{f}}$	0.045	-0.022	-0.032	-0.002	1

Table 23: Correlation matrix of the systematic uncertainties for the $B_s^0 \rightarrow D_s^\mp K^\pm$ observables [52].

	C_f	$A_f^{\Delta\Gamma}$	$A_{\bar{f}}^{\Delta\Gamma}$	S_f	$S_{\bar{f}}$
C_f	1	-0.22	-0.22	-0.04	0.03
$A_f^{\Delta\Gamma}$	-0.22	1	0.96	0.17	-0.14
$A_{\bar{f}}^{\Delta\Gamma}$	-0.22	0.96	1	0.17	-0.14
S_f	-0.04	0.17	0.17	1	-0.09
$S_{\bar{f}}$	0.03	-0.14	-0.14	-0.09	1

D External constraint values and uncertainties

D.1 Input from global fit to charm data

The values and uncertainties are taken from Ref. [22]. The observables are

$$\begin{aligned}
 x_D &= 0.0037 \pm 0.0016, \\
 y_D &= 0.0066 \pm 0.0009, \\
 \delta_D^{K\pi} &= 3.35 \pm 0.21 \text{ rad}, \\
 R_D^{K\pi} &= 0.00349 \pm 0.00004, \\
 A_{\pi\pi}^{\text{dir}} &= 0.0010 \pm 0.0015, \\
 A_{KK}^{\text{dir}} &= -0.0015 \pm 0.0014.
 \end{aligned}$$

Here the value of $\delta_D^{K\pi}$ has been shifted by π to comply with the phase convention used in the combination. The correlations of the charm parameters are given in Table 24.

D.2 Input for $D^0 \rightarrow K^\pm \pi^\mp \pi^+ \pi^-$ and $D^0 \rightarrow K^\pm \pi^\mp \pi^0$ decays

The values and uncertainties are taken from Ref. [58]. The values used are

$$\begin{aligned}
 \kappa_D^{K3\pi} &= 0.43 \pm 0.17, \\
 \delta_D^{K3\pi} &= 2.23 \pm 0.49 \text{ rad}, \\
 \kappa_D^{K2\pi} &= 0.81 \pm 0.06, \\
 \delta_D^{K2\pi} &= 3.46 \pm 0.26 \text{ rad}, \\
 r_D^{K3\pi} &= 0.0549 \pm 0.0006, \\
 r_D^{K2\pi} &= 0.0447 \pm 0.0012.
 \end{aligned}$$

The correlation matrix is given in Table 25.

D.3 CP content of $D \rightarrow h^+ h^- \pi^0$ and $D \rightarrow \pi^+ \pi^- \pi^+ \pi^-$ decays

The values and uncertainties are taken from Ref. [59]. The values used are

$$\begin{aligned}
 F_{\pi\pi\pi^0} &= 0.973 \pm 0.017, \\
 F_{KK\pi^0} &= 0.732 \pm 0.055, \\
 F_{\pi\pi\pi\pi} &= 0.737 \pm 0.032.
 \end{aligned}$$

D.4 Input for $D \rightarrow K_s^0 K^- \pi^+$ parameters

The following constraints from Ref. [60] are used:

$$\begin{aligned} R_D^{K_S K \pi} &= 0.356 \pm 0.034 \pm 0.007, \\ \delta_D^{K_S K \pi} &= -0.29 \pm 0.32 \text{ rad}, \\ \kappa_D^{K_S K \pi} &= 0.94 \pm 0.16. \end{aligned}$$

In addition the following constraint from Ref. [61] is used

$$R_D^{K_S K \pi} = 0.370 \pm 0.003 \pm 0.012.$$

The correlation between $\delta_D^{K_S K \pi}$ and $\kappa_D^{K_S K \pi}$ is determined from the experimental likelihood to be $\rho(\delta_D^{K_S K \pi}, \kappa_D^{K_S K \pi}) = -0.60$.

D.5 Constraints on the $B^0 \rightarrow DK^{*0}$ hadronic parameters

The values and uncertainties are taken from Ref. [50]. The values used are

$$\begin{aligned} \kappa_B^{DK^{*0}} &= 0.958 \pm 0.008 \pm 0.024, \\ \bar{R}_B^{DK^{*0}} &= 1.020 \pm 0.020 \pm 0.060, \\ \Delta \bar{\delta}_B^{DK^{*0}} &= 0.020 \pm 0.025 \pm 0.110 \text{ rad}, \end{aligned}$$

where the first uncertainty is statistical and the second systematic. These are taken to be uncorrelated.

D.6 Constraint on ϕ_s

The value used is taken from Ref. [62] as

$$\phi_s = -0.010 \pm 0.039 \text{ rad}.$$

E Uncertainty correlations for the external constraints

Table 24: Correlations of the HFAG charm parameters (CHARM 2015, “Fit 3”, CP violation allowed) [22].

	x_D	y_D	$\delta_D^{K\pi}$	$R_D^{K\pi}$	$A_{\pi\pi}^{\text{dir}}$	A_{KK}^{dir}
x_D	1	-0.361	-0.332	0.234	0.117	0.146
y_D	-0.361	1	0.941	0.234	-0.180	-0.221
$\delta_D^{K\pi}$	-0.332	0.941	1	0.439	-0.200	-0.237
$R_D^{K\pi}$	0.234	0.234	0.439	1	-0.078	-0.067
$A_{\pi\pi}^{\text{dir}}$	0.117	-0.180	-0.200	-0.078	1	0.726
A_{KK}^{dir}	0.146	-0.221	-0.237	-0.067	0.726	1

Table 25: Correlations of the $D^0 \rightarrow K^\pm \pi^\mp \pi^+ \pi^-$ and $D^0 \rightarrow K^\pm \pi^\mp \pi^0$ parameters from CLEO and LHCb [58].

	$\kappa_D^{K3\pi}$	$\delta_D^{K3\pi}$	$\kappa_D^{K2\pi}$	$\delta_D^{K2\pi}$	$r_D^{K3\pi}$	$r_D^{K2\pi}$
$\kappa_D^{K3\pi}$	1	-0.67	0.04	-0.05	-0.48	-0.04
$\delta_D^{K3\pi}$	-0.67	1	0.02	0.15	0.12	0.08
$\kappa_D^{K2\pi}$	0.04	0.02	1	0.23	-0.04	-0.04
$\delta_D^{K2\pi}$	-0.05	0.15	0.23	1	-0.02	0.36
$r_D^{K3\pi}$	-0.48	0.12	-0.04	-0.02	1	-0.03
$r_D^{K2\pi}$	-0.04	0.08	-0.04	0.36	-0.03	1

F Fit parameter correlations

F.1 DK combination

Table 26: Fit parameter correlations for the DK combination. The fit results are given in Table 3

	γ	r_B^{DK}	δ_B^{DK}	$r_B^{DK^*0}$	$\delta_B^{DK^*0}$
γ	1	0.54	0.44	0.21	-0.15
r_B^{DK}	0.54	1	0.39	0.11	-0.08
δ_B^{DK}	0.44	0.39	1	0.08	-0.05
$r_B^{DK^*0}$	0.21	0.11	0.08	1	-0.13
$\delta_B^{DK^*0}$	-0.15	-0.08	-0.05	-0.13	1

F.2 Dh combination

Table 27: Fit parameter correlations for the Dh combination solution 1. The fit results are given in Table 4

	γ	r_B^{DK}	δ_B^{DK}	$r_B^{DK^*0}$	$\delta_B^{DK^*0}$	$r_B^{D\pi}$	$\delta_B^{D\pi}$
γ	1	0.19	0.23	0.10	-0.07	-0.59	-0.22
r_B^{DK}	0.19	1	0.23	0.02	0	-0.20	0.02
δ_B^{DK}	0.23	0.23	1	0.02	0	-0.09	0.42
$r_B^{DK^*0}$	0.10	0.02	0.02	1	-0.10	-0.06	-0.03
$\delta_B^{DK^*0}$	-0.07	0	0	-0.10	1	0.04	0.03
$r_B^{D\pi}$	-0.59	-0.20	-0.09	-0.06	0.04	1	0.45
$\delta_B^{D\pi}$	-0.22	0.02	0.42	-0.03	0.03	0.45	1

Table 28: Fit parameter correlations for the Dh combination solution 2. The fit results are given in Table 4

	γ	r_B^{DK}	δ_B^{DK}	$r_B^{DK^*0}$	$\delta_B^{DK^*0}$	$r_B^{D\pi}$	$\delta_B^{D\pi}$
γ	1	0.52	0.51	0.22	-0.16	-0.12	0.01
r_B^{DK}	0.52	1	0.41	0.11	-0.08	0.03	0.10
δ_B^{DK}	0.51	0.41	1	0.11	-0.06	-0.19	-0.01
$r_B^{DK^*0}$	0.22	0.11	0.11	1	-0.13	-0.02	0
$\delta_B^{DK^*0}$	-0.16	-0.08	-0.06	-0.13	1	0.01	0
$r_B^{D\pi}$	-0.12	0.03	-0.19	-0.02	0.01	1	0.83
$\delta_B^{D\pi}$	0.01	0.10	-0.01	0	0	0.83	1

References

- [1] A. D. Sakharov, *Violation of CP Invariance, C Asymmetry, and Baryon Asymmetry of the Universe*, Pisma Zh. Eksp. Teor. Fiz. **5** (1967) 32, [Usp. Fiz. Nauk161,61(1991)].
- [2] N. Cabibbo, *Unitary symmetry and leptonic decays*, Phys. Rev. Lett. **10** (1963) 531.
- [3] M. Kobayashi and T. Maskawa, *CP violation in the renormalizable theory of weak interaction*, Prog. Theor. Phys. **49** (1973) 652.
- [4] M. B. Gavela, P. Hernandez, J. Orloff, and O. Pène, *Standard model CP violation and baryon asymmetry*, Mod. Phys. Lett. **A9** (1994) 795, arXiv:hep-ph/9312215.
- [5] L. Wolfenstein, *Parametrization of the Kobayashi-Maskawa Matrix*, Phys. Rev. Lett. **51** (1983) 1945.
- [6] L.-L. Chau and W.-Y. Keung, *Comments on the parametrization of the Kobayashi-Maskawa Matrix*, Phys. Rev. Lett. **53** (1984) 1802.
- [7] A. J. Buras, M. E. Lautenbacher, and G. Ostermaier, *Waiting for the top quark mass, $K^+ \rightarrow \pi^+ \nu \bar{\nu}$, $B_s^0 - \bar{B}_s^0$ mixing and CP asymmetries in B decays*, Phys. Rev. **D50** (1994) 3433, arXiv:hep-ph/9403384.
- [8] M. Gronau and D. Wyler, *On determining a weak phase from CP asymmetries in charged B decays*, Phys. Lett. **B265** (1991) 172.
- [9] M. Gronau and D. London, *How to determine all the angles of the unitarity triangle from $B^0 \rightarrow DK_s^0$ and $B_s^0 \rightarrow D\phi$* , Phys. Lett. **B253** (1991) 483.
- [10] D. Atwood, I. Dunietz, and A. Soni, *Enhanced CP violation with $B \rightarrow KD^0$ (\bar{D}^0) modes and extraction of the CKM angle γ* , Phys. Rev. Lett. **78** (1997) 3257, arXiv:hep-ph/9612433.
- [11] D. Atwood, I. Dunietz, and A. Soni, *Improved methods for observing CP violation in $B^\pm \rightarrow KD$ and measuring the CKM phase γ* , Phys. Rev. **D63** (2001) 036005, arXiv:hep-ph/0008090.
- [12] J. Brod, A. Lenz, G. Tetlalmatzi-Xolocotzi, and M. Wiebusch, *New physics effects in tree-level decays and the precision in the determination of the quark mixing angle γ* , Phys. Rev. **D92** (2015) 033002, arXiv:1412.1446.
- [13] J. Brod and J. Zupan, *The ultimate theoretical error on γ from $B \rightarrow DK$ decays*, JHEP **01** (2014) 051, arXiv:1308.5663.
- [14] A. Bondar, *Proceedings of BINP special analysis meeting on Dalitz analysis*, 24–26 Sep, 2002. Unpublished.
- [15] A. Giri, Y. Grossman, A. Soffer, and J. Zupan, *Determining γ using $B^\pm \rightarrow DK^\pm$ with multibody D decays*, Phys. Rev. **D68** (2003) 054018, arXiv:hep-ph/0303187.
- [16] Y. Grossman, Z. Ligeti, and A. Soffer, *Measuring γ in $B^\pm \rightarrow K^\pm(KK^*)_D$ decays*, Phys. Rev. **D67** (2003) 071301, arXiv:hep-ph/0210433.

- [17] R. Fleischer, *New strategies to obtain insights into CP violation through $B_s^0 \rightarrow D_s^\pm K^\mp$, $D_s^{*\pm} K^\mp$, ... and $B^0 \rightarrow D^\pm \pi^\mp$, $D_s^\pm \pi^\mp$, ... decays*, Nucl. Phys. **B671** (2003) 459, [arXiv:hep-ph/0304027](#).
- [18] R. Aleksan, I. Dunietz, and B. Kayser, *Determining the CP violating phase γ* , Z. Phys. **C54** (1992) 653.
- [19] I. Dunietz and R. G. Sachs, *Asymmetry between inclusive charmed and anticharmed modes in B^0 , \bar{B}^0 decay as a measure of CP violation*, Phys. Rev. **D37** (1988) 3186.
- [20] T. Gershon, *On the measurement of the unitarity triangle angle γ from $B^0 \rightarrow DK^{*0}$ decays*, Phys. Rev. **D79** (2009) 051301, [arXiv:0810.2706](#).
- [21] T. Gershon and M. Williams, *Prospects for the measurement of the unitarity triangle angle γ from $B^0 \rightarrow DK^+\pi^-$ decays*, Phys. Rev. **D80** (2009) 092002, [arXiv:0909.1495](#).
- [22] Heavy Flavor Averaging Group (HFAG), Y. Amhis *et al.*, *Averages of b-hadron, c-hadron, and τ -lepton properties as of summer 2014*, [arXiv:1412.7515](#), updated results and plots available at <http://www.slac.stanford.edu/xorg/hfag/>.
- [23] M. Kenzie, M. Martinelli, and N. Tuning, *Estimating $r_B^{D\pi}$ as an input to the determination of the CKM angle γ* , Phys. Rev. **D94** (2016) 054021, [arXiv:1606.09129](#).
- [24] K. De Bruyn *et al.*, *Exploring $B_s \rightarrow D_s^{(*)\pm} K^\mp$ Decays in the Presence of a Sizable Width Difference $\Delta\Gamma_s$* , Nucl. Phys. **B868** (2013) 351, [arXiv:1208.6463](#).
- [25] Particle Data Group, K. A. Olive *et al.*, *Review of particle physics*, Chin. Phys. **C38** (2014) 090001, and 2015 update.
- [26] CKMfitter group, J. Charles *et al.*, *CP violation and the CKM matrix: Assessing the impact of the asymmetric B factories*, Eur. Phys. J. **C41** (2005) 1, [arXiv:hep-ph/0406184](#), updated results and plots available at: <http://ckmfitter.in2p3.fr>.
- [27] UTfit collaboration, M. Bona *et al.*, *The 2004 UTfit collaboration report on the status of the unitarity triangle in the standard model*, JHEP **07** (2005) 028, [arXiv:hep-ph/0501199](#), updated results and plots available at: <http://www.utfit.org/UTfit/>.
- [28] LHCb collaboration, *Improved constraints on γ : CKM2014 update*, LHCb-CONF-2014-004.
- [29] LHCb collaboration, *A measurement of γ from a combination of $B^\pm \rightarrow DK^\pm$ analyses including first results using 2 fb^{-1} of 2012 data*, LHCb-CONF-2013-006.
- [30] LHCb collaboration, R. Aaij *et al.*, *A measurement of the CKM angle γ from a combination of $B^\pm \rightarrow Dh^\pm$ analyses*, Phys. Lett. **B726** (2013) 151, [arXiv:1305.2050](#).
- [31] LHCb collaboration, *LHCb γ combination update from $B \rightarrow DKX$ decays*, LHCb-CONF-2016-001.

- [32] T. Gershon and V. V. Gligorov, *CP violation in the B system*, arXiv:1607.06746.
- [33] M. Nayak *et al.*, *First determination of the CP content of $D \rightarrow \pi^+\pi^-\pi^0$ and $D \rightarrow K^+K^-\pi^0$* , Phys. Lett. **B740** (2015) 1, arXiv:1410.3964.
- [34] LHCb collaboration, R. Aaij *et al.*, *Determination of the sign of the decay width difference in the B_s^0 system*, Phys. Rev. Lett. **108** (2012) 241801, arXiv:1202.4717.
- [35] C. C. Meca and J. P. Silva, *Detecting new physics contributions to the $D^0-\bar{D}^0$ mixing through their effects on B decays*, Phys. Rev. Lett. **81** (1998) 1377, arXiv:hep-ph/9807320.
- [36] J. P. Silva and A. Soffer, *Impact of $D^0-\bar{D}^0$ mixing on the experimental determination of γ* , Phys. Rev. **D61** (2000) 112001, arXiv:hep-ph/9912242.
- [37] M. Rama, *Effect of $D-\bar{D}^0$ mixing in the extraction of γ with $B^- \rightarrow D^0K^-$ and $B^- \rightarrow D^0\pi^-$ decays*, Phys. Rev. **D89** (2014) 014021, arXiv:1307.4384.
- [38] W. Wang, *CP violation effects on the measurement of the Cabibbo-Kobayashi-Maskawa angle γ from $B \rightarrow DK$* , Phys. Rev. Lett. **110** (2013) 061802, arXiv:1211.4539.
- [39] M. Martone and J. Zupan, *$B^\pm \rightarrow DK^\pm$ with direct CP violation in charm*, Phys. Rev. **D87** (2013) 034005, arXiv:1212.0165.
- [40] B. Bhattacharya, D. London, M. Gronau, and J. L. Rosner, *Shift in weak phase γ due to CP asymmetries in D decays to two pseudoscalar mesons*, Phys. Rev. **D87** (2013) 074002, arXiv:1301.5631.
- [41] A. Bondar, A. Dolgov, A. Poluektov, and V. Vorobiev, *Effect of direct CP violation in charm on γ extraction from $B \rightarrow DK^\pm$, $D \rightarrow K_S^0\pi^+\pi^-$ Dalitz plot analysis*, Eur. Phys. J. **C73** (2013) 2476, arXiv:1303.6305.
- [42] LHCb collaboration, R. Aaij *et al.*, *Measurement of the difference of time-integrated CP asymmetries in $D^0 \rightarrow K^-K^+$ and $D^0 \rightarrow \pi^-\pi^+$ decays*, Phys. Rev. Lett. **116** (2016) 191601, arXiv:1602.03160.
- [43] Y. Grossman and M. Savastio, *Effects of $K^0-\bar{K}^0$ mixing on determining γ from $B^\pm \rightarrow DK^\pm$* , JHEP **1403** (2014) 008, arXiv:1311.3575.
- [44] LHCb collaboration, R. Aaij *et al.*, *Measurement of CP observables in $B^\pm \rightarrow DK^\pm$ and $B^\pm \rightarrow D\pi^\pm$ with two- and four-body D meson decays*, Phys. Lett. **B760** (2016) 117, arXiv:1603.08993.
- [45] LHCb collaboration, R. Aaij *et al.*, *A study of CP violation in $B^\mp \rightarrow Dh^\mp$ ($h = K, \pi$) with the modes $D \rightarrow K^\mp\pi^\pm\pi^0$, $D \rightarrow \pi^+\pi^-\pi^0$ and $D \rightarrow K^+K^-\pi^0$* , Phys. Rev. **D91** (2015) 112014, arXiv:1504.05442.
- [46] LHCb collaboration, R. Aaij *et al.*, *Measurement of the CKM angle γ using $B^\pm \rightarrow DK^\pm$ with $D \rightarrow K_S^0\pi^+\pi^-$, $K_S^0K^+K^-$ decays*, JHEP **10** (2014) 097, arXiv:1408.2748.

- [47] LHCb collaboration, R. Aaij *et al.*, *A study of CP violation in $B^\pm \rightarrow DK^\pm$ and $B^\pm \rightarrow D\pi^\pm$ decays with $D \rightarrow K_S^0 K^\pm \pi^\mp$ final states*, Phys. Lett. **B733** (2014) 36, arXiv:1402.2982.
- [48] LHCb collaboration, R. Aaij *et al.*, *Study of $B^- \rightarrow DK^- \pi^+ \pi^-$ and $B^- \rightarrow D\pi^- \pi^+ \pi^-$ decays and determination of the CKM angle γ* , Phys. Rev. **D92** (2015) 112005, arXiv:1505.07044.
- [49] LHCb collaboration, R. Aaij *et al.*, *Measurement of CP violation parameters in $B^0 \rightarrow DK^{*0}$ decays*, Phys. Rev. **D90** (2014) 112002, arXiv:1407.8136.
- [50] LHCb collaboration, R. Aaij *et al.*, *Constraints on the unitarity triangle angle γ from Dalitz plot analysis of $B^0 \rightarrow DK^+ \pi^-$ decays*, Phys. Rev. **D93** (2016) 112018, arXiv:1602.03455.
- [51] LHCb collaboration, R. Aaij *et al.*, *Measurement of the CKM angle γ using $B^0 \rightarrow DK^{*0}$ with $D \rightarrow K_S^0 \pi^+ \pi^-$ decays*, JHEP **08** (2016) 137, arXiv:1605.01082.
- [52] LHCb collaboration, R. Aaij *et al.*, *Measurement of CP asymmetry in $B_s^0 \rightarrow D_s^\mp K^\pm$ decays*, JHEP **11** (2014) 060, arXiv:1407.6127.
- [53] LHCb collaboration, R. Aaij *et al.*, *Observation of CP violation in $B^\pm \rightarrow DK^\pm$ decays*, Phys. Lett. **B712** (2012) 203, Erratum *ibid.* **B713** (2012) 351, arXiv:1203.3662.
- [54] LHCb collaboration, R. Aaij *et al.*, *Observation of the suppressed ADS modes $B^\pm \rightarrow [\pi^\pm K^\mp \pi^+ \pi^-]_D K^\pm$ and $B^\pm \rightarrow [\pi^\pm K^\mp \pi^+ \pi^-]_D \pi^\pm$* , Phys. Lett. **B723** (2013) 44, arXiv:1303.4646.
- [55] LHCb collaboration, R. Aaij *et al.*, *Measurement of CP violation and constraints on the CKM angle γ in $B^\pm \rightarrow DK^\pm$ with $D \rightarrow K_S^0 \pi^+ \pi^-$ decays*, Nucl. Phys. **B888** (2014) 169, arXiv:1407.6211.
- [56] BaBar collaboration, P. del Amo Sanchez *et al.*, *Measurement of D^0 - \bar{D}^0 mixing parameters using $D^0 \rightarrow K_S^0 \pi^+ \pi^-$ and $D^0 \rightarrow K_S^0 K^+ K^-$ decays*, Phys. Rev. Lett. **105** (2010) 081803, arXiv:1004.5053.
- [57] LHCb collaboration, R. Aaij *et al.*, *Model-independent measurement of the CKM angle γ using $B^0 \rightarrow DK^{*0}$ decays with $D \rightarrow K_S^0 \pi^+ \pi^-$ and $K_S^0 K^+ K^-$* , JHEP **06** (2016) 131, arXiv:1604.01525.
- [58] T. Evans *et al.*, *Improved determination of the $D \rightarrow K^- \pi^+ \pi^+ \pi^-$ coherence factor and associated hadronic parameters from a combination of $e^+ e^- \rightarrow \psi(3770) \rightarrow c\bar{c}$ and $pp \rightarrow c\bar{c}X$ data*, Phys. Lett. **B757** (2016) 520, arXiv:1602.07430, Erratum *ibid.* submitted to Phys. Lett. B.
- [59] S. Malde *et al.*, *First determination of the CP content of $D \rightarrow \pi^+ \pi^- \pi^+ \pi^-$ and updated determination of the CP contents of $D \rightarrow \pi^+ \pi^- \pi^0$ and $D \rightarrow K^+ K^- \pi^0$* , Phys. Lett. **B747** (2015) 9, arXiv:1504.05878.
- [60] CLEO collaboration, J. Insler *et al.*, *Studies of the decays $D^0 \rightarrow K_S^0 K^- \pi^+$ and $D^0 \rightarrow K_S^0 K^+ \pi^-$* , Phys. Rev. **D85** (2012) 092016, Erratum *ibid.* **D94** (2016) 099905, arXiv:1203.3804.

- [61] LHCb collaboration, R. Aaij *et al.*, *Studies of the resonance structure in $D^0 \rightarrow K_s^0 K^\pm \pi^\mp$ decays*, Phys. Rev. **D93** (2016) 052018, [arXiv:1509.06628](#).
- [62] LHCb collaboration, R. Aaij *et al.*, *Precision measurement of CP violation in $B_s^0 \rightarrow J/\psi K^+ K^-$ decays*, Phys. Rev. Lett. **114** (2015) 041801, [arXiv:1411.3104](#).
- [63] LHCb collaboration, R. Aaij *et al.*, *First observation of $D^0 - \bar{D}^0$ oscillations in $D^0 \rightarrow K^+ \pi^+ \pi^- \pi^-$ decays and a measurement of the associated coherence parameters*, Phys. Rev. Lett. **116** (2016) 241801, [arXiv:1602.07224](#).
- [64] B. Sen, M. Walker, and M. Woodroffe, *On the unified method with nuisance parameters*, Statistica Sinica **19** (2009) 301.

LHCb collaboration

R. Aaij⁴⁰, B. Adeva³⁹, M. Adinolfi⁴⁸, Z. Ajaltouni⁵, S. Akar⁶, J. Albrecht¹⁰, F. Alessio⁴⁰, M. Alexander⁵³, S. Ali⁴³, G. Alkhazov³¹, P. Alvarez Cartelle⁵⁵, A.A. Alves Jr⁵⁹, S. Amato², S. Amerio²³, Y. Amhis⁷, L. An⁴¹, L. Anderlini¹⁸, G. Andreassi⁴¹, M. Andreotti^{17,g}, J.E. Andrews⁶⁰, R.B. Appleby⁵⁶, F. Archilli⁴³, P. d'Argent¹², J. Arnau Romeu⁶, A. Artamonov³⁷, M. Artuso⁶¹, E. Aslanides⁶, G. Auriemma²⁶, M. Baalouch⁵, I. Babuschkin⁵⁶, S. Bachmann¹², J.J. Back⁵⁰, A. Badalov³⁸, C. Baesso⁶², S. Baker⁵⁵, W. Baldini¹⁷, R.J. Barlow⁵⁶, C. Barschel⁴⁰, S. Barsuk⁷, W. Barter⁴⁰, M. Baszczyk²⁷, V. Batozskaya²⁹, B. Batsukh⁶¹, V. Battista⁴¹, A. Bay⁴¹, L. Beaucourt⁴, J. Beddow⁵³, F. Bedeschi²⁴, I. Bediaga¹, L.J. Bel⁴³, V. Bellee⁴¹, N. Belloli^{21,i}, K. Belous³⁷, I. Belyaev³², E. Ben-Haim⁸, G. Bencivenni¹⁹, S. Benson⁴³, J. Benton⁴⁸, A. Berezhnoy³³, R. Bernet⁴², A. Bertolin²³, F. Betti¹⁵, M.-O. Bettler⁴⁰, M. van Beuzekom⁴³, I. Bezshyiko⁴², S. Bifani⁴⁷, P. Billoir⁸, T. Bird⁵⁶, A. Birnkraut¹⁰, A. Bitadze⁵⁶, A. Bizzeti^{18,u}, T. Blake⁵⁰, F. Blanc⁴¹, J. Blouw^{11,†}, S. Blusk⁶¹, V. Bocci²⁶, T. Boettcher⁵⁸, A. Bondar^{36,w}, N. Bondar^{31,40}, W. Bonivento¹⁶, A. Borgheresi^{21,i}, S. Borghi⁵⁶, M. Borisyak³⁵, M. Borsato³⁹, F. Bossu⁷, M. Boubdir⁹, T.J.V. Bowcock⁵⁴, E. Bowen⁴², C. Bozzi^{17,40}, S. Braun¹², M. Britsch¹², T. Britton⁶¹, J. Brodzicka⁵⁶, E. Buchanan⁴⁸, C. Burr⁵⁶, A. Bursche², J. Buytaert⁴⁰, S. Cadeddu¹⁶, R. Calabrese^{17,g}, M. Calvi^{21,i}, M. Calvo Gomez^{38,m}, A. Camboni³⁸, P. Campana¹⁹, D. Campora Perez⁴⁰, D.H. Campora Perez⁴⁰, L. Capriotti⁵⁶, A. Carbone^{15,e}, G. Carboni^{25,j}, R. Cardinale^{20,h}, A. Cardini¹⁶, P. Carniti^{21,i}, L. Carson⁵², K. Carvalho Akiba², G. Casse⁵⁴, L. Cassina^{21,i}, L. Castillo Garcia⁴¹, M. Cattaneo⁴⁰, Ch. Cauet¹⁰, G. Cavallero²⁰, R. Cenci^{24,t}, M. Charles⁸, Ph. Charpentier⁴⁰, G. Chatzikonstantinidis⁴⁷, M. Chefdeville⁴, S. Chen⁵⁶, S.-F. Cheung⁵⁷, V. Chobanova³⁹, M. Chrzaszcz^{42,27}, X. Cid Vidal³⁹, G. Ciezarek⁴³, P.E.L. Clarke⁵², M. Clemencic⁴⁰, H.V. Cliff⁴⁹, J. Closier⁴⁰, V. Coco⁵⁹, J. Cogan⁶, E. Cogneras⁵, V. Cogoni^{16,40,f}, L. Cojocariu³⁰, G. Collazuol^{23,o}, P. Collins⁴⁰, A. Comerma-Montells¹², A. Contu⁴⁰, A. Cook⁴⁸, G. Coombs⁴⁰, S. Coquereau³⁸, G. Corti⁴⁰, M. Corvo^{17,g}, C.M. Costa Sobral⁵⁰, B. Couturier⁴⁰, G.A. Cowan⁵², D.C. Craik⁵², A. Crocombe⁵⁰, M. Cruz Torres⁶², S. Cunliffe⁵⁵, R. Currie⁵⁵, C. D'Ambrosio⁴⁰, F. Da Cunha Marinho², E. Dall'Occo⁴³, J. Dalseno⁴⁸, P.N.Y. David⁴³, A. Davis⁵⁹, O. De Aguiar Francisco², K. De Bruyn⁶, S. De Capua⁵⁶, M. De Cian¹², J.M. De Miranda¹, L. De Paula², M. De Serio^{14,d}, P. De Simone¹⁹, C.-T. Dean⁵³, D. Decamp⁴, M. Deckenhoff¹⁰, L. Del Buono⁸, M. Demmer¹⁰, D. Derkach³⁵, O. Deschamps⁵, F. Dettori⁴⁰, B. Dey²², A. Di Canto⁴⁰, H. Dijkstra⁴⁰, F. Dordei⁴⁰, M. Dorigo⁴¹, A. Dosil Suárez³⁹, A. Dovbnya⁴⁵, K. Dreimanis⁵⁴, L. Dufour⁴³, G. Dujany⁵⁶, K. Dungs⁴⁰, P. Durante⁴⁰, R. Dzhelyadin³⁷, A. Dziurda⁴⁰, A. Dzyuba³¹, N. Deléage⁴, S. Easo⁵¹, M. Ebert⁵², U. Egede⁵⁵, V. Egorychev³², S. Eidelman^{36,w}, S. Eisenhardt⁵², U. Eitschberger¹⁰, R. Ekelhof¹⁰, L. Eklund⁵³, Ch. Elsasser⁴², S. Ely⁶¹, S. Esen¹², H.M. Evans⁴⁹, T. Evans⁵⁷, A. Falabella¹⁵, N. Farley⁴⁷, S. Farry⁵⁴, R. Fay⁵⁴, D. Fazzini^{21,i}, D. Ferguson⁵², V. Fernandez Albor³⁹, A. Fernandez Prieto³⁹, F. Ferrari^{15,40}, F. Ferreira Rodrigues¹, M. Ferro-Luzzi⁴⁰, S. Filippov³⁴, R.A. Fini¹⁴, M. Fiore^{17,g}, M. Fiorini^{17,g}, M. Firlej²⁸, C. Fitzpatrick⁴¹, T. Fiutowski²⁸, F. Fleuret^{7,b}, K. Fohl⁴⁰, M. Fontana^{16,40}, F. Fontanelli^{20,h}, D.C. Forshaw⁶¹, R. Forty⁴⁰, V. Franco Lima⁵⁴, M. Frank⁴⁰, C. Frei⁴⁰, J. Fu^{22,q}, E. Furfaro^{25,j}, C. Färber⁴⁰, A. Gallas Torreira³⁹, D. Galli^{15,e}, S. Gallorini²³, S. Gambetta⁵², M. Gandelman², P. Gandini⁵⁷, Y. Gao³, L.M. Garcia Martin⁶⁸, J. García Pardiñas³⁹, J. Garra Tico⁴⁹, L. Garrido³⁸, P.J. Garsed⁴⁹, D. Gascon³⁸, C. Gaspar⁴⁰, L. Gavardi¹⁰, G. Gazzoni⁵, D. Gerick¹², E. Gersabeck¹², M. Gersabeck⁵⁶, T. Gershon⁵⁰, Ph. Ghez⁴, S. Gianì⁴¹, V. Gibson⁴⁹, O.G. Girard⁴¹, L. Giubega³⁰, K. Gizdov⁵², V.V. Gligorov⁸, D. Golubkov³², A. Golutvin^{55,40}, A. Gomes^{1,a}, I.V. Gorelov³³, C. Gotti^{21,i}, M. Grabalosa Gándara⁵, R. Graciani Diaz³⁸, L.A. Granado Cardoso⁴⁰, E. Graugés³⁸, E. Graverini⁴², G. Graziani¹⁸, A. Greco³⁰, P. Griffith⁴⁷, L. Grillo^{21,40,i}, B.R. Gruberg Cazon⁵⁷, O. Grünberg⁶⁶, E. Gushchin³⁴, Yu. Guz³⁷, T. Gys⁴⁰,

C. Göbel⁶², T. Hadavizadeh⁵⁷, C. Hadjivasiliou⁵, G. Haefeli⁴¹, C. Haen⁴⁰, S.C. Haines⁴⁹,
 S. Hall⁵⁵, B. Hamilton⁶⁰, X. Han¹², S. Hansmann-Menzemer¹², N. Harnew⁵⁷, S.T. Harnew⁴⁸,
 J. Harrison⁵⁶, M. Hatch⁴⁰, J. He⁶³, T. Head⁴¹, A. Heister⁹, K. Hennessy⁵⁴, P. Henrard⁵,
 L. Henry⁸, J.A. Hernando Morata³⁹, E. van Herwijnen⁴⁰, M. Heß⁶⁶, A. Hicheur², D. Hill⁵⁷,
 C. Hombach⁵⁶, H. Hopchev⁴¹, W. Hulsbergen⁴³, T. Humair⁵⁵, M. Hushchyn³⁵, N. Hussain⁵⁷,
 D. Hutchcroft⁵⁴, M. Idzik²⁸, P. Ilten⁵⁸, R. Jacobsson⁴⁰, A. Jaeger¹², J. Jalocha⁵⁷, E. Jans⁴³,
 A. Jawahery⁶⁰, F. Jiang³, M. John⁵⁷, D. Johnson⁴⁰, C.R. Jones⁴⁹, C. Joram⁴⁰, B. Jost⁴⁰,
 N. Jurik⁶¹, S. Kandybei⁴⁵, W. Kanso⁶, M. Karacson⁴⁰, J.M. Kariuki⁴⁸, S. Karodia⁵³,
 M. Kecke¹², M. Kelsey⁶¹, I.R. Kenyon⁴⁷, M. Kenzie⁴⁹, T. Ketel⁴⁴, E. Khairullin³⁵,
 B. Khanji^{21,40,i}, C. Khurewathanakul⁴¹, T. Kirn⁹, S. Klaver⁵⁶, K. Klimaszewski²⁹, S. Koliiev⁴⁶,
 M. Kolpin¹², I. Komarov⁴¹, R.F. Koopman⁴⁴, P. Koppenburg⁴³, A. Kosmyntseva³²,
 A. Kozachuk³³, M. Kozeiha⁵, L. Kravchuk³⁴, K. Kreplin¹², M. Kreps⁵⁰, P. Krokovny^{36,w},
 F. Kruse¹⁰, W. Krzemien²⁹, W. Kucewicz^{27,l}, M. Kucharczyk²⁷, V. Kudryavtsev^{36,w},
 A.K. Kuonen⁴¹, K. Kurek²⁹, T. Kvaratskheliya^{32,40}, D. Lacarrere⁴⁰, G. Lafferty⁵⁶, A. Lai¹⁶,
 D. Lambert⁵², G. Lanfranchi¹⁹, C. Langenbruch⁹, T. Latham⁵⁰, C. Lazzeroni⁴⁷, R. Le Gac⁶,
 J. van Leerdam⁴³, J.-P. Lees⁴, A. Leflat^{33,40}, J. Lefrançois⁷, R. Lefèvre⁵, F. Lemaitre⁴⁰,
 E. Lemos Cid³⁹, O. Leroy⁶, T. Lesiak²⁷, B. Leverington¹², Y. Li⁷, T. Likhomanenko^{35,67},
 R. Lindner⁴⁰, C. Linn⁴⁰, F. Lionetto⁴², B. Liu¹⁶, X. Liu³, D. Loh⁵⁰, I. Longstaff⁵³, J.H. Lopes²,
 D. Lucchesi^{23,o}, M. Lucio Martinez³⁹, H. Luo⁵², A. Lupato²³, E. Luppi^{17,g}, O. Lupton⁵⁷,
 A. Lusiani²⁴, X. Lyu⁶³, F. Machefert⁷, F. Maciuc³⁰, O. Maev³¹, K. Maguire⁵⁶, S. Malde⁵⁷,
 A. Malinin⁶⁷, T. Maltsev³⁶, G. Manca⁷, G. Mancinelli⁶, P. Manning⁶¹, J. Maratas^{5,v},
 J.F. Marchand⁴, U. Marconi¹⁵, C. Marin Benito³⁸, P. Marino^{24,t}, J. Marks¹², G. Martellotti²⁶,
 M. Martin⁶, M. Martinelli⁴¹, D. Martinez Santos³⁹, F. Martinez Vidal⁶⁸, D. Martins Tostes²,
 L.M. Massacrier⁷, A. Massafferri¹, R. Matev⁴⁰, A. Mathad⁵⁰, Z. Mathe⁴⁰, C. Matteuzzi²¹,
 A. Mauri⁴², B. Maurin⁴¹, A. Mazurov⁴⁷, M. McCann⁵⁵, J. McCarthy⁴⁷, A. McNab⁵⁶,
 R. McNulty¹³, B. Meadows⁵⁹, F. Meier¹⁰, M. Meissner¹², D. Melnychuk²⁹, M. Merk⁴³,
 A. Merli^{22,q}, E. Michielin²³, D.A. Milanes⁶⁵, M.-N. Minard⁴, D.S. Mitzel¹², A. Mogini⁸,
 J. Molina Rodriguez⁶², I.A. Monroy⁶⁵, S. Monteil⁵, M. Morandin²³, P. Morawski²⁸, A. Mordà⁶,
 M.J. Morello^{24,t}, J. Moron²⁸, A.B. Morris⁵², R. Mountain⁶¹, F. Muheim⁵², M. Mulder⁴³,
 M. Mussini¹⁵, D. Müller⁵⁶, J. Müller¹⁰, K. Müller⁴², V. Müller¹⁰, P. Naik⁴⁸, T. Nakada⁴¹,
 R. Nandakumar⁵¹, A. Nandi⁵⁷, I. Nasteva², M. Needham⁵², N. Neri²², S. Neubert¹²,
 N. Neufeld⁴⁰, M. Neuner¹², A.D. Nguyen⁴¹, C. Nguyen-Mau^{41,n}, S. Nieswand⁹, R. Niet¹⁰,
 N. Nikitin³³, T. Nikodem¹², A. Novoselov³⁷, D.P. O'Hanlon⁵⁰, A. Oblakowska-Mucha²⁸,
 V. Obraztsov³⁷, S. Ogilvy¹⁹, R. Oldeman⁴⁹, C.J.G. Onderwater⁶⁹, J.M. Otalora Goicochea²,
 A. Otto⁴⁰, P. Owen⁴², A. Oyanguren⁶⁸, P.R. Pais⁴¹, A. Palano^{14,d}, F. Palombo^{22,q},
 M. Palutan¹⁹, J. Panman⁴⁰, A. Papanestis⁵¹, M. Pappagallo^{14,d}, L.L. Pappalardo^{17,g},
 W. Parker⁶⁰, C. Parkes⁵⁶, G. Passaleva¹⁸, A. Pastore^{14,d}, G.D. Patel⁵⁴, M. Patel⁵⁵,
 C. Patrignani^{15,e}, A. Pearce^{56,51}, A. Pellegrino⁴³, G. Penso²⁶, M. Pepe Altarelli⁴⁰, S. Perazzini⁴⁰,
 P. Perret⁵, L. Pescatore⁴⁷, K. Petridis⁴⁸, A. Petrolini^{20,h}, A. Petrov⁶⁷, M. Petruzzo^{22,q},
 E. Picatoste Olloqui³⁸, B. Pietrzyk⁴, M. Pikiés²⁷, D. Pinci²⁶, A. Pistone²⁰, A. Piucci¹²,
 S. Playfer⁵², M. Plo Casasus³⁹, T. Poikela⁴⁰, F. Polci⁸, A. Poluektov^{50,36}, I. Polyakov⁶¹,
 E. Polcarpo², G.J. Pomery⁴⁸, A. Popov³⁷, D. Popov^{11,40}, B. Popovici³⁰, S. Poslavskii³⁷,
 C. Potterat², E. Price⁴⁸, J.D. Price⁵⁴, J. Prisciandaro³⁹, A. Pritchard⁵⁴, C. Prouve⁴⁸,
 V. Pugatch⁴⁶, A. Puig Navarro⁴¹, G. Punzi^{24,p}, W. Qian⁵⁷, R. Quagliani^{7,48}, B. Rachwal²⁷,
 J.H. Rademacker⁴⁸, M. Rama²⁴, M. Ramos Pernas³⁹, M.S. Rangel², I. Raniuk⁴⁵, G. Raven⁴⁴,
 F. Redi⁵⁵, S. Reichert¹⁰, A.C. dos Reis¹, C. Remon Alepuz⁶⁸, V. Renaudin⁷, S. Ricciardi⁵¹,
 S. Richards⁴⁸, M. Rihl⁴⁰, K. Rinnert⁵⁴, V. Rives Molina³⁸, P. Robbe^{7,40}, A.B. Rodrigues¹,
 E. Rodrigues⁵⁹, J.A. Rodriguez Lopez⁶⁵, P. Rodriguez Perez^{56,†}, A. Rogozhnikov³⁵, S. Roiser⁴⁰,
 A. Rollings⁵⁷, V. Romanovskiy³⁷, A. Romero Vidal³⁹, J.W. Ronayne¹³, M. Rotondo¹⁹,
 M.S. Rudolph⁶¹, T. Ruf⁴⁰, P. Ruiz Valls⁶⁸, J.J. Saborido Silva³⁹, E. Sadykhov³², N. Sagidova³¹,

B. Saitta^{16,f}, V. Salustino Guimaraes², C. Sanchez Mayordomo⁶⁸, B. Sanmartin Sedes³⁹, R. Santacesaria²⁶, C. Santamarina Rios³⁹, M. Santimaria¹⁹, E. Santovetti^{25,j}, A. Sarti^{19,k}, C. Satriano^{26,s}, A. Satta²⁵, D.M. Saunders⁴⁸, D. Savrina^{32,33}, S. Schael⁹, M. Schellenberg¹⁰, M. Schiller⁴⁰, H. Schindler⁴⁰, M. Schlupp¹⁰, M. Schmelling¹¹, T. Schmelzer¹⁰, B. Schmidt⁴⁰, O. Schneider⁴¹, A. Schopper⁴⁰, K. Schubert¹⁰, M. Schubiger⁴¹, M.-H. Schune⁷, R. Schwemmer⁴⁰, B. Sciascia¹⁹, A. Sciubba^{26,k}, A. Semennikov³², A. Sergi⁴⁷, N. Serra⁴², J. Serrano⁶, L. Sestini²³, P. Seyfert²¹, M. Shapkin³⁷, I. Shapoval⁴⁵, Y. Shcheglov³¹, T. Shears⁵⁴, L. Shekhtman^{36,w}, V. Shevchenko⁶⁷, A. Shires¹⁰, B.G. Siddi^{17,40}, R. Silva Coutinho⁴², L. Silva de Oliveira², G. Simi^{23,o}, S. Simone^{14,d}, M. Sirendi⁴⁹, N. Skidmore⁴⁸, T. Skwarnicki⁶¹, E. Smith⁵⁵, I.T. Smith⁵², J. Smith⁴⁹, M. Smith⁵⁵, H. Snoek⁴³, M.D. Sokoloff⁵⁹, F.J.P. Soler⁵³, B. Souza De Paula², B. Spaan¹⁰, P. Spradlin⁵³, S. Sridharan⁴⁰, F. Stagni⁴⁰, M. Stahl¹², S. Stahl⁴⁰, P. Stefko⁴¹, S. Stefkova⁵⁵, O. Steinkamp⁴², S. Stemmler¹², O. Stenyakin³⁷, S. Stevenson⁵⁷, S. Stoica³⁰, S. Stone⁶¹, B. Storaci⁴², S. Stracka^{24,p}, M. Straticiu³⁰, U. Straumann⁴², L. Sun⁵⁹, W. Sutcliffe⁵⁵, K. Swientek²⁸, V. Syropoulos⁴⁴, M. Szczekowski²⁹, T. Szumlak²⁸, S. T'Jampens⁴, A. Tayduganov⁶, T. Tekampe¹⁰, G. Tellarini^{17,g}, F. Teubert⁴⁰, E. Thomas⁴⁰, J. van Tilburg⁴³, M.J. Tilley⁵⁵, V. Tisserand⁴, M. Tobin⁴¹, S. Tolck⁴⁹, L. Tomassetti^{17,g}, D. Tonelli⁴⁰, S. Topp-Joergensen⁵⁷, F. Toriello⁶¹, E. Tournefier⁴, S. Tourneur⁴¹, K. Trabelsi⁴¹, M. Traill⁵³, M.T. Tran⁴¹, M. Tresch⁴², A. Trisovic⁴⁰, A. Tsaregorodtsev⁶, P. Tsopelas⁴³, A. Tully⁴⁹, N. Tuning⁴³, A. Ukleja²⁹, A. Ustyuzhanin³⁵, U. Uwer¹², C. Vacca^{16,f}, V. Vagnoni^{15,40}, A. Valassi⁴⁰, S. Valat⁴⁰, G. Valenti¹⁵, A. Vallier⁷, R. Vazquez Gomez¹⁹, P. Vazquez Regueiro³⁹, S. Vecchi¹⁷, M. van Veghel⁴³, J.J. Velthuis⁴⁸, M. Veltri^{18,r}, G. Veneziano⁴¹, A. Venkateswaran⁶¹, M. Vernet⁵, M. Vesterinen¹², B. Viaud⁷, D. Vieira¹, M. Vieites Diaz³⁹, X. Vilasis-Cardona^{38,m}, V. Volkov³³, A. Vollhardt⁴², B. Voneki⁴⁰, A. Vorobyev³¹, V. Vorobyev^{36,w}, C. Voß⁶⁶, J.A. de Vries⁴³, C. Vázquez Sierra³⁹, R. Waldi⁶⁶, C. Wallace⁵⁰, R. Wallace¹³, J. Walsh²⁴, J. Wang⁶¹, D.R. Ward⁴⁹, H.M. Wark⁵⁴, N.K. Watson⁴⁷, D. Websdale⁵⁵, A. Weiden⁴², M. Whitehead⁴⁰, J. Wicht⁵⁰, G. Wilkinson^{57,40}, M. Wilkinson⁶¹, M. Williams⁴⁰, M.P. Williams⁴⁷, M. Williams⁵⁸, T. Williams⁴⁷, F.F. Wilson⁵¹, J. Wimberley⁶⁰, J. Wishahi¹⁰, W. Wislicki²⁹, M. Witek²⁷, G. Wormser⁷, S.A. Wotton⁴⁹, K. Wraight⁵³, S. Wright⁴⁹, K. Wyllie⁴⁰, Y. Xie⁶⁴, Z. Xing⁶¹, Z. Xu⁴¹, Z. Yang³, H. Yin⁶⁴, J. Yu⁶⁴, X. Yuan^{36,w}, O. Yushchenko³⁷, K.A. Zarebski⁴⁷, M. Zavertyaev^{11,c}, L. Zhang³, Y. Zhang⁷, Y. Zhang⁶³, A. Zhelezov¹², Y. Zheng⁶³, A. Zhokhov³², X. Zhu³, V. Zhukov⁹, S. Zucchelli¹⁵.

¹ Centro Brasileiro de Pesquisas Físicas (CBPF), Rio de Janeiro, Brazil

² Universidade Federal do Rio de Janeiro (UFRJ), Rio de Janeiro, Brazil

³ Center for High Energy Physics, Tsinghua University, Beijing, China

⁴ LAPP, Université Savoie Mont-Blanc, CNRS/IN2P3, Annecy-Le-Vieux, France

⁵ Clermont Université, Université Blaise Pascal, CNRS/IN2P3, LPC, Clermont-Ferrand, France

⁶ CPPM, Aix-Marseille Université, CNRS/IN2P3, Marseille, France

⁷ LAL, Université Paris-Sud, CNRS/IN2P3, Orsay, France

⁸ LPNHE, Université Pierre et Marie Curie, Université Paris Diderot, CNRS/IN2P3, Paris, France

⁹ I. Physikalisches Institut, RWTH Aachen University, Aachen, Germany

¹⁰ Fakultät Physik, Technische Universität Dortmund, Dortmund, Germany

¹¹ Max-Planck-Institut für Kernphysik (MPIK), Heidelberg, Germany

¹² Physikalisches Institut, Ruprecht-Karls-Universität Heidelberg, Heidelberg, Germany

¹³ School of Physics, University College Dublin, Dublin, Ireland

¹⁴ Sezione INFN di Bari, Bari, Italy

¹⁵ Sezione INFN di Bologna, Bologna, Italy

¹⁶ Sezione INFN di Cagliari, Cagliari, Italy

¹⁷ Sezione INFN di Ferrara, Ferrara, Italy

¹⁸ Sezione INFN di Firenze, Firenze, Italy

¹⁹ Laboratori Nazionali dell'INFN di Frascati, Frascati, Italy

²⁰ Sezione INFN di Genova, Genova, Italy

²¹ Sezione INFN di Milano Bicocca, Milano, Italy

- ²² *Sezione INFN di Milano, Milano, Italy*
- ²³ *Sezione INFN di Padova, Padova, Italy*
- ²⁴ *Sezione INFN di Pisa, Pisa, Italy*
- ²⁵ *Sezione INFN di Roma Tor Vergata, Roma, Italy*
- ²⁶ *Sezione INFN di Roma La Sapienza, Roma, Italy*
- ²⁷ *Henryk Niewodniczanski Institute of Nuclear Physics Polish Academy of Sciences, Kraków, Poland*
- ²⁸ *AGH - University of Science and Technology, Faculty of Physics and Applied Computer Science, Kraków, Poland*
- ²⁹ *National Center for Nuclear Research (NCBJ), Warsaw, Poland*
- ³⁰ *Horia Hulubei National Institute of Physics and Nuclear Engineering, Bucharest-Magurele, Romania*
- ³¹ *Petersburg Nuclear Physics Institute (PNPI), Gatchina, Russia*
- ³² *Institute of Theoretical and Experimental Physics (ITEP), Moscow, Russia*
- ³³ *Institute of Nuclear Physics, Moscow State University (SINP MSU), Moscow, Russia*
- ³⁴ *Institute for Nuclear Research of the Russian Academy of Sciences (INR RAN), Moscow, Russia*
- ³⁵ *Yandex School of Data Analysis, Moscow, Russia*
- ³⁶ *Budker Institute of Nuclear Physics (SB RAS), Novosibirsk, Russia*
- ³⁷ *Institute for High Energy Physics (IHEP), Protvino, Russia*
- ³⁸ *ICCUB, Universitat de Barcelona, Barcelona, Spain*
- ³⁹ *Universidad de Santiago de Compostela, Santiago de Compostela, Spain*
- ⁴⁰ *European Organization for Nuclear Research (CERN), Geneva, Switzerland*
- ⁴¹ *Ecole Polytechnique Fédérale de Lausanne (EPFL), Lausanne, Switzerland*
- ⁴² *Physik-Institut, Universität Zürich, Zürich, Switzerland*
- ⁴³ *Nikhef National Institute for Subatomic Physics, Amsterdam, The Netherlands*
- ⁴⁴ *Nikhef National Institute for Subatomic Physics and VU University Amsterdam, Amsterdam, The Netherlands*
- ⁴⁵ *NSC Kharkiv Institute of Physics and Technology (NSC KIPT), Kharkiv, Ukraine*
- ⁴⁶ *Institute for Nuclear Research of the National Academy of Sciences (KINR), Kyiv, Ukraine*
- ⁴⁷ *University of Birmingham, Birmingham, United Kingdom*
- ⁴⁸ *H.H. Wills Physics Laboratory, University of Bristol, Bristol, United Kingdom*
- ⁴⁹ *Cavendish Laboratory, University of Cambridge, Cambridge, United Kingdom*
- ⁵⁰ *Department of Physics, University of Warwick, Coventry, United Kingdom*
- ⁵¹ *STFC Rutherford Appleton Laboratory, Didcot, United Kingdom*
- ⁵² *School of Physics and Astronomy, University of Edinburgh, Edinburgh, United Kingdom*
- ⁵³ *School of Physics and Astronomy, University of Glasgow, Glasgow, United Kingdom*
- ⁵⁴ *Oliver Lodge Laboratory, University of Liverpool, Liverpool, United Kingdom*
- ⁵⁵ *Imperial College London, London, United Kingdom*
- ⁵⁶ *School of Physics and Astronomy, University of Manchester, Manchester, United Kingdom*
- ⁵⁷ *Department of Physics, University of Oxford, Oxford, United Kingdom*
- ⁵⁸ *Massachusetts Institute of Technology, Cambridge, MA, United States*
- ⁵⁹ *University of Cincinnati, Cincinnati, OH, United States*
- ⁶⁰ *University of Maryland, College Park, MD, United States*
- ⁶¹ *Syracuse University, Syracuse, NY, United States*
- ⁶² *Pontifícia Universidade Católica do Rio de Janeiro (PUC-Rio), Rio de Janeiro, Brazil, associated to ²*
- ⁶³ *University of Chinese Academy of Sciences, Beijing, China, associated to ³*
- ⁶⁴ *Institute of Particle Physics, Central China Normal University, Wuhan, Hubei, China, associated to ³*
- ⁶⁵ *Departamento de Física, Universidad Nacional de Colombia, Bogota, Colombia, associated to ⁸*
- ⁶⁶ *Institut für Physik, Universität Rostock, Rostock, Germany, associated to ¹²*
- ⁶⁷ *National Research Centre Kurchatov Institute, Moscow, Russia, associated to ³²*
- ⁶⁸ *Instituto de Física Corpuscular (IFIC), Universitat de Valencia-CSIC, Valencia, Spain, associated to ³⁸*
- ⁶⁹ *Van Swinderen Institute, University of Groningen, Groningen, The Netherlands, associated to ⁴³*
- ^a *Universidade Federal do Triângulo Mineiro (UFTM), Uberaba-MG, Brazil*
- ^b *Laboratoire Leprince-Ringuet, Palaiseau, France*
- ^c *P.N. Lebedev Physical Institute, Russian Academy of Science (LPI RAS), Moscow, Russia*
- ^d *Università di Bari, Bari, Italy*
- ^e *Università di Bologna, Bologna, Italy*
- ^f *Università di Cagliari, Cagliari, Italy*

- ^g *Università di Ferrara, Ferrara, Italy*
^h *Università di Genova, Genova, Italy*
ⁱ *Università di Milano Bicocca, Milano, Italy*
^j *Università di Roma Tor Vergata, Roma, Italy*
^k *Università di Roma La Sapienza, Roma, Italy*
^l *AGH - University of Science and Technology, Faculty of Computer Science, Electronics and Telecommunications, Kraków, Poland*
^m *LIFAEELS, La Salle, Universitat Ramon Llull, Barcelona, Spain*
ⁿ *Hanoi University of Science, Hanoi, Viet Nam*
^o *Università di Padova, Padova, Italy*
^p *Università di Pisa, Pisa, Italy*
^q *Università degli Studi di Milano, Milano, Italy*
^r *Università di Urbino, Urbino, Italy*
^s *Università della Basilicata, Potenza, Italy*
^t *Scuola Normale Superiore, Pisa, Italy*
^u *Università di Modena e Reggio Emilia, Modena, Italy*
^v *Iligan Institute of Technology (IIT), Iligan, Philippines*
^w *Novosibirsk State University, Novosibirsk, Russia*

[†] *Deceased*